INFLUENCE OF SEA LEVEL ON THE GROWTH AND COMPOSITION OF INTERTIDAL OYSTER REEFS

Justin Tyler Ridge

A dissertation submitted to the faculty at the University of North Carolina at Chapel Hill in partial fulfillment of the requirements for the degree of Doctor of Philosophy in the Department of Marine Sciences in the College of Arts and Sciences.

Chapel Hill
2017

Approved by:

Antonio B. Rodriguez

F. Joel Fodrie

Michael F. Piehler

Brent A. McKee

Jonathan H. Grabowski

ABSTRACT

Justin Tyler Ridge: Influence of sea level on the growth and composition of intertidal oyster reefs
(Under the direction of Antonio B. Rodriguez and F. Joel Fodrie)

Oyster reefs play an important role in the estuarine landscape but have been globally decimated over the past century from overharvesting, deteriorating water quality, and disease. Expanding our knowledge of how these habitats are responding to anthropogenic and climate driven changes will help improve management strategies. This work explored the growth and composition of intertidal oyster reefs in the euhaline estuaries of North Carolina using high-resolution mapping (terrestrial lidar), density sampling, and cores of reefs. The first chapter examined mature, constructed patch reefs (isolated on sandflats) to elucidate that oyster reef growth is strongly linked to specific elevation ranges within the intertidal zone. Building upon these findings, the second chapter determined this pattern holds true on marsh-fringing reefs, and as the reefs transgress the marsh with sea-level rise (SLR) they also protect carbonaceous marsh sediment from erosion. The third chapter observed reefs of varying age, both constructed and natural, over five years to discover that oyster reefs are in a dynamic equilibrium with sea level, responding rapidly (< 1 year) to fluctuations in sea level. Similarly, examining oyster reefs across time scales, from ancient reefs (~4,000-2,000 years old) to extant natural reefs (150 years old) and recently constructed reefs (5-10 years old), chapter four provided evidence that oyster reefs exhibit catch-up and keep-up growth phases tied to SLR, which was first described for coral reefs. Within this context, reefs experience exceptional rates of shell production and

organic carbon accumulation while catching up to sea level, but these values are at least a magnitude less in reefs that are keeping up with sea level. Burial of ancient reefs is likely a result of estuarine changes related to the migration of adjacent barrier islands, indicating oyster reefs existing near the limits of suitable conditions could be fatally impaired by estuarine modifications, either anthropogenic (inlet and river dynamics) or climate driven (storms).

To all of my family
for their unwavering support.

ACKNOWLEDGEMENTS

First and foremost, I want to thank the support and guidance of my two advisors, Tony Rodriguez and Joel Fodrie. I was beyond lucky to find my way to North Carolina and work with these two extremely talented researchers. While I have deeply enjoyed working with both labs, a majority of my time has been spent in the Rodriguez Lab, which has become family with boundless support and welcoming friendship. Tony, I could not have asked for a better mentor during this process, and I have felt more like a colleague than a student these past few years. Your enthusiasm and commitment to both research and teaching opportunities is infectious, and it has been great to chat endlessly about exciting research questions as well as books and movies, and even donuts. Joel, while I may have relied less on you during this time, I have truly benefited from your perspective and expertise, and I knew that I could always seek your advice at any hour. I have learned so much about how to be a great researcher from you two, and I look forward to collaborating on future projects as colleagues and friends.

I also would not have done this well without the love and support of my wife, Michelle Brodeur. I could not have dreamed how great life would get coming to North Carolina, and I am incredibly blessed to have you by my side. I was also fortunate to find a brother and partner in crime, Ethan Theuerkauf. You and Kristen helped make North Carolina home, and I cannot wait for the many adventures to come for us. And to my family (both blood and chosen), I cannot thank you enough for your limitless support and love.

I very much appreciate the help of my committee members, Michael Piehler, Brent McKee, and Jon Grabowski, for their ever-useful feedback and advice that has provided perspective for my research. I would also be remiss if I did not thank the constant support and guidance from John Fear, who helped steer a random guy looking for a job in North Carolina to a place he would want to call home. From the Rodriguez Lab family, I must thank the following people for their assistance with my dissertation work (and friendship) over the past five years: Beth VanDusen, Anna Atencio, Mariah Livernois, Taylor Bennett, Kieu Tran, Noel Anderson, Quin Walker, Caroline White-Nockleby, Rachel Quindlen, Morgan Freese, Robin Kim, Max Tice-Lewis, Charlie Deaton, Carson Miller, Rich Mahoney, Molly Bost, and (best for last) Emily Woodward. And to the rest of my IMS family, old and new, thank you for creating an environment that fosters friendship and makes each day a joy to come to work.

TABLE OF CONTENTS

LIST OF TABLES

LIST OF FIGURES

LIST OF ABBREVIATIONS AND SYMBOLS

~	approximately
°C	degrees Celsius
µm	micrometer
AD	Anno Domini
ANOVA	Analysis of Variance
BP	Before Present
Cy	clay
Cal	calibrated
CE	Common Era
CEB	Critical Exposure Boundary
CI	Carrot Island
cm	centimeter
C_{org}	organic carbon
DEM	Digital Elevation Model
e.g.	for example
ENSO	El Niño-Southern Oscillation
et al.	and colleagues
etc.	etcetera
g C	grams carbon
g	gram
GPS	Global Positioning System
HSD	Highest Significant Difference

i.e.	that is
ID	identification
kg	Kilogram
L	liter
LOI	loss on ignition
m	meter
MARS	Merrick Advanced Remote Sensing
MLW	Mean Low Water
MM	Middle Marsh
mm	millimeter
MSL	Mean Sea Level
NAO	North Atlantic Oscillation
NAVD88	North American Vertical Datum of 1988
NC	North Carolina
NCNERR	North Carolina National Estuarine Research Reserve
NOAA	National Oceanic and Atmospheric Administration
NOS	National Ocean Service
NOSAMS	National Ocean Sciences Accelerator Mass Spectrometry
NRM	North River Marsh
OGZ	Optimal Growth Zone
ppt	parts per thousand
psu	practical salinity units
refs	reference(s)

RSLR	relative sea-level rise
RTK	Real-Time Kinematic
Sd	sand
SD	standard deviation
SLR	sea-level rise
St	silt
T	time
US	United States
USA	United States of America
USDA	United States Department of Agriculture
yr	year
Δ	delta (change)

CHAPTER 1: MAXIMIZING OYSTER-REEF GROWTH SUPPORTS GREEN INFRASTRUCTURE WITH ACCELERATING SEA-LEVEL RISE[1]

1.1. Introduction

Species distributions result from distinct regions of optimal fitness conditions, defined by critical boundaries regulated by physiological and external stressors (Connell 1972, Menge and Sutherland 1987). As such, biological zonation is expressed both globally (e.g., latitudinal range limits) and locally, as in the intertidal zone for foundation species such as saltmarsh, mangrove and reef-forming bivalves. The forecasted acceleration in SLR (IPCC 2014) will shift the position of critical boundaries in littoral systems. Thus, the resilience of sessile species confined to a narrow intertidal zone and their associated shorelines (both natural and developed) will be defined by the species' ability to respond to moving boundary conditions. However, migration of coastal foundation species (e.g., oyster reefs and saltmarsh) will be hindered by shoreline development as part of the coastal squeeze (Pontee 2013), resulting in reduced area suitable for colonization. Therefore, this anthropogenically-induced phenomenon accentuates the importance of self-maintaining accretional habitats that can match SLR (Nicholls et al. 1999). Failure to maintain their position within the tidal range or migrate landward will result in replacement of biogenic reefs or marshes by unstructured habitats like sandflats (Nicholls et al. 1999, Borsje et al. 2011).

[1]This chapter previously appeared as an article in *Scientific Reports*. The original citation is as follows: Ridge JT, Rodriguez AB, Fodrie FJ *et al.* (2015) Maximizing oyster-reef growth supports green infrastructure with accelerating sea-level rise. *Scientific Reports*, **5**, 14785.

Intertidal habitats can provide disproportionately high levels of ecosystem services, such that coastal and estuarine ecosystems are among the most valuable on earth (Costanza et al. 1997, Coen et al. 1999, Peterson and Lipcius 2003, Grabowski and Peterson 2007, Barbier et al. 2011, Grabowski et al. 2012). Unfortunately, continued population growth in coastal areas globally has led to the degradation of these ecosystems and reduced service delivery (Vitousek 1997, Halpern et al. 2008, Barbier et al. 2011), stimulating efforts to explore how these systems will respond to current and future anthropogenic stressors, such as accelerated SLR. As one of the only natural hard substrates along the Mid and South Atlantic Coast (USA), oyster reef habitat has been recognized as green infrastructure for shoreline protection (Borsje et al. 2011, Arkema et al. 2013) and conservation of natural capital in the face of damaging storms and wave erosion (Piazza et al. 2005, Scyphers et al. 2011, Cheong et al. 2013, La Peyre et al. 2014), even though they now occupy a small fraction of their distribution prior to massive harvesting during the last three centuries (Kirby 2004, Beck et al. 2011, zu Ermgassen 2012). The effectiveness of using oyster reefs to enhance shoreline resiliency and reduce storm hazards along estuarine shorelines depends on understanding the biologically- and environmentally-driven thresholds separating oyster-reef production and growth from imminent degradation.

At whole-estuary scales, oyster growth responds to two overarching factors: salinity and aerial exposure, the amount of time intertidal oysters are exposed (or emerge) during a tidal cycle. Free-swimming oyster larvae require hard substrate to settle onto and typically grow on other oysters, which will form patches of unconsolidated oyster clusters that can eventually develop into large cohesive reef mounds (>1 km^2) with densities exceeding 1000 individuals m^{-2} (Bahr and Lanier 1981, Kennedy et al. 1996). Historical observations (Bahr and Lanier 1981, Wilber 1992, Hargis and Haven 1999) of oyster abundances along estuarine gradients provide a

foundational understanding of oyster response to varying salinity and aerial exposure. The euhaline (high salinity, between 30-35 psu) waters commonly found near coastal inlets are not conducive to subtidal oyster reef formation due to high levels of biotic stress on individual oysters from marine predators, competitors, bioeroders and pathogens (Chu et al. 1993, White and Wilson 1996, Fodrie et al. 2014, Johnson and Smee 2014). However, mesohaline and polyhaline waters (moderate salinities, 5-18 and 18-30 psu respectively) offer oysters refuge from these marine stressors that are not tolerant of lower salinities, thereby allowing oyster reefs to persist subtidally unless they are exposed to hypoxic/anoxic (low oxygen) events (Lenihan 1999, Lenihan et al. 1999) or overharvesting (Rothschild et al. 1994, Jackson et al. 2001, Wilberg et al. 2011). The decimation to oyster populations as well as anthropogenic and SLR-driven changes to water quality have made restoration and sustainability difficult (Mann and Powell 2007, Mann et al. 2009, Seavey et al. 2011), but there have been promising efforts (Piazza et al. 2005, Powers et al. 2009, Schulte et al. 2009, Rodriguez et al. 2014) that indicate restoration, recovery and sustainability are possible. Rates of oyster-reef growth appear comparable to rates of SLR (DeAlteris 1988), and while intertidal oyster reefs have also exhibited the capacity for even greater growth (Rodriguez et al. 2014), it remains unclear as to which environmental conditions will provide the greatest return on investment from restoration efforts and ensure persistence with accelerations in SLR. Optimizing conservation and restoration efforts of oyster populations along our coasts requires a more precise understanding of how intertidal reefs grow in response to exposure-flooding cycles and forecasted SLR.

We investigated whole- and across-reef vertical growth, along with oyster density, on natural and constructed *Crassostrea virginica* (eastern oyster) reefs within the Rachel Carson National Estuarine Research Reserve, Back Sound, North Carolina (tidal range 0.92 m, salinity

30-35 psu). In total, 43 reefs provided spectrums of sizes (15 – 850 m^2), ages (<1 – >100 years old), and tidal elevations (intertidal to subtidal) for our investigations. Constructed intertidal oyster reefs were created by forming dead oyster shells into 3 x 5 x 0.15 m piles in 1997, 2000, and 2011 that developed via natural oyster recruitment, growth and survivorship patterns (Grabowski et al. 2005, Fodrie et al. 2014). We used a terrestrial laser scanner to measure variation in vertical growth across entire reefs constructed in 1997 and 2000, over a two-year time step (measured between 2010 and 2012, Fig. 1.1). Water-level data were collected within the study area in order to transform the reef elevations into the amount of time each portion of the reef spent emerged from the water (percent aerial exposure) during a tidal cycle (water level referenced to elevations using the North American Vertical Datum of 1988 [NAVD88]). We examined the relationship between reef growth and associated elevation to determine growth thresholds relative to an oyster reef's position in the intertidal zone. Subsequently, we used those empirical data to develop a model that illustrates impacts of accelerating SLR on existing reefs and future reef construction as large-scale green infrastructure.

1.2. Results and Discussion

Decade-old oyster reefs exhibited a unimodal relationship between average vertical-accretion rate and aerial exposure (Fig. 1.2a). Areas of highest mean growth were exposed 20-40% of the time, and this range represents an optimal-growth zone (OGZ). These reefs, along with natural oyster reefs, consistently exhibit a plateau morphology at 0.03 m NAVD88 (± 0.05 m) (Appendix 1.1), indicating that 55% (± 1.5%) exposure is the upper zero-growth boundary (growth ceiling) for reefs in this region. The 10% exposure, occurring at -0.43 m NAVD88 in the Reserve, coincides with mean low water (MLW) and represents the lower zero-growth boundary for oyster reefs where accretional and erosional forces are balanced. Below 10%

inundation, increases in accretion resulted from deposition of sediment and dead oyster shell at the reef edge. As an oyster reef is physically and biologically weathered (Fodrie et al. 2014, Johnson and Smee 2014), material is transported from higher reef elevations downslope, mainly during periods of high wave and current energy, promoting lateral expansion. The lower portions of an oyster reef may experience increased vertical growth as the physical processes of sedimentation build those areas in to the OGZ. For example, a majority of reef MF3-1997 had just reached the center of the OGZ at the beginning of the study period and experienced the most vertical growth of all the decade-old oyster reefs (Figs. 1,2a).

To verify these exposure boundaries, in 2011 we constructed oyster reefs along a gradient of sandflat exposures ranging from 0.01 to 18.0% (Appendix 1.2 and Table 1.1) and average vertical reef growth was measured in 2014 using a Trimble 5800 GPS receiver (±1.5 cm vertical). The initial reef-top exposures ranged from 0.30 to 32.4%, which were comparable to the lower edge to mid-slope of natural, mature oyster-reef mounds located in the area. Those 3-year old reefs followed the same growth pattern as the decade-old reefs, with increasing aerial exposures resulting in greater reef growth rates, and little to no growth when those older reef were located below 10% exposure (Fig. 1.2b). Although the shallower reefs exhibited rapid vertical growth (4-8 cm yr^{-1}), with the shallowest reef reaching 45% exposure at the end of the study period, our observation period was too short for these reefs to reach the growth ceiling and become confined by the stress of limited inundation. Reefs below MLW did not sustain growth, and anomalously-high accretion rates measured on some reefs were caused by migrating sand ripples converting the deep shell piles into sand mounds (Fig. 1.2b), as has been observed in other sandy environments (Taylor and Bushek 2008). While this overall growth pattern reinforces our results from decade-old reefs, it also indicates that newly-constructed oyster reefs

have the potential to grow twice as fast as mature reefs. Thus, there likely is a progression of diminishing vertical growth from substrate colonization to reef maturation as the oyster reef approaches the growth ceiling and the area of the OGZ narrows to the reef flanks (Fig. 1.1c).

Oyster recruitment, growth and survival collectively mediate oyster reef accretion rates, and therefore, oyster density should generally be correlated with reef accretion. Adult oyster density in both natural and restored reefs also matched the observed reef growth pattern, except at the highest elevations of the reef (>OGZ), where density continues to increase as oysters recruit and fill the interstitial space (Fig. 1.2c) but are still limited in overall growth by desiccation stress (growth ceiling). Adult oyster densities were greater on natural reefs than restored reefs in all but the topmost region of the reefs (Fig. 1.2c). Very low adult oyster density below 10% exposure further supports our observation that reef accretion at the base (Fig. 1.2a) is from accumulation of sediment and shell material, not oyster growth.

While rising sea level will shift the growth boundaries landward and to higher elevations, accelerations in SLR will exacerbate the loss of substrate elevations suitable for oyster reef growth. Similar to models of productivity in saltmarsh habitats (Morris et al. 2002), our oyster-reef growth model reveals the rates of SLR for a given oyster reef to remain in equilibrium with rising water levels (Fig. 1.3a). At current rates of local SLR (~ 0.3 cm yr^{-1}, Kemp et al. 2011), the 12% exposure depth represents a critical-exposure boundary (CEB) where rates of reef growth and SLR are equal. At substrate depths above the CEB, oyster reefs will form and persist as a consequence of reduced stressors such as disease, predation, and sedimentation. However, an increase in the rate of SLR to 0.5 cm yr^{-1} (well within most predictions of SLR by 2100, Rahmstorf 2010) may render substrates below 15% exposure unsuitable for intertidal oyster-reef habitat because below that level, oyster-reef accretion cannot keep pace with this SLR scenario

(Fig. 1.3b). In contrast, the growth ceiling, while adjusting in elevation with SLR, will remain at the 55% exposure. Therefore, and most notably, this strong link between oyster growth and aerial exposure means accelerating SLR will reduce the estuarine area suitable for oyster reef occupation (Fig. 1.3c,d) between the shifting CEB (e.g., 12% to 15% exposure) and the constant growth ceiling (55%). The amount of oyster-reef habitat area lost locally further depends on nearshore sedimentation rates and changing bathymetry as the shoreface responds to SLR and fluctuations in sediment supply. Considering the model is crucial for newly forming oyster reefs (both natural and constructed), as we have witnessed failed reef growth below the CEB within the first year of construction (Fodrie et al. 2014), making this boundary an immediate consideration for restoration efforts. Because our results suggest that oyster-reef growth in the intertidal zone is dependent upon percent aerial exposure, the range of suitable substrate depths (above the CEB) and the OGZ boundaries will likely expand in other estuaries of the U.S. with increasing tidal range as the intertidal zone is stretched across a greater depth spectrum (Appendix 1.3). It also bears noting that the growth ceiling, depending upon oyster tolerance to desiccation and other stresses of exposure, may differ in warmer and colder latitudes, as more extreme temperatures could diminish the upper growth limit.

Older established oyster reefs that reached the growth ceiling are resilient to accelerating SLR because growth rates will increase on top of the reef as oysters exploit increased inundation time and subaqueous space. That increased productivity at the reef top could in turn lead to an increase in biogenic sediment flux to the reef base and enhance lateral and vertical accretion rates around the CEB. This resiliency is contingent upon limited disturbance; harvesting that lowers an oyster reef below the CEB will ultimately result in the loss of the habitat. Conservation efforts should limit harvesting practices from reducing oyster reef elevation below

the OGZ to maximize the potential for rebound and to maintain optimal reef growth levels that would ensure the highest productivity of the fishery.

As development along low-elevation sheltered coastlines and rates of SLR continue to increase, so does our need for new decision-support tools that both reduce the risk of human societies to coastal hazards and maintain the vast natural capital that coastal habitats provide. In high salinity portions of estuaries, oyster-reef restoration in front of either saltmarsh shorelines or stabilization structures like riprap revetments will increase and help sustain ecosystem services, but only if restoration efforts consider the CEB and OGZ during project design, implementation, and future harvesting practices. Notably, the range of suitable substrate elevations for colonization, restoration, and maintenance of oysters and likely other intertidal foundation species is a moving and narrowing target with accelerating sea-level rise.

1.3. Methods

We constructed reefs from 60 bushels of shucked oyster shell (cultch) formed into 3 x 5 x 0.15 m boxes in 1997, 2000, and 2011 on sandflats or adjacent to saltmarsh (*Spartina alterniflora* dominated; see Appendices 1.1 and 1.4; Grabowski et al. 2005, Fodrie et al. 2014). Constructed reefs are located within the Rachel Carson National Estuarine Research Reserve and are protected from harvesting. The natural reefs are located within the Rachel Carson National Estuarine Research Reserve and adjacent to Cape Lookout National Seashore and are not protected.

Ten-minute water-level data were obtained over the course of 6 months (June – December 2010) using HOBO® U20 Water Level Loggers (Onset Computer Corporation; ± 0.3 cm accuracy) located in three areas of Middle Marsh. Loggers were placed in a stilling well (slotted PVC pipe) attached to rebar that was driven into the substrate to refusal (~3 m deep).

Elevations were surveyed at both deployment and data collection, which occurred every month, with a Trimble® RTK GPS. Pressure data were corrected for local fluctuations in barometric pressure using a fourth pressure sensor deployed on land, and water-levels were verified with independent field measurements obtained with a level measuring staff at time of deployment and readout. Survey data were used to transform the water-level data in to the North American Vertical Datum established in 1988 (NAVD88) with average vertical precisions of 1.5 cm. We divided the tidal data into 1-cm bins to ascertain mean percent aerial exposure at each elevation, which we used to convert all elevation measurements obtained from the oyster reefs to percent exposure.

Following previously established methods (Rodriguez et al. 2014), we measured cm-scale vertical growth rates across the entire surface of six sandflat reefs over a 2-year period. These reefs were chosen because they incorporated a wide range of intertidal elevations and were fully exposed during the most extreme spring low tides, which is necessary for our methods of measuring reef growth. Reefs were scanned using a Riegl three-dimensional LMSZ210ii terrestrial laser scanner in 2010 and 2012 and point clouds were processed to isolate ground returns using RiSCAN Pro software. We utilized Surfer 10 (Golden Software) to generate digital elevation models (1-cm cell size) of the six sandflat reefs from 600,000 to 1,000,000 laser returns (number depends on reef size) spaced <1 cm apart. Elevation changes >1.4 cm are resolvable with this method. The 2010 reef grid-cell elevations were subtracted from 2012 counterparts (> 500,000 observations per reef) to obtain elevation changes between measurements. This allowed us to create a table of XYZ and elevation change (2010 value for Z), which we sorted by descending 2010 elevation values. Those data were separated into 2-cm elevation bins (2010 elevations) and mean elevation change between 2010 and 2012 for each bin were calculated (i.e.,

mean vertical accretion rate for every 2-cm change in reef elevation across the entire reef surface). An overall mean vertical accretion rate among reefs was then calculated for each 2-cm elevation bin. Reef MF4-2000 was excluded from the overall mean because it showed signs of significant harvesting between our 2-yr time step (even though the reef was protected), and this was supported by laser-scan data and field observations.

Recently constructed reefs (2011) were placed on sandflats at approximate substrate elevations of -0.9 m, -0.75 m, -0.6 m, and -0.5 m NAVD88 (exposure range: 0.01-18%, Kennedy et al. 1996, Fodrie et al. 2014). To assess the growth of recently-constructed (2011) reefs over their lifetimes, we surveyed a grid across each reef using the RTK-GPS at 0.25-m horizontal intervals. Reefs were surveyed in the fall and winter of 2011, spring of 2013, and spring of 2014. The highest 10% of points within each grid were averaged and designated as the elevation of the reef top. For each reef, we subtracted top elevations between the longest available time step and then normalized by the time interval. For comparison, reef accretions were averaged after binning by original cultch surface exposures: 0-15%, 15-30%, and >30%.

To ascertain size-abundance patterns at different aerial exposures we measured oyster density and oyster-shell height across intertidal elevations. We randomly placed 0.25-m^2 quadrats at varying elevations (surveyed using the Trimble® GPS) on decade-old reefs to obtain 2-3 quadrat samples per reef (N = 22) for density and SH. To sample natural reefs (N = 7), parallel transects, from reef crest to base, were placed 1 meter apart, and one randomly-placed quadrat was sampled along each transect. Samples within reefs were not pooled because they were collected from areas with different exposure conditions, and our primary interest was to determine if exposure regulates reef dynamics. Oyster-reef material was sampled to a depth of approximately 15 cm (or to the depth where sediment was anoxic) and the number and shell

height of live oysters was quantified in the field. Samples were broken into 4 different aerial exposure bins: less than mean low water (<MLW), from MLW to 20% aerial exposure (MLW), from 20% to 40% aerial exposure or the optimal-growth zone (OGZ), and greater than 40% aerial exposure (>OGZ). Adult-oyster densities (oysters >2.5 cm long) were then analyzed among aerial exposure bins and between natural and constructed reefs using a two-way analysis of variance (ANOVA). We used a *post-hoc* Tukey Honest Significant Difference (HSD) test ($\alpha = 0.05$) to determine density differences among exposure zones and between reef types.

The tidal-growth model (Fig. 1.3a) was developed using water-level data and the oyster-reef-growth curve (Fig. 1.2a). Critical boundaries were defined as the elevation where reef growth equaled the current or forecasted rate of sea-level rise. NOAA tide data from Fort Pulaski, Georgia (Station ID: 8670870) were used to extrapolate the model into a larger tidal range (2.25 m)(Appendix 1.3). Tidal elevations were transformed to aerial exposure and indexed to corresponding reef-growth rates using the North Carolina growth curve.

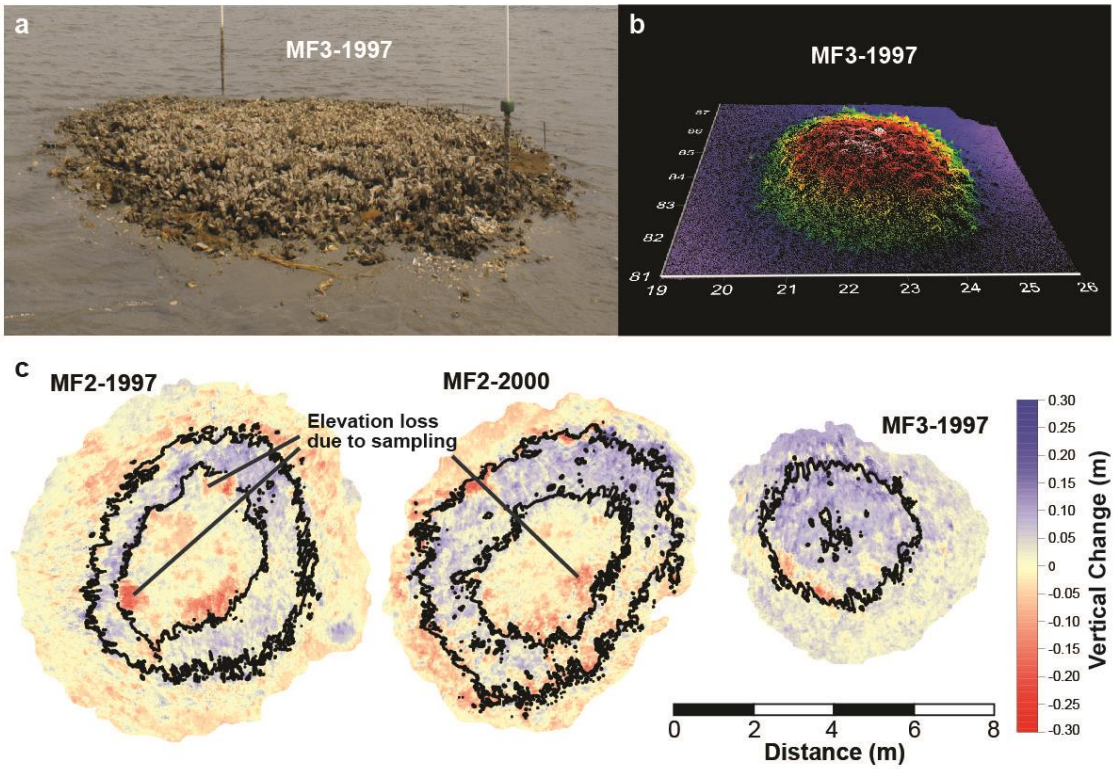

Figure 1.1 Measuring fine-scale growth on oyster reefs. (**a**) Photo and (**b**) oblique point cloud of oyster reef MF3-1997, both obtained in 2010 using a terrestrial laser scanner. (**c**) Digital elevation model subtraction maps of reefs constructed in 1997 and 2000. Reef scans were conducted in 2010 and 2012. Contour lines represent the 20% and 40% aerial exposure elevations in 2010.

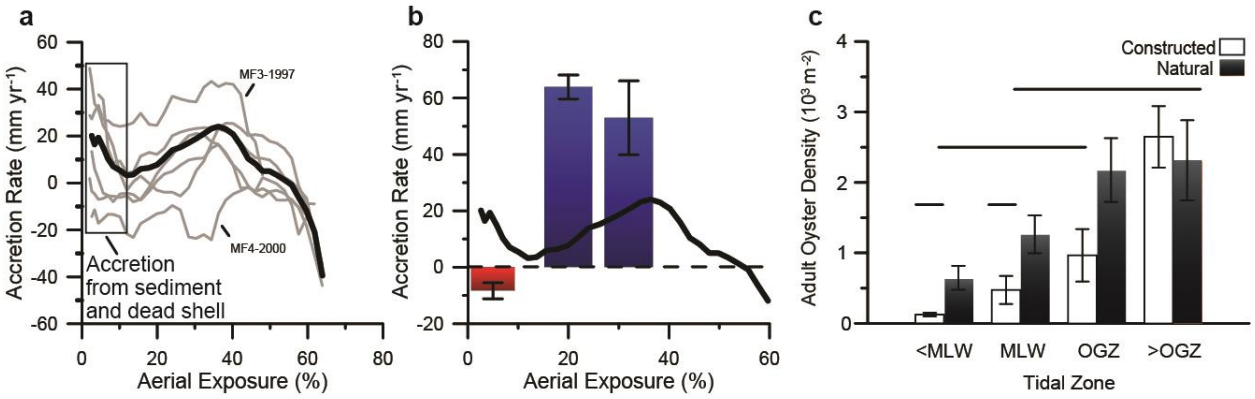

Figure 1.2 Analysis of oyster-reef growth and density over an aerial exposure gradient. (**a**) Mean vertical accretion rates by aerial exposure for decade-old constructed oyster reefs in Back Sound, North Carolina. Thick black line represents the mean vertical accretion rate from 2010 to 2012 for five of the decade-old reefs, excluding reef MF4-2000, which was heavily fished during the study period. (**b**) Bars represent the growth of newly constructed oyster reefs from 2011 (date of origin) to 2014 (mean ± standard error). Red and blue bars indicate loss and accretion respectively. Thick black line is the mean vertical accretion rate from the decade-old constructed reefs (from **a**). (**c**) Average adult oyster densities for natural (black) and constructed (white) reefs divided into four intertidal zones (mean ± standard error). The four zones include: below mean low water (<MLW), from MLW to 20% aerial exposure (MLW), the optimal-growth zone (OGZ, encompassing 20-40% aerial exposure), and above the OGZ (from 40% to approximately 60% aerial exposure). Tiered horizontal bars represent statistical similarity ($\alpha = 0.05$).

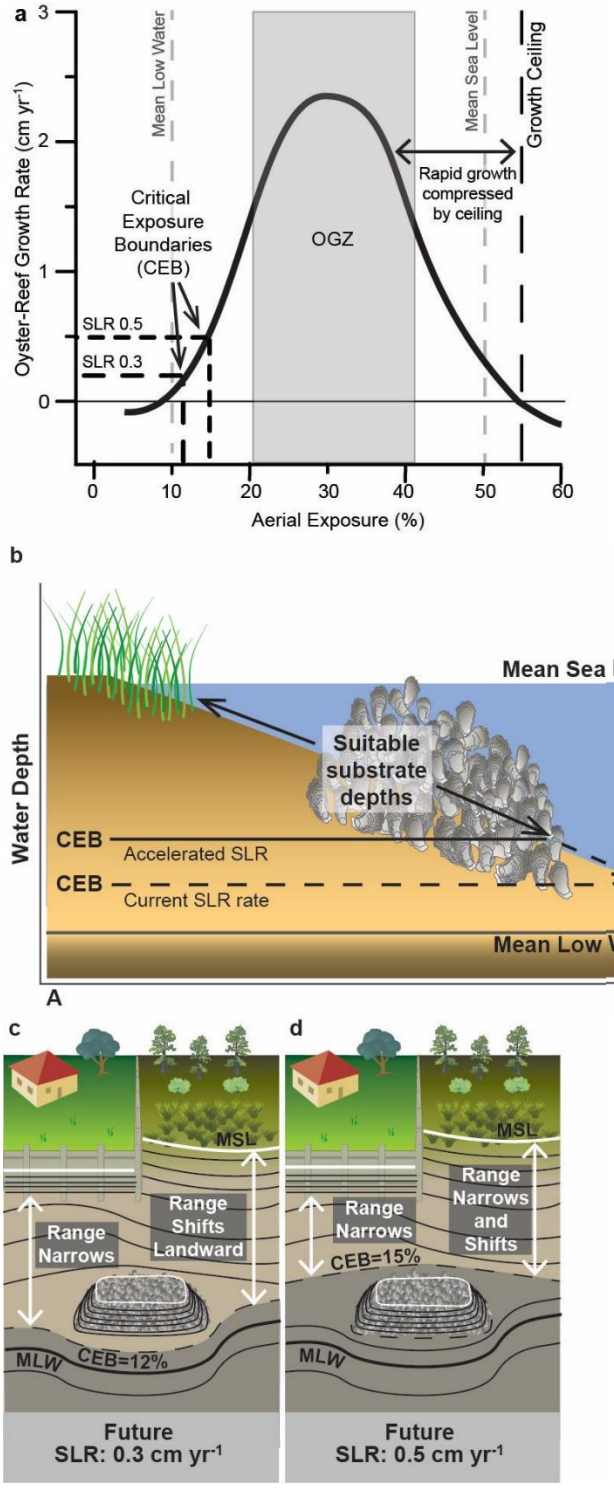

Figure 1.3 Modeling oyster-reef growth with aerial exposure and considering accelerations in SLR through time. (**a**) Greatest oyster-reef growth occurs at exposures between 20-40% (optimal-growth zone, OGZ) and returns to zero at 55% (growth ceiling) and 10% (mean low water). Critical-exposure boundaries (CEBs) represent reef growths in equilibrium with rates of local sea-level rise (0.3 cm yr^{-1} or 0.5 cm yr^{-1}). (**b**) Suitable substrate (unshaded), or range of viable habitat, for oyster reef development on developed and natural (retreating marsh) shorelines at initial time (Present) with a conceptual model of changing suitable substrate depths with reference to how differing rates of SLR will immediately change the CEB (SLR: 0.3 cm yr^{-1}, SLR: 0.5 cm yr^{-1}) along transect A-A′. For example, an oyster reef developing at 13% exposure can grow and persist at current rates of SLR, whereas an acceleration in SLR (0.5 cm yr^{-1}) will result in the reef growth rate falling farther beneath the CEB (**a**) as sea levels rise at a faster rate than reef growth, leading to the reef's eventual failure. (**c-d**) Future changes in suitable substrate (unshaded) with CEBs considering SLR rates of 0.3 cm yr^{-1} (no change; **c**) and 0.5 cm yr^{-1} (accelerated; **d**). Future projections assume that nearshore sedimentation is not keeping pace with SLR. The range of suitable substrate depths will narrow against a developed shoreline, whereas natural shorelines will allow oyster reefs to shift shoreward (**c**). However, accelerations in SLR will raise the CEB, overall narrowing the range of suitable substrate depth regardless of the shoreface configuration (**d**). Incorporated symbols courtesy of the Integration and Application Network, University of Maryland Center for Environmental Science (ian.umces.edu/symbols/).

REFERENCES

Arkema, K. K. *et al.* 2013. Coastal habitats shield people and property from sea-level rise and storms. *Nat. Clim. Chang.* 3, 913–918.

Bahr, L. M. & Lanier, W. P. in *The ecology of intertidal oyster reefs of the South Atlantic Coast: a community profile*. Ch. 3-4, 37-62 (U.S. Fish and Wildlife Service, 1981).

Barbier, E. B. *et al.* 2011. The value of estuarine and coastal ecosystem services. *Ecol. Monogr.* 81, 169–193.

Beck, M. W. *et al.* 2011. Oyster Reefs at Risk and Recommendations for Conservation, Restoration, and Management. *Bioscience* 61, 107–116.

Borsje, B. W. *et al.* 2011. How ecological engineering can serve in coastal protection. *Ecol. Eng.* 37, 113–122.

Cheong, S.-M. *et al.* 2013. Coastal adaptation with ecological engineering. *Nat. Clim. Chang.* 3, 787–791.

Chu, F.-L. E., La Peyre, J. F. & Burreson, C. S. 1993. Perkinsus marinus infection and potential defense-related activities in Eastern Oysters, Crassostrea virginica: salinity effects. *J. Invertebr. Pathol.* 62, 226–232.

Coen, L. D., Luckenbach, M. W., & Breitburg, D. L. 1999. The role of oyster reefs as essential fish habitat: A review of current knowledge and some new perspectives. *Am Fish S S* 22, 438-454.

Connell, J. H. 1972. Community Interactions on Marine Rocky Intertidal Shores. *Annu. Rev. Ecol. Syst.* 3, 169–192.

Costanza, R. *et al.* 1997. The value of the world's ecosystem services and natural capital. *Nature* 387, 253–260.

DeAlteris, J. T. 1988. The Geomorphic Development of Wreck Shoal , a Subtidal Oyster Reef of the James River , Virginia. *Estuaries* 11, 240–249.

Fodrie, F. J. *et al.* 2014. Classic paradigms in a novel environment: inserting food web and productivity lessons from rocky shores and saltmarshes into biogenic reef restoration. *J. Appl. Ecol.* 51, 1314–1325.

Grabowski, J. H. & Peterson, C. H. 2007. Restoring oyster reefs to recover ecosystem services in *Ecosystem Engineers: Concepts, Theory and Applications*, (eds., Cuddington, K., Byers, J.

E., Wilson, W. G., & Hastings, A.) Elsevier/Academic Press, Netherlands. Ecosystem Engineers: Concepts, Theory and Application. Netherlands, Elsevier/Academic Press. pp. 281-298.

Grabowski, J. H. *et al.* 2012. Economic Valuation of Ecosystem Services Provided by Oyster Reefs. *Bioscience* 62, 900–909.

Grabowski, J. H., Hughes, A. R., Kimbro, D. L. & Dolan, M. A. 2005. How Habitat Setting Influences Restored Oyster Reef Communities. *Ecology* 86, 1926–1935.

Halpern, B. S. *et al.* 2008. A global map of human impact on marine ecosystems. *Science* 319, 948–52.

Hargis, W. J. & Haven, D. S. in *Oyster reef habitat restoration: a synopsis and synthesis of approaches* (eds. Luckenbach, M. W., Mann, R. & Wesson, J. A.) Ch. 23, 329–358 (Virginia Institute of Marine Science Press,1999).

IPCC. in *Climate Change 2014: Impacts, Adaptation and Vulnerability - Contributions of the Working Group II to the Fifth Assessment Report of the Intergovernmental Panel on Climate Change* (eds. Field, C. B. et al.) 1–32 (Cambridge University Press, 2014). doi:10.1016/j.renene.2009.11.012

Jackson, J. B. C. *et al.* 2001. Historical overfishing and the recent collapse of coastal ecosystems. *Science* 293, 629–37.

Johnson, K. D. & Smee, D. L. 2014. Predators influence the tidal distribution of oysters (Crassostrea virginica). *Mar. Biol.* 161, 1557–1564.

Kemp, A. C. *et al.* 2011. Climate related sea-level variations over the past two millennia. *Proc. Natl. Acad. Sci. U. S. A.* 108, 11017–22.

Kennedy, V. S., Newell, R. I. E. & Eble, A. F (Eds) 1996. *The eastern oyster Crassostrea virginica* Maryland Sea Grant College.

Kirby, M. X. 2004. Fishing down the coast: historical expansion and collapse of oyster fisheries along continental margins. *Proc. Natl. Acad. Sci. U. S. A.* 101, 13096–9.

La Peyre, M. K., Humphries, A. T., Casas, S. M. & La Peyre, J. F. 2014. Temporal variation in development of ecosystem services from oyster reef restoration. *Ecol. Eng.* 63, 34–44.

Lenihan, H. S. 1999. Physical – biological coupling on oyster reefs: how habitat structure influences individual performance. *Ecol. Monogr.* 69, 251–275.

Lenihan, H. S., Micheli, F., Shelton, S. W. & Peterson, C. H. 1999. The influence of multiple environmental stressors on susceptibility to parasites: an experimental determination with oysters. *Limnol. Oceanogr.* 44, 910–924.

Mann, R. & Powell, E. N. 2007. Why oyster restoration goals in the Chesapeake Bay are not and probably cannot be achieved. *J. Shellfish Res.* 26, 905–917.

Mann, R., Harding, J. M. & Southworth, M. J. 2009. Reconstructing pre-colonial oyster demographics in the Chesapeake Bay, USA. *Estuar. Coast. Shelf Sci.* 85, 217–222.

Menge, B. A. & Sutherland, J. P. 1987. Community Regulation: Variation in Disturbance, Competition, and Predation in Relation to Environmental Stress and Recruitment. *Am. Nat.* 130, 730–757.

Morris, J. T., Sundareshwar, P. V., Nietch, C. T., Kjerfve, B. & Cahoon, D. R. 2002. Responses of coastal wetlands to rising sea level. *Ecology* 83, 2869–2877.

Nicholls, R. J., Hoozemans, F. M. J. & Marchand, M. 1999. Increasing flood risk and wetland losses due to global sea-level rise: regional and global analyses. *Glob. Environ. Chang.* 9, S69–S87.

Peterson, C. H. & Lipcius. R. N. 2003. Conceptual progress towards predicting quantitative ecosystem benefits of ecological restorations. *Mar. Ecol. Prog. Ser.* 264: 297-307.

Piazza, B. P., Banks, P. D. & Peyre, M. K. La. 2005. The Potential for Created Oyster Shell Reefs as a Sustainable Shoreline Protection Strategy in Louisiana. *Restor. Ecol.* 13, 499–506.

Pontee, N. 2013. Defining coastal squeeze: A discussion. *Ocean Coast. Manag.* 84, 204–207.

Powers, S. P., Peterson, C. H., Grabowski, J. H., & Lenihan, H. S. 2009. Evaluating the success of constructed oyster reefs in no-harvest sanctuaries: implications for restoration. *Mar. Ecol. Prog. Ser.* 389: 159-170.

Rahmstorf, S. 2010. A new view on sea level rise. *Nat. Reports Clim. Chang.* 44–45. doi:10.1038/climate.2010.29

Rodriguez, A. B. *et al.* 2014. Oyster reefs can outpace sea-level rise. *Nat. Clim. Chang.* 4, 493–497.

Rothschild, B. J., Ault, J. S., Goulletquer, P., & Heral, M. 1994. Decline of the Chesapeake Bay oyster population: A century of habitat destruction and overfishing. *Mar. Ecol. Prog. Ser.* 111: 29-39.

Schulte, D. M., Burke, R. P. & Lipcius, R. N. 2009. Unprecedented restoration of a native oyster metapopulation. *Science* 325, 1124–8.

Scyphers, S. B., Powers, S. P., Heck, K. L. & Byron, D. 2011. Oyster reefs as natural breakwaters mitigate shoreline loss and facilitate fisheries. *PLoS One* 6, e22396.

Seavey, J. R., Pine, W. E., Frederick, P., Sturmer, L. & Berrigan, M. 2011. Decadal changes in oyster reefs in the Big Bend of Florida's Gulf Coast. *Ecosphere* 2, art114.

Taylor, J. & Bushek, D. 2008. Intertidal oyster reefs can persist and function in a temperate North American Atlantic estuary. *Mar. Ecol. Prog. Ser.* 361, 301–306.

Vitousek, P. M. 1997. Human Domination of Earth's Ecosystems. *Science* 277, 494–499.

White, M. E. & Wilson, E. A. in *The eastern oyster Crassostrea virginica* (eds. Kennedy, V. S., Newell, R. I. E. & Eble, A. F.) 559–580 (Maryland Sea Grant College, 1996).

Wilber, D. H. 1992. Associations between freshwater inflows and oyster productivity in Apalachicola Bay, Florida. *Estuar. Coast. Shelf Sci.* 35, 179–190.

Wilberg, M., Livings, M., Barkman, J., Morris, B. & Robinson, J. 2011. Overfishing, disease, habitat loss, and potential extirpation of oysters in upper Chesapeake Bay. *Mar. Ecol. Prog. Ser.* 436, 131–144.

Zu Ermgassen, P. S. E. *et al.* 2012. Historical ecology with real numbers: past and present extent and biomass of an imperilled estuarine habitat. *Proc. R. Soc. / Biol. Sci.* 279, 3393–400.

CHAPTER 2: SALT MARSH AND FRINGING OYSTER REEF TRANSGRESSION IN A SHALLOW TEMPERATE ESTUARY: IMPLICATIONS FOR RESTORATION, CONSERVATION AND BLUE CARBON[2]

2.1. Introduction

Climate change poses a significant threat to coastal ecosystems with the expectation of increased flooding with sea-level rise (SLR) and storms. Low relief coastal environments are highly susceptible to erosion and inundation from accelerating SLR and storms, as well as anthropogenic stressors like increased development and boat wakes. While many developed areas use hardened structures to protect their shorelines in the form of bulkheads and rock revetments, there has been a movement to utilize more natural methods, such as living shorelines. Living shorelines exploit the innate ability of natural habitats (e.g., oyster reefs and salt marsh) to dissipate wave and current energy (Broome et al. 1992; Currin et al. 2010; Gedan et al. 2011; Gittman et al. 2014; Davis et al. 2015). Regaining lost shoreline habitats through restoration, which in many instances have been lost through development (salt marsh; Kennish 2001; Lotze et al. 2006) and exploitation of resources and/or disease (oyster reefs; Beck et al. 2011; zu Ermgassen et al. 2012), not only increases shoreline and property resistance to wave energy and resultant erosion but also enhances overall service delivery of the estuarine ecosystem (Coen et al. 2007; Grabowski and Peterson 2007).

[2] This chapter previously appeared as an article in *Estuaries and Coasts*. The original citation is as follows: Ridge, Justin T., Antonio B. Rodriguez, and F. Joel Fodrie. 2016. Salt Marsh and Fringing Oyster Reef Transgression in a Shallow Temperate Estuary: Implications for Restoration, Conservation and Blue Carbon. *Estuaries and Coasts*. 1–15. doi:10.1007/s12237-016-0196-8.

Tidal wetlands provide a number of ecosystem services, making them one of the most valuable ecosystems in the world (Costanza et al. 1997). Marsh grasses form expansive platforms along estuarine shorelines of low relief and elevation, providing a number of benefits for shores under pressure from SLR and storm waves. *Spartina alterniflora* can trap sediment by baffling current and wave energy (Leonard and Croft 2006) and significantly reduce wave height (~90% decrease) within 20 m of the marsh edge (Knutson et al. 1982). Marshes can be resilient to SLR because they have the ability to increase their elevation by augmenting belowground biomass (Cahoon et al. 2004), and they can exhibit greater productivity with increased inundation (Morris et al. 2002). However, Morris et al. (2002) also describe a threshold occurring near MSL where increased inundation will result in diminished marsh productivity, and rapid SLR could destabilize many marsh shorelines. This could result in major loss of marsh services along the estuarine coastline, including wave dampening, provision of essential fish habitat and carbon sequestration (Peterson and Turner 1994; Barbier et al. 2011; Murray et al. 2011; Moller et al. 2014).

More than 50% of wetlands have been lost in the US alone within the last century (Kennish et al. 2001, Lotze et al. 2006) from both natural and anthropogenic sources, with an estimated minimum global loss of 1-2% per year (Duarte et al. 2008). Along with coastal development of marshland, the combined pressure of accelerating SLR (Reed 1995; Nicholls et al. 2007; Craft et al. 2009) and sediment starvation (Syvitski et al. 2009) will lead to the eventual drowning of marshes along some coasts (Kirwan et al. 2010). An entire marsh platform can transform into a subtidal sand- or mud-flat environment as conditions change, and marsh-edge erosion is pervasive along both highly productive and degraded marshes, resulting in a decrease in area and associated ecosystem services.

Oyster reefs fringe many natural salt marshes, and are more resistant to erosion and positioned lower in the tidal frame than marsh platforms. With multiple stressors reducing the integrity of the marsh, the use of synergistic ecological engineering (Halpern et al. 2007; Milbrandt et al. 2015), like coupling oyster reef with marsh, is a viable coastal adaptation that should provide greater shoreline protection and stability (Cheong et al. 2013). This type of shoreline modification is applying the sequence of environments found naturally along many undisturbed, stable estuarine coastlines, encompassing subtidal sand- or mud-flat in the open bay to oyster reef and then marsh platform moving landward. The installation of substrates like oyster cultch (recycled shell) or other hard materials at the edge of vegetated habitats is commonly implemented with the expectation that a living reef will grow and protect the adjacent habitat edge from erosion. Increasing our understanding of the conditions that promote the vertical and lateral growth of reefs that fringe vegetated habitats and the subsequent evolution of the habitat boundary will better guide restoration practices for maximum return on investment in terms of time, money, and sustained shoreline protection. In addition, constraining the growth patterns and optimal growth conditions of fringing reefs will improve predictions of coastal landscape response to climate-induced changes to estuaries in the absence of intervention.

Oyster reefs are self-accreting structures through deposition of shell and biodeposits but are degraded at varying rates through predation, bioerosion, dissolution, and disturbance (Powell et al. 2006; Mann and Powell 2007; Powell and Klinck 2007; Green et al. 2009). Salinity and exposure to air during tidal cycles (aerial exposure) constitute two of the main controls on oyster reef growth (Baggett et al. 2015; Walles et al. 2016). Exposure provides a refuge from competition and predation in the high salinity lower estuary (Fodrie et al. 2015), while the fresher water of the upper estuary provides this refuge for reef growth deeper in the water

column. Oysters naturally colonize hard substrate located on sand or mudflats, isolated from other habitats (patch reefs), or along the distal edge of salt marshes (fringing reefs; Grabowski et al. 2005). Previous work examining intertidal oyster patch-reef growth has shown that, like marshes, oyster reefs have the capacity to grow at rates equal to or greater than present rates of SLR (Rodriguez et al. 2014; Ridge et al. 2015).

The proximity of a habitat with other structurally complex habitats can alter hydrodynamics (Borsje et al. 2011; Sharma et al. 2016a; Sharma et al. 2016b) as well as predator utilization along these habitat boundaries (Irlandi and Crawford 1997; Lewis and Eby 2002; Carroll et al. 2015). Oyster reefs may produce a shadow effect, attenuating hydrodynamic energy, reducing erosion and promoting expansion of adjacent vegetated habitats (Sharma et al. 2016a, Sharma et al. 2016b). However, reduced flow around the marsh-reef complex may decrease food delivery to oysters and allogenic sedimentation in both the reef and marsh. These interactions may ultimately result in diminished reef growth and marsh accretion, as well as changes in sediment composition within both habitats.

Vertical accretion and shoreline evolution are particularly important for carbon sequestration potential as marshes are considered a blue carbon habitat (Murray et al. 2011), capturing a disproportionately high amount of carbon compared to the global area they occupy (Chmura et al. 2003; Duarte et al. 2005). Theuerkauf et al. (2015) observed marsh shoreline erosion in North Carolina on the order of 0.65-0.76 m yr^{-1}. This process has resulted in total ravinement (loss to erosion) of carbonaceous marsh sediments spanning hundreds of years, highlighting the importance of carbon export explicitly through lateral erosion when modeling marsh carbon budgets (Theuerkauf et al. 2015). During transgression, the presence of a fringing oyster reef could change the ravinement process and preservation of marsh sediments. To better

understand fringing oyster reef development and the lateral trajectory of the marsh-reef boundary (and implications for the carbon-related storage services of marsh habitat), this study addresses three main questions: 1) Are fringing reefs following the same growth paradigm with regards to aerial exposure as observed on patch reefs (sensu Ridge et al. 2015)? 2) What is the trajectory of marsh-oyster reef boundaries (shorelines) in the Southeast US? and 3) What are the consequent implications for the carbon storage potential of these environments?

2.1.1. Conceptual model of estuarine shoreline evolution

The depositional environments that exist around marsh shorelines can evolve in a number of ways depending on the local hydrodynamics, sediment supply, and rate of SLR (Mariotti and Fagherazzi 2010, Fagherazzi et al. 2012, Fagherazzi et al. 2013, Kirwan et al. 2016; Fig. 2.1). The stratigraphy of coastal areas preserves a record of the trajectory of the boundary between depositional environments. Assuming a productive marsh platform and the absence of a fringing oyster reef, a salt marsh may grow laterally and/or vertically with adequate sediment supply and relatively low hydrodynamic energy and rates of local SLR (LSLR). Conversely, sediment starved areas can experience wave-induced shoreline erosion even without SLR. As a salt marsh shoreline erodes under conditions of increasing hydrodynamic energy and/or rapid SLR, salt marsh area is reduced and typically transformed into a subtidal sand- or mud-flat environment. Depending on the depth of wave- and current-induced erosion and thickness of the salt marsh, some marsh peat could be preserved under the new sandflat environment, retaining a portion of the buried carbon that accumulated in the past. Increasing the depth of erosion, or ravinement, and decreasing marsh thickness decreases the preservation potential of old marsh peat as the marsh edge transgresses.

A productive salt marsh platform fringed with oyster reef may have a different evolution under conditions of increasing hydrodynamic energy and/or accelerating SLR than the scenario described above, because an oyster reef is more resistant to erosion than the adjacent marsh. Under these conditions, the boundary between the fringing oyster reef and salt marsh could experience four different evolutionary responses, including: 1. regression, 2. stasis, 3. transgression, or 4. disconnection as the boundary between environments widens (Fig. 2.1). If the oyster reef dampens the hydrodynamic energy impacting the boundary and accretion of both environments is keeping up with the rate of LSLR, then the boundary will either regress and the marsh would expand over the oyster reef or the boundary will remain static as both environments accrete vertically. Alternatively, if the oyster reef does not sufficiently dampen the hydrodynamic energy impacting the boundary and accretion of both environments lags behind the rate of LSLR, then the boundary will either transgress, through the displacement of oyster reef on top of salt marsh, or the marsh edge will erode landward at a faster rate than the oyster reef, and the fringing reef will transform into a patch reef (disconnection).

2.2. Methods

2.2.1. Study site and reef selection

Back Sound and the North River Estuary, North Carolina, were chosen for the study because they contain natural and restored fringing oyster reefs (*Crassostrea virginica*) and salt marshes (*S. alterniflora*) that are experiencing edge erosion (Fig. 2.2). The marshes and oyster reefs included in the study are located around Middle Marsh (MM), North River Marsh (NRM), and Carrot Island (CI) (Fig. 2.2). Middle Marsh and North River Marsh are part of a relic flood tidal delta that formed approximately 4000-2000 years ago (Berelson and Heron 1985). It is an extensive network of salt marsh, tidal channels, natural and constructed oyster reefs, and

sandflats, many of which are occupied by seasonal seagrass beds. This area experiences a semidiurnal tide with a range of 0.9 m (U.S. Army Corps of Engineers 1976; Rodriguez et al. 2014) and salinities between 30-35 ppt.

Oyster-reef growth, and evolution of the reef-marsh contact were studied using natural and constructed reefs (Table 2.1). The natural fringing reefs and back-reef marshes examined were along straight portions of the marsh shoreline and along marsh headlands. The oyster reefs at marsh headlands were narrow (~10 m) and long extending (20-40 m) off the headland into the adjacent estuary (groin reefs). The other natural marsh-fringing reefs are oriented with their long axis parallel to the marsh shoreline extending ~100 m and 10 m in the along- and cross-shore directions, respectively. Constructed fringing reefs were built from recycled oyster shell placed at the edge of the salt marsh in 3 m x 5 m x 0.15 m boxes (long dimension oriented parallel to the marsh shoreline) around Middle Marsh in 1997 and 2000 (Grabowski et al. 2005) (Fig. 2.2).

2.2.2. Reef growth

Growth of natural and constructed fringing reefs were assessed using remote sensing and coring. Terrestrial laser scanning has proven to be a highly accurate method for measuring reef growth and elevation changes >1.4 cm (Rodriguez et al. 2014, Ridge et al. 2015). This method only works for areas exposed during a tidal cycle and data were collected during spring low tides when the maximum reef area was exposed. The natural and constructed fringing reefs were scanned twice between 2010 and 2015 using a RIEGL three-dimensional LMSZ210ii terrestrial laser scanner to create digital elevation models (DEM) from 600,000 to 1,000,000 laser returns spaced <1 cm apart. Point clouds were processed using RiSCAN Pro software (RIEGL LMS), extraneous points were removed using the MARS 7 software package (Merrick® Advanced Remote Sensing Software), and DEMs of the reefs were generated at a 5-cm grid-cell spacing

using Surfer 11 (Golden Software, Inc.) (Fig. 2.3). Reef grid cell elevations were subtracted from its second-scan counterpart to obtain elevation changes between measurements, then those differences were sorted into 2-cm elevation bins, based on the first scan for each bin, and averaged (i.e., mean vertical accretion for every 2-cm reef elevation bin across the entire surface of the reefs; Ridge et al. 2015). Intertidal elevations were converted to percent aerial exposure, or relative amount of time spent out of the water during an average tidal cycle, as described by Ridge et al. (2015), because aerial exposure is an important determinant of reef growth in the high-salinity seaward portions of estuaries (Walles et al. 2016). This provided fine-scale vertical growth measurements for determining if aerial exposure impacts the growth of fringing reefs similarly to patch reefs. All elevations are reported in reference to the North American Vertical Datum of 1988 (NAVD88).

To supplement the laser scan data, we took cores through the middle of 10 constructed reefs to coarsely measure reef growth from date of construction to 2010. Core locations were surveyed using a Real Time Kinematic Global Positioning System (RTK-GPS) to determine the exact elevations of the reef surface relative to mean sea level (MSL). To core the reefs, a 10-cm diameter aluminum pipe was driven into the surface using a jackhammer. In the lab, cores were split longitudinally, sectioned continuously in 5-cm increments from the top, photographed, and described. In addition to the date of oyster-reef construction, we used the distance between the reef surface and the top of oyster cultch shell to calculate vertical growth rates. The oyster cultch shell is morphologically distinct and easily discernable from new oyster growth because the cultch shell was sourced from subtidal oyster beds that have wider and thicker shells compared to the narrower thinner shells of intertidal reefs.

2.2.3. Live oyster and salt marsh density

Oyster density is an indication of oyster population, recruitment and survivorship, while size provides additional information on the age structure of a reef (Kraeuter et al. 2007). Along natural reefs, at least four transects running from the reef crest to base were spaced one meter apart. Each transect was divided into four zones down the reef slope, and a random sample was taken within each zone using a 0.06-m^2 quadrat. Quadrats were excavated to the depth that all living oysters were collected, typically where the reef became anoxic (Baggett et al. 2015). All plot elevations were recorded at the surface of the reef using the RTK-GPS. Along with oyster density, the shell heights of all oysters were measured to ascertain the number of adult oysters (>2.5 cm).

Marsh-grass densities were measured using a 0.25-m^2 quadrat at the farthest extent of grass adjacent to the fringing reef, the marsh platform levee, and the interior of the marsh (5-10 m from the levee). Stem heights of 10 grass blades were recorded within each plot. These measurements were also taken at 5 non-reef marsh sites for reference (Fig. 2.2).

2.2.4. Reef-marsh evolution

To assess the evolution of the reef-marsh interface, we collected a core transect perpendicular to the reef-marsh contact across 7 natural fringing-reef shorelines. Each transect is composed of four cores (10-cm aluminum pipe) collected at the seaward edge of the reef, at the reef crest, in the zone occupied by both living oysters and marsh grass, and in the marsh beyond the extent of living oysters. Using the RTK-GPS, we collected elevation profiles by walking from the bayward edge of the reef into the marsh to demark the boundaries and overlap of habitats. For reference, we also cored areas of marsh with no oyster occurring on the shoreline using two cores 1 m from the marsh edge in both directions. Concurrently, transects of push cores were taken at non-reef marsh sites progressing away from the marsh edge (furthest extent

of living grass) at 1-m intervals. This provided the thickness and extent of marsh sediments preserved following marsh shoreline retreat. We used the jackhammer method of collecting cores on the reef and some salt marshes were cored using a sledgehammer to drive the 10-cm diameter aluminum pipe into the subsurface.

Once taken, cores were processed similarly to the oyster-reef cores obtained to measure vertical reef growth. The similar depth of strata between adjacent cores indicates that what little compaction was introduced during the coring process (<5 cm, defined as the distance between the top of the core and the adjacent substrate measured before the core was extracted) is ubiquitous within and among the cores. For the natural reefs, we estimated the timing of first oyster colonization and lateral reef expansion, by obtaining Carbon-14 dates from shell fragments cut from the umbo of articulated oysters sampled at the base of reefs. Additionally, we radiocarbon dated marsh material collected just below the reef-marsh contact in the mid-reef core of two natural groin reefs (MM2 & NRM2). The National Ocean Sciences Accelerator Mass Spectrometry Facility at the Woods Hole Oceanographic Institution provided the radiocarbon ages. Ages were calibrated to years before present (AD 1950 = 0 BP) and calendar years at the 95.45% confidence interval (2 sigma) obtained by using the CALIB 7.1 program (Stuiver and Reimer 1993; Reimer et al. 2013).

2.2.5. Sedimentary analyses

Coastal depositional environments form distinct lithofacies, arranged in a vertical succession dictated by the evolution of an area through time with laterally shifting habitats. In addition to visual description, we measured grain size on each 5-cm section of the cores to aid in defining lithofacies. Samples were wet-sieved to separate the >2-mm size fraction, which was weighed. The remaining finer-grained sediment was dried, weighed, subsampled, and processed

through a Cilas 1180 laser particle-size analyzer to obtain a grain-size distribution from 0.04 to 2000 microns split into 100 bins.

Percent organic carbon in reef and marsh sediments was obtained using a combination of Loss on Ignition (LOI) and a Perkins-Elmer CHN analyzer. CHN analysis was conducted on 6-10 samples (< 2-mm size fraction) from most cores, and LOI was used on the > 2-mm size fraction for each sample. We also used LOI to further supplement this dataset from the remaining cores, which consisted of separately combusting sediments <2 mm and organic material >2 mm (mainly blades, stems and roots) at 550°C for 4 hours. A calibration (Craft et al. 1991) was applied to more accurately estimate the organic C content from organic matter combusted during LOI, making these results directly comparable and combinable with CHN data. Mean percent organic carbon (sediment + organics, mass by volume) was calculated for marsh strata in each core, and then averaged across sites for the interior marsh carbon inventory ($kg\ m^{-2}$). Next, using the dimensions of marsh sediment preserved below oyster reef obtained from the cross-sections, we calculated average carbon inventory below each study reef. Finally, prior to the formation of these fringing reefs, marsh shorelines likely stretched beyond the present extent of their preserved sediments, and we determined the percent carbon conserved at each shoreline using respective carbon inventories and the trapezoidal area bounded by the two oyster-reef cores with marsh sediments (cross sections) at relevant sites (MM2, MM3, and NRM2). Our study areas fall along the edges of historical aerial imagery, and the distance from reliable benchmarks for georectification make it difficult to reliably track shoreline changes at each of our sites. Therefore, for a conservative estimate of percent carbon preserved by the reefs, we assumed the greatest erosion scenario in that the current lateral extent of marsh sediment along eroding shores was once occupied by a fully formed marsh platform.

2.3. Results and Interpretation

2.3.1. Reef growth and density

Elevation measurements from the laser scans of the natural fringing reef (CI-1) yielded a parabolic growth response with elevation (Fig. 2.3), having the greatest growth (1.4 cm yr^{-1}) between 18% and 28% aerial exposure (-0.35 and -0.25 m NAVD88, respectively). Overall, the entire reef area examined exhibited growth, which dropped to <0.5 cm yr^{-1} at 10% (mean low water, MLW) and 52% exposure (-0.43 and -0.1 m NAVD88, respectively). Scans of the constructed fringing reef (SG3-1997) revealed a similar trend in the 3-yr time step, but in the first scan (2010), reef substrate only incorporated elevations up to -0.25 m NAVD88. Most of SG3-1997 experienced little or no growth (predominantly loss), with growth spiking at the highest elevations (Fig. 2.3A).

The cores from constructed reefs in Middle Marsh sampled the cultch surfaces of all but two reefs (SG3-2000 and SM1-1997) below MLW and the mean thickness of the reefs above the cultch were only 10.5 ± 5.7 cm (Mean ± SD). Thus, we observed the same pattern as the laser scanning results with little growth below MLW, based on the overall reef growth since their construction (mean growth rate of 0.89 ± 0.51 cm yr^{-1}). Greatest growth (20 cm or 2.0 cm yr^{-1}) occurred on constructed reef SG3-2000 (Fig. 2.3B), which had the highest cultch surface exposure (14%).

Adult oyster density increased with exposure, with greatest densities occurring near the tops of natural reefs around MSL (Fig. 2.4). Constructed fringing reefs mainly occupy areas at and below MLW, and oyster densities in those lower tidal-zone regions, while being less abundant, followed the pattern found on natural reefs.

Salt marsh density and average stem height between reef and non-reef sites were not significantly different (density: t = -0.966, df = 34, P = 0.34; height: t = 1.88, df = 34, P = 0.069; Appendix 2.1). Mean stem densities in non-reef and reef marshes were 128 ± 49.2 m^{-2} and 112 ± 50.2 m^{-2} (Mean ± SD), respectively, while mean stem heights were 48.2 ± 10.2 cm (non-reef) and 54.5 ± 9.93 cm (reef).

2.3.2. Sedimentary units and stacking patterns

Cores sampled the same three sedimentary units in all transects along natural shorelines. The deepest unit was a fine-grained silty sand (mean grain size ~150 μm) with less than 1% shell fragments. This unit was interpreted as a sandflat and is similar to the modern sandflat that exists throughout Middle Marsh. Above the sand flat, we sampled a carbonaceous muddy sand (mean grain size ~ 100 μm) to sandy mud (mean grain size ~50 μm) with abundant roots and stems of *S. alterniflora*. This unit was interpreted as salt marsh peat and extends below and in direct contact with all but the natural reef NRM1 (Fig. 2.5, Appendix 2.2). While older, deeper marsh sediments were uniformly muddy sand, inner marsh cores (Core 1 for each transect) all exhibited a fining upwards trend (the transition from coarse-dominant to fine-dominant sediment up core). Marsh cores closer to the reef (Core 2 of each transect) were sandier overall. In most transects, the marsh unit was continuous and thickened toward the reef-marsh boundary.

Oyster reef strata were composed of >15% shell with sandy mud or muddy sand filling the pore space, and the taphonomically active zone (zone of living oysters) having between 80-98% shell with relatively open pore space. Similar to the marsh cores, reef cores exhibited a fining upwards trend in grain size. Laterally, reefs experienced a midpoint peak thickness and thinned toward both the sandflat and salt marsh boundaries. The maximum thickness of the reefs

varied, with the groin reefs MM2 and NRM2 being the thickest reefs sampled (0.6 m and 0.85 m thick, respectively).

Radiocarbon dates from the deepest section of North River reef NRM2 revealed the reef first formed 110-208 cal yr BP (~1819 AD). Dates from the base of the Middle Marsh reef MM2 suggested it formed after 1950 AD (Fig. 2.5), and aerial photography from the United States Department of Agriculture (USDA) in 1958 indicated that a smaller precursor reef was present. For both groin reefs, MM2 and NRM2, dates taken up the slope of the reef-marsh contact demonstrated that these reefs expanded over the marsh after 1950. Similar to NRM2, shell material from CI-1 showed the reef was as old as 65-211 cal yr BP (~1877 AD).

Preservation of the marsh sediment under the study reefs reached 5-15 m from the farthest extent of living marsh (Figs. 2.5,2.6), while marsh sediments at all non-reef sites were completely absent at some distance within 5 m of the marsh edge (Fig. 2.6). Interior marsh cores had an average soil carbon density of 0.0208 ± 0.004 g C cm^{-3} and organic carbon inventory of 12.5 ± 2.41 kg C m^{-2} (average of four cores and standard deviation). Carbon inventories for marsh sediments below reefs ranged from 0.382 to 9.72 kg m^{-2} among individual cores and reef sites with an overall average below-reef inventory of 5.29 ± 2.69 kg C m^{-2} and soil carbon density of 0.0199 ± 0.007 g C cm^{-3}. The natural low-relief fringing reefs, MM3 and MM4, yielded average below-reef marsh carbon inventories of 3.50 ± 2.37 kg C m^{-2} and 1.81 ± 2.01 kg C m^{-2}, respectively (averages of two cores each). Marsh sediments under the high-relief fringing reef, MM1, contained 8.27 kg C m^{-2} (one core), while the marsh sediments below the groin reefs NRM2 and MM2 contained 7.44 kg C m^{-2} (one core) and 5.44 ± 3.78 kg C m^{-2} (three cores), respectively.

To calculate the percent carbon preserved by the reefs during transgression, we used a conservative date for oyster-reef presence on the marsh shorelines (1950 AD, modern by radiocarbon analysis). This meant the marsh platform would have been approximately 15-cm lower at historical rates of LSLR (2.8 mm yr^{-1}, Beaufort, NC, NOAA Tides and Currents, Station ID 8656483). The corresponding interior marsh core at each site was used to estimate the potential carbon within the hypothetical marsh platform bounded by the relevant oyster cores. Compared to the current extent of buried marsh sediment and corresponding carbon inventories, carbon preservation under reefs MM3, NRM2, and MM2 equaled 22.2%, 28.3%, and 58.4%, respectively. Just relating the interior marsh cores to cores taken within the reef-marsh interface indicated that an average of 64.4% ± 13.4% (standard error) was capped by the transgressing reef.

2.4. Discussion

2.4.1. Reef growth

Natural fringing reefs appear to be following a parabolic exposure-growth curve, with a peak in reef growth between MLW and MSL. This growth pattern follows previous fine-scale examinations of constructed intertidal patch-reef growth, which exhibited a parabolic growth pattern with greatest rates occurring in the mid-low intertidal (optimal growth zone, OGZ; Ridge et al. 2015) with zero-growth boundaries forming near MLW and MSL (growth ceiling). However, unlike constructed patch-reef growth curves, the natural fringing reef exhibited growth lower in the tidal range, from 15-30% as opposed to the 20-40% previously described. It also experienced net accretion across all elevations sampled, only decreasing to 3.9 mm yr^{-1} around MLW and 2.3 mm yr^{-1} near MSL, roughly the rate of local LSLR (2.8 ± 0.37 mm yr^{-1}). This inconsistency may indicate that natural reef growth behaves differently than constructed reef

growth due to a variety of factors. Growth may manifest differently with varying levels of reef maturity (Rodriguez et al. 2014). The fringing reef's location adjacent to salt marsh may impact the growth curve due to flow modification (Leonard and Croft 2006) and/or predator accessibility and behavior (Irlandi and Crawford 1997; Lewis and Eby 2002; Carroll et al. 2015). While proximity to the marsh would not change the tidal exposure-elevation gradient, baffled flow near the marsh could reduce food delivery, and the higher elevations of the reef nearer the marsh edge may experience increased predation. This reef may have also experienced a different aerial exposure regime during this study period than the elevation-exposure calibration we derived from Middle Marsh water levels earlier in 2011 as a result of annual fluctuations in sea level between 2012 and 2015, with annual mean sea level changing ± 4 cm between years (Beaufort, NC, Mean Sea Level Trends; NOAA Tides and Currents, Station ID 8656483). Because the tidal range in this area is just below a meter, each centimeter change in water level would correspond to a shift of slightly more than one percent aerial exposure when referencing our baseline water level data. A 4-cm drop in water level could explain the OGZ appearing at 15% aerial exposure instead of 20% when compared to the same 2011 baseline water levels.

Constructed fringing reefs in Middle Marsh are experiencing little to no growth, and in some instances, substantial elevation losses as the substrate is slowly redistributed (e.g. the abundant loss on SG3-1997, Fig. 2.3). The scanned constructed reef (SG3-1997) experienced a growth peak at its highest elevation (26% exposure). While that peak did occur within the previously defined OGZ for constructed patch reefs (Ridge et al. 2015), the critical exposure boundary (the depth at which growth is equivalent to LSLR) of this constructed fringing reef also falls within the previously defined OGZ. Therefore, from a restoration standpoint, it appears that

the optimal placement of material along some marsh shorelines could be defined by an even narrower depth range than previously suggested from examining patch reefs.

In comparison to constructed patch reefs in Middle Marsh (Rodriguez et al. 2014; Ridge et al. 2015), many of these constructed fringing reefs were placed lower in the tidal range, with much of their surface below MLW (Figs. 2.3,2.4). A detailed inspection of the shell material within each core section (Appendix 2.3) reveals that the "growth" displayed by most of these reefs is only a cluster of oysters that spans one to two generations. When we exclude the taphonomically active zone (zone of living oysters), which is the top 5-10 cm of each core, the only reef that showed growth is SG3-2000. Reef SG3-2000 was the only constructed-fringing-reef site where cultch material was placed near the OGZ, which further supports the paradigm that reef material placed too low in the water column will not produce a prolific reef in lower estuarine systems.

Oyster recruitment, growth and survival collectively mediate oyster-reef accretion rates, and therefore, oyster density should generally be correlated with reef accretion. Adult oyster density in both natural and restored fringing reefs matched the observed reef-growth pattern, increasing growth with exposure, except at the highest elevations of the reef (> OGZ), where oyster densities were high but growth rates were low. These areas of the reef near MSL are most likely older sections of the reef that have been confined by the growth ceiling (~55% aerial exposure in this area). Over time, oyster recruitment within the interstitial space has increased density (Fig. 2.4) while oyster growth is still being limited by desiccation stress. Most of the restored fringing reefs included in this study fall on the deeper end of the growth spectrum and thus have markedly lower densities than the more mature, natural fringing reefs.

It is possible that the constructed-reef locations along marsh shorelines, which did not have substantial natural oyster reefs prior to cultch placement, are not suitable for reef development due to factors other than aerial exposure. Recent work has indicated that some shorelines may be unsuitable for oyster reef growth due to high wave exposure (Theuerkauf et al. 2016). Flow and sedimentation, which were not measured here, have been used to model reef development (Jordan-Cooley et al. 2011; Housego and Rosman 2015), primarily for subtidal oyster reefs. Flow has a major influence on the growth and condition of oysters (Grizzle et al. 1992; Lenihan et al. 1996; Lenihan 1999), and the baffling of flow around the marsh may inhibit food delivery to oysters and increase sediment deposition. Several studies (MacKenzie 1981; Colden and Lipcius 2015) have linked sedimentation to oyster mortality, and studies conducted by Lenihan (1999), Taylor and Bushek (2008), and Colden and Lipcius (2015) found that sediment burial could be detrimental to reef development. Solomon et al. (2014) found that sedimentation was positively correlated with increased inundation in the intertidal; thus, low flow and high sedimentation could explain why the constructed reef SM1-1997, which was placed just above MLW but in a very sheltered area, still exhibited little growth (Fig. 2.3). This coupled with the high growth of SG3-2000, which had the greatest cultch material thickness (i.e. highest relief; Appendix 2.3), may indicate that the importance of flow and sedimentation with relation to subtidal reef height (Lenihan 1999; Schulte et al. 2009; Jordan-Cooley et al. 2011) could be applicable to intertidal reefs. While it is possible that we are witnessing a localized effect, these data still support the need for proper siting of oyster restoration projects.

2.4.2. Reef-marsh evolution

Core transects revealed that most of the natural fringing reefs in Back Sound are in a state of transgression (Fig. 2.1, Response C), as old marsh sediment was found beneath 5 of the 7

natural reefs studied. Radiocarbon dating of marsh-sandflat contacts from around Back Sound indicates that marsh grass colonized and fully occupied intertidal sandflats as early as the 16th century (Theuerkauf et al. 2015). The increased rate of SLR during the last two centuries combined with anthropogenic disturbances have driven marsh area loss along our coasts (Nicholls et al. 1999). Lateral retreat of marsh shorelines in response to these changes in estuarine conditions is associated with some degree of ravinement of old marsh sediment from waves and currents. Prior to oyster-reef formation, it is likely that the areal extent of the marsh platform extended seaward. This assumption is supported by core transects across marsh shorelines in this study that sampled marsh below oyster reef (Fig. 2.6) and other research conducted in nearby areas (Mattheus et al. 2010; Theuerkauf et al. 2015) that showed over 20 m of shoreline erosion since 1958 (the oldest, discernable shoreline from aerial photographs). In places of eroding marsh, the non- or sparsely-vegetated, shoreface may have provided an intertidal surface for deposition of shell material allowing reefs to gain a foothold. Radiocarbon dating of basal oysters from three reefs suggests these reefs occupied their present position within the last 200 years, and dates obtained from the reef/marsh sediment contact in cores 3 and 4 of the natural groin reef MM2 (Fig. 2.5) show that transgression has primarily happened within the last century.

Grain-size data reinforce that the upper portions of the marsh sediment column were eroded prior to- or during transgression of the fringing oyster reef. Cores from the marsh interior show that basal marsh sediment is sandy, and this old marsh was deposited during initial colonization of the sandflat, when allogenic marsh sediment was being sourced from the surrounding sandflats. As the marsh accreted and increased in areal extent, the allogenic sediment source transitioned from the adjacent sandflat to the finer grains suspended in the water

column, demonstrated by the fining upwards sequence present in interior marsh cores. This process is mirrored in the oyster reefs, with the pore space in less developed reefs being predominantly filled with sandy allogenic sediment. Pore space of the higher relief, mature reefs is fining upward (Fig. 2.5). The tops of those reefs are now disconnected from the adjacent sandflat and pore space is primarily being filled with fine-grained sediments, likely biodeposits of oyster feces and pseudofeces. Marsh sampled below the oyster reefs show the same fining upward sequence as the interior marsh cores, but upper muddy marsh sediment is thinner than what was sampled in the marsh interior, and we interpret the difference in thickness between the interior marsh and the marsh preserved below the oyster reef being due to ravinement processes.

Cores taken within the transition area between the marsh and oyster reef (Core 2 in most transects) display a sandier marsh unit throughout except in the high-relief natural reefs MM1 and MM2. This is most likely due to the reconnection of allogenic sediment sourcing from the adjacent sandflat as the shoreline retreated, and probably further mixed by bioturbation from burrowing organisms. The siltier mid-transect cores (Core 2) from MM1 and MM2 are likely due to the fringing reefs being more mature with greater vertical relief than other sites. The mature fringing reefs reduced the connection of the marsh with the adjacent sandflat, protecting that marsh sediment from reworking through exposure to erosive forces. This provides further evidence that larger reefs with higher relief exhibit enhanced protection of the shoreline.

At the point of reef maturation, when the reef reaches its growth ceiling, the transition zone between reef and marsh reaches peak stabilization. The ravinement of marsh sediment has been reduced or halted as seen in MM1 and MM2, but it is unlikely that the reef-marsh transition zone will remain static with both habitats accreting at the same rate. Rather, it is more likely that the reef will consolidate as it intrudes into the marsh and increased oyster density crowds out the

marsh grass as rising sea level elevates the growth ceiling and the transition zone transgresses. In many cases, it is improbable that the rate of oyster reef transgression would supersede upland migration of the marsh, but in instances where the marsh cannot traverse the upland boundary, or has no upland to expand upon (Middle Marsh), this will result in the loss of the marsh platform area over time, gradually decreasing its carbon sequestration potential.

2.4.3. Carbon reservoir

Marsh-carbon inventories from our study sites (both interior marsh and below reef) were the same magnitude as inventories obtained in nearby salt marshes (5-8 kg C m^{-2}, Theuerkauf et al. 2015). These values are also equivalent to carbon inventories observed in Florida in middle and high marsh areas (10 ± 5 kg C m^{-2}) but less than low marsh observations (25 ± 4 kg C m^{-2}) (Choi and Wang 2004). Likewise, our soil-carbon densities from interior marsh and below the reefs were on the low end of the marsh-carbon density spectrum (see review in Chmura et al. 2003).

Ravinement of the marsh shoreline results in export of stored carbon to the estuary that can far outweigh the marsh's capacity to trap carbon (Theuerkauf et al. 2015). Fringing reefs, regardless of morphology, did not impact marsh grass density or overall stem height (Appendix 2.1), and thus the natural hardening of the shoreline by oyster reefs is principally responsible for mitigating the depth of ravinement and consequent loss of carbonaceous marsh sediment. This study indicates that, from a fringing reef's inception, it can preserve a quarter to half the carbon stored within an eroding marsh shoreline. These percent preservation values are conservative, because it is possible that the marsh was already eroded prior to oysters colonizing the shoreline, which would increase the relative percent carbon preserved by the reefs. In the process of a reef growing vertically and laterally along the marsh edge, erosion of marsh sediments was likely

reduced correspondingly to the maturity of the reef. This is further evidenced by the cores taken within the habitat overlap (the reef-marsh interface), which indicate that nearly two-thirds of the marsh carbon is being preserved under recently transgressed areas; the highest preserved carbon values being in the reefs with the greatest relief.

No marsh sediment was preserved >5 m bayward of the marsh edge at reference sites where no oyster reef was present, indicating total ravinement of carbonaceous sediments. When compared to the annual rate of carbon being lost from nearby eroding marsh sites without oyster reefs (annual shoreline retreat: 0.65 m; average carbon inventory: 6.79 kg C m^{-2}; Theuerkauf et al. 2015), carbon preservation under the reefs MM1 and MM2 is equivalent to approximately 1.5 and 18.9 years of unimpeded marsh erosion, respectively (6.70 ± 7.16 yr, average for all sites). This presents a new view of how reefs can help enhance ecosystem services of marshes, by preserving buried marsh carbon during transgression. This process is likely occurring throughout the Southeastern US and other parts of the world where oyster reefs fringe wetland environments.

Beyond capping carbonaceous marsh sediments, there still remains the question of what role oyster reefs play in estuarine carbon budgets. It has been speculated that reefs can act as carbon sinks (Peterson and Lipcius 2003; Grabowski and Peterson 2007), although there is a lack of empirical evidence to support this postulation. As seen in the marsh, finer sediments (silts and clays) are generally richer in organic carbon, and the fine sediments trapped in the pore space of upper sections of mature reefs may be evidence for the reef's capacity to trap large amounts of carbon within the reef matrix. However, most of that carbon is likely allogenic, and it is yet to be determined if this burial is enough to offset overall reef respiration and the CO_2 produced during the calcification process (Ware et al. 1992).

2.5. Conclusions

Salt marshes and oyster reefs are highly threatened habitats but are crucial components to a coastal landscape that has experienced alarming changes since the end of the 19th century (Beck et al. 2001; zu Ermgassen et al. 2012). This study demonstrates that marsh shorelines in central North Carolina, and likely other locations along the Southeast coast of the US, are in a general state of retreat and that fringing oyster reefs naturally transgress these habitats. Natural fringing oyster reefs exhibit a similar pattern of growth to highly productive constructed patch reefs, having a peak in growth occurring between MLW and local MSL, and we have also shown that constructing fringing reefs above MLW in lower estuaries is important for promoting reef growth. As reefs mature, they not only slow marsh retreat but also preserve buried marsh carbon during transgression. Careful consideration of tidal placement and hydrodynamic conditions will help promote growth of constructed reefs, and coupled restoration and preservation of reef and marsh environments will help ensure prolonged ecosystem functioning in impacted estuaries.

Table 2.1 Description of study reefs and sampling conducted on each.

			Sampling Methods			
Reef	**Type**	**Vertical Relief†**	**Laser Scan**	**Core**	**Core Transect**	**Density**
Natural Reefs						
MM1	Fringing	High		X	X	X
MM2	Groin	High		X	X	X
MM3	Fringing	Low		X	X	X
MM4	Fringing	Low		X	X	X
NRM1	Disconnect	High		X	X	
NRM2	Groin	High		X	X	X
CI-1	Fringing	High	X	X	X	X
Constructed Reefs						
SG3-1997	Fringing	Low	X	X		X
SG3-2000	Fringing	Low		X		X
SM1-1997	Fringing	Low		X		X

†Low relief fringing reefs are less than 0.25 m in vertical relief, while high relief reefs are greater than 0.25 m in vertical relief

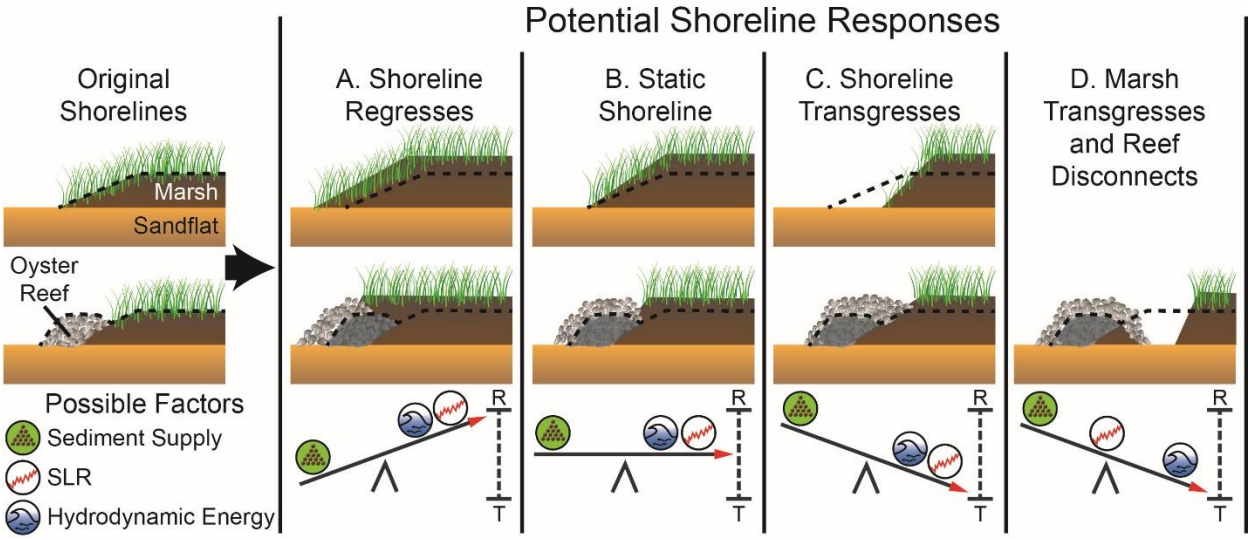

Figure 2.1 Potential responses of marsh shorelines with and without adjacent oyster reefs to an increase in relative sea level, considering relative sediment supply and local hydrodynamic energy. The dashed black line represents the original shoreline at Time 1. Within each shoreline response, a combination of possible factors is included along a fulcrum to illustrate how their relative contributions will impact the balance between shoreline regression (R) or transgression (T). For example, the shoreline response A. Shoreline Regresses can occur when sediment supply offsets the impact of SLR and/or hydrodynamic energy. As another example, response D. Marsh Transgresses and Reef Disconnects may occur when hydrodynamic energy far outweighs sediment supply, regardless of the rate of SLR.

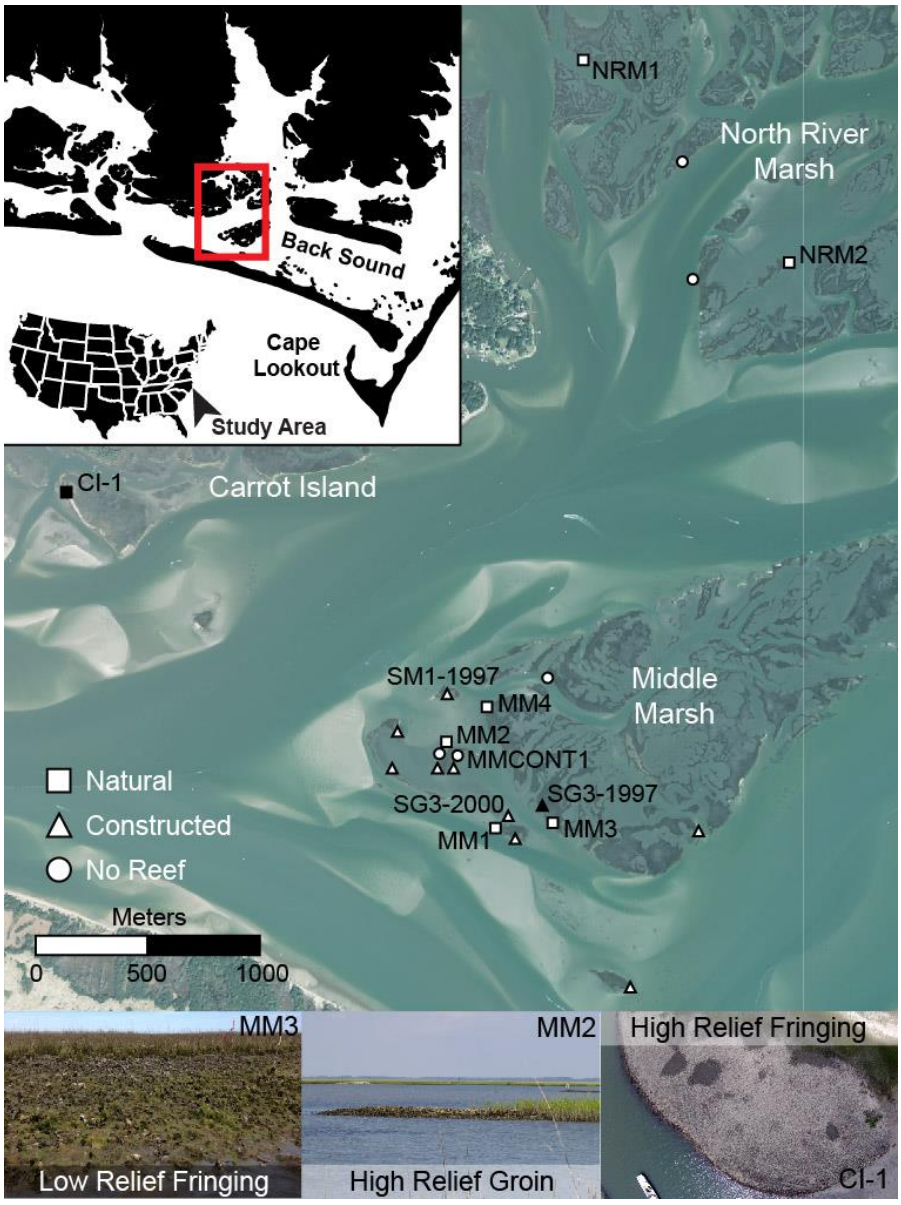

Figure 2.2 Study area map of Back Sound and North River Estuary in North Carolina. Marsh sites with reefs (natural and constructed) and without reefs are indicated with symbols. Black filled symbols represent reefs that were scanned using terrestrial lidar. All reef sites were cored and oyster densities sampled. Labels are placed at sites mentioned in the text.

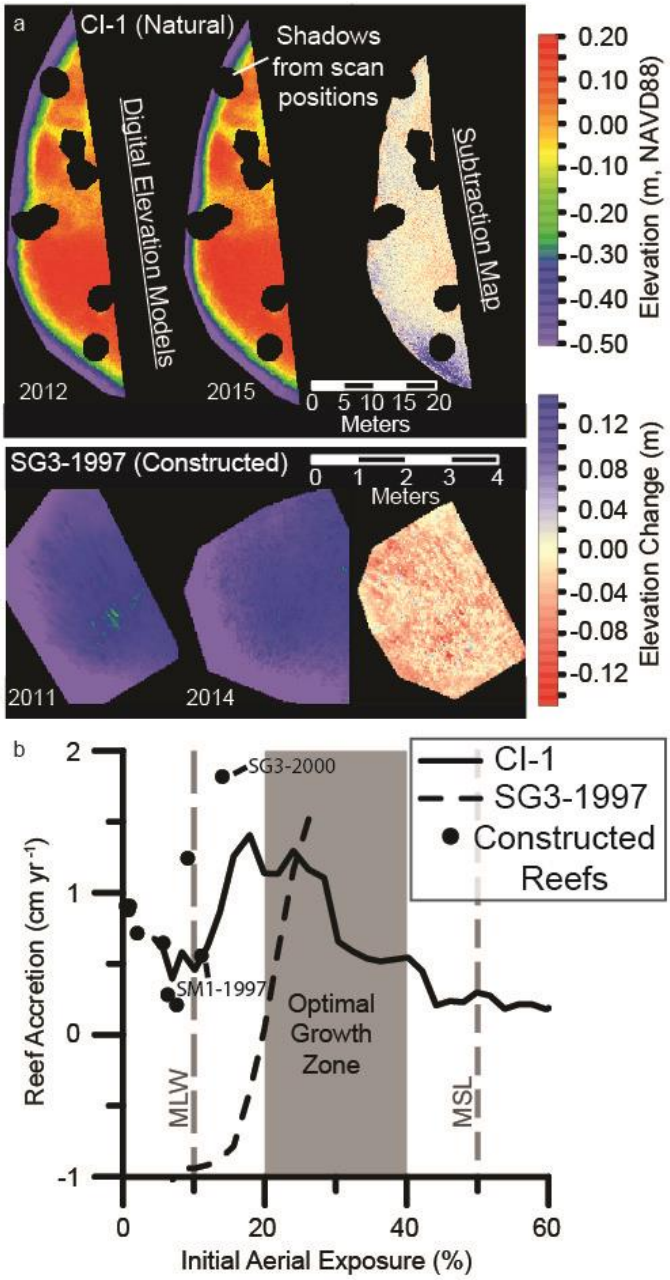

Figure 2.3 Growth of natural and restored fringing oyster reefs. a) Digital elevation models (DEMs) constructed from laser scans of natural (CI-1) and restored fringing reefs (SG3-1997). Subtraction maps (right panels) denote elevation change between the two scans. Holes on maps represent scan shadows with insufficient data to accurately construct the DEMs. **b**) Mean vertical growth rate across a natural fringing oyster reef (CI-1, solid line) and constructed fringing oyster reef (SG3-1997, dotted line) based on consecutive laser scans and binned by the aerial exposure of initial scan. Dots represent growth rates of constructed oyster reefs based on core data and plotted by the initial aerial exposure of the cultch shell surface at construction. Mean low water (MLW) occurs at 10% aerial exposure, and the Optimal Growth Zone (OGZ) spans 20-40% aerial exposure as established in Ridge et al. 2015.

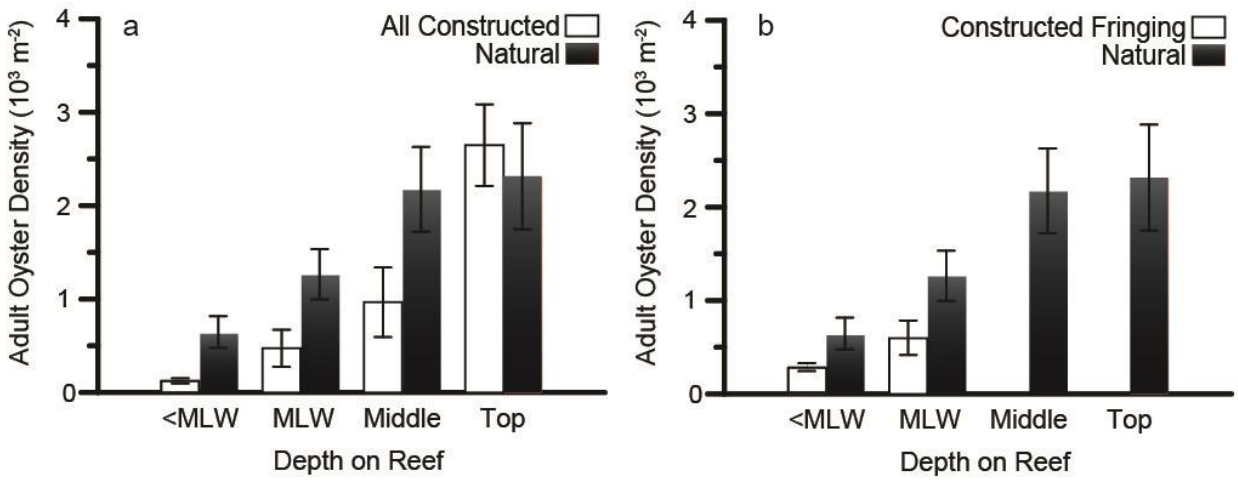

Figure 2.4 Adult oyster densities on natural and constructed reefs. a) Natural and Middle Marsh constructed reefs (adapted from Ridge et al. 2015) and **b**) comparing constructed fringing reefs with natural reefs. Elevation-exposure bins for depths on reef include <MLW (<10% exposure), MLW (10-20% exposure), Middle (20-40% exposure), and Top (>40% exposure).

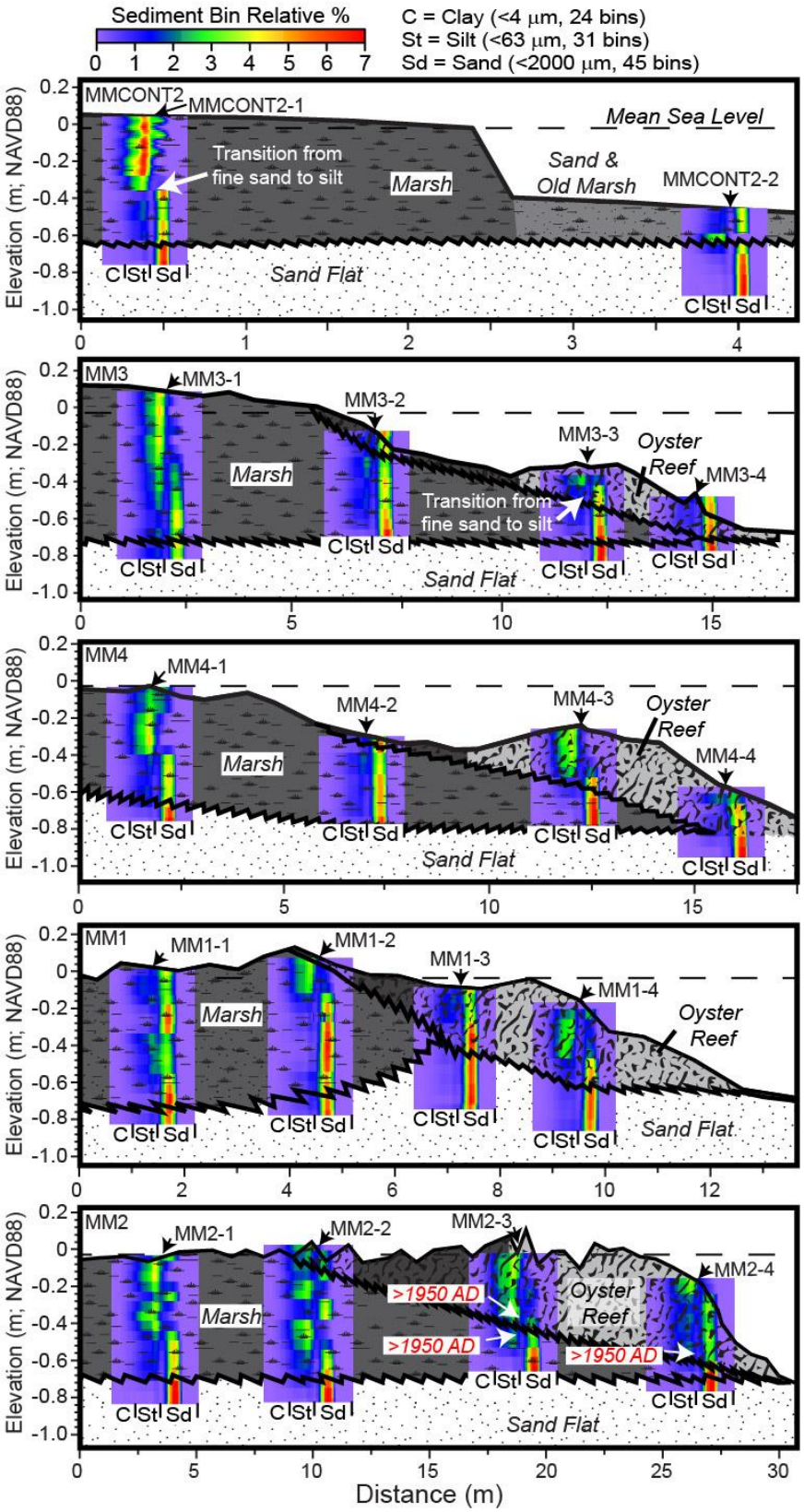

Figure 2.5 Cross sections of five study sites with corresponding grain size color maps from labeled cores. Shaded oyster reef represents units that are mix oyster and marsh sediments (overlap of living marsh and oyster). Radiocarbon dates are labeled in red with arrows pointing to approximate depths sampled. Grain size composition with depth was transformed into a colored grid using a relative percentage histogram of the 100 grain size bins. Within each color map, the y-axis corresponds to the core depth embedded in the cross-section, and the x-axis is divided into the 100 grain size bins from 0.04 μm to 2000 μm. The x-axis has been subdivided into the grain size categories of Clay (C; < 4 μm), Silt (St; < 63 μm), and Sand (Sd; < 2000 μm) for ease of reference. Grain size maps exclude the gravel fraction (>2 mm) from each section, which is predominantly shell material in oyster reefs and plant material in the marsh sediments.

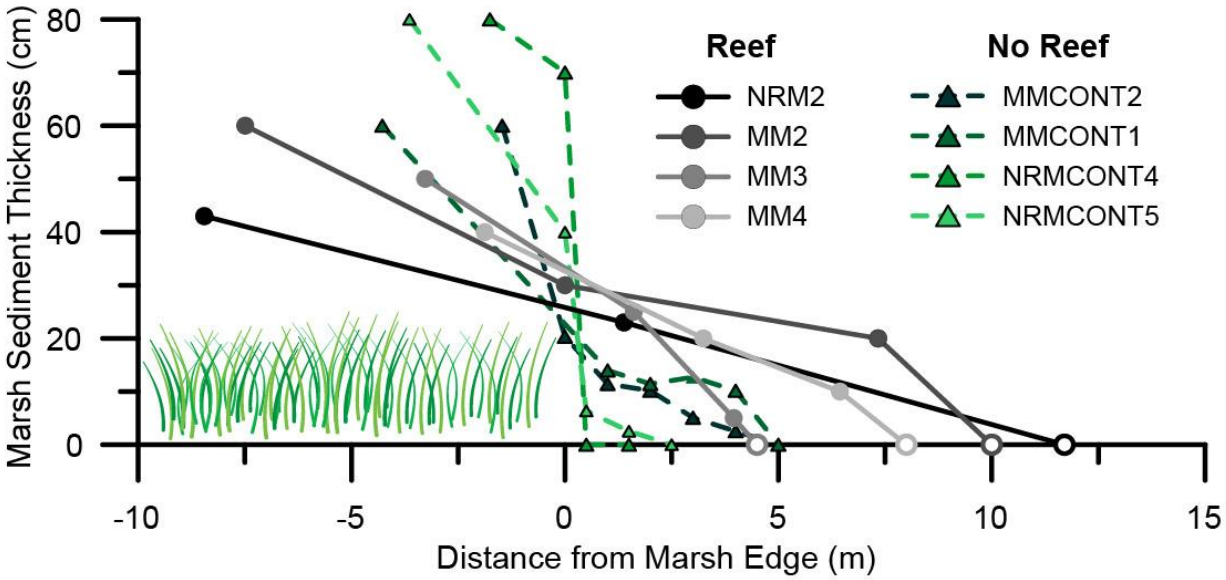

Figure 2.6 Preservation of marsh sediments in both oyster reef and non-reef shorelines. Reef site data to the left of zero were obtained from cores taken in the overlapping zone of living oyster and marsh grass. Using the cross sections (Fig. 2.5), a midpoint value was chosen between the outermost core that sampled marsh sediment under the reef and the presumed extent of marsh sediment assuming the continuous depth of the marsh-sandflat contact (represented by the open circles along the x-axis).

REFERENCES

Baggett, Lesley P., Sean P. Powers, Robert D. Brumbaugh, Loren D. Coen, Bryan M. DeAngelis, Jennifer K. Greene, Boze T. Hancock, et al. 2015. Guidelines for evaluating performance of oyster habitat restoration. *Restoration Ecology* 23, 737–745. doi:10.1111/rec.12262.

Barbier, Edward B., Sally D. Hacker, Chris Kennedy, Evamaria W. Koch, Adrian C. Stier, and Brian R. Silliman. 2011. The value of estuarine and coastal ecosystem services. *Ecological Monographs* 81. Ecological Society of America, 169–193. doi:10.1890/0012-9615-81.2.169.

Beck, Michael W., Robert D. Brumbaugh, Laura Airoldi, Alvar Carranza, Loren D. Coen, Christine Crawford, Omar Defeo, et al. 2011. Oyster Reefs at Risk and Recommendations for Conservation, Restoration, and Management. *BioScience* 61, 107–116. doi:10.1525/bio.2011.61.2.5.

Beck, Michael W, Kenneth L Heck Jr, Kenneth W Able, Daniel L Childers, David B Eggleston, Bronwyn M Gillanders, Benjamin Halpern, et al. 2001. The Identification, Conservation, and Management of Estuarine and Marine Nurseries for Fish and Invertebrates. *BioScience* 51, 633–641.

Berelson, William M., and S. Duncan Heron, Jr. 1985. Correlations between Holocene flood tidal delta and barrier island inlet fill sequences: Back Sound-Shackleford Banks, North Carolina. *Sedimentology* 32, 215–222. doi:10.1111/j.1365-3091.1985.tb00504.x.

Bishop, Melanie J, and Charles H Peterson. 2006. Direct effects of physical stress can be counteracted by indirect benefits: oyster growth on a tidal elevation gradient. *Oecologia* 147, 426–33. doi:10.1007/s00442-005-0273-3.

Borsje, Bas W., Bregje K. van Wesenbeeck, Frank Dekker, Peter Paalvast, Tjeerd J. Bouma, Marieke M. van Katwijk, and Mindert B. de Vries. 2011. How ecological engineering can serve in coastal protection. *Ecological Engineering* 37, 113–122. doi:10.1016/j.ecoleng.2010.11.027.

Broome, Stephen W., Spencer M. Rogers, Jr., and Ernest D. Seneca. 1992. Shoreline erosion control using marsh vegetation and low-cost structures: Raleigh, N.C., North Carolina Sea Grant Program Publication UNC-SG-92-12.

Cahoon, Donald R, Mark A Ford, and Philippe F Hensel. 2004. Ecogeomorphology of *Spartina patens*-Dominated Tidal Marshes' Soil Organic Matter Accumulation, Marsh Elevation Dynamics, and Disturbance. *Coastal and Estuarine Studies* 59, 247–266.

Carroll, John M., John P. Marion, and Christopher M. Finelli. 2015. A field test of the effects of mesopredators and landscape setting on juvenile oyster, *Crassostrea virginica*, consumption on intertidal reefs. *Marine Biology* 162, 993–1003. doi:10.1007/s00227-015-2643-7.

Cheong, So-Min, Brian Silliman, Poh Poh Wong, Bregje van Wesenbeeck, Choong-Ki Kim, and Greg Guannel. 2013. Coastal adaptation with ecological engineering. *Nature Climate Change* 3, 787–791. doi:10.1038/nclimate1854.

Chmura, G L, S C Anisfeld, D R Cahoon, and J C Lynch. 2003. Global carbon sequestration in tidal, saline wetland soils. *Global Biogeochemical Cycles* 17, 12. doi:1111 10.1029/2002gb001917.

Chmura, Gail L. 2013. What do we need to assess the sustainability of the tidal salt marsh carbon sink? *Ocean and Coastal Management* 83, 25–31. doi:10.1016/j.ocecoaman.2011.09.006.

Choi, Yonghoon, and Yang Wang. 2004. Dynamics of carbon sequestration in a coastal wetland using radiocarbon measurements. *Global Biogeochemical Cycles* 18, 1–12. doi:10.1029/2004GB002261.

Coen, Loren D., Robert D. Brumbaugh, David Bushek, Ray Grizzle, Mark W. Luckenbach, Martin H. Posey, Sean P. Powers, and S. Gregory Tolley. 2007. Ecosystem services related to oyster restoration. *Marine Ecology Progress Series* 341, 303–307. doi:10.3354/meps341303.

Costanza, Robert, Ralph D'Arge, Rudolf de Groot, Stephen Farber, Monica Grasso, Bruce Hannon, Karin Limburg, et al. 1997. The value of the world's ecosystem services and natural capital. *Nature* 387, 253–260. doi:10.1038/387253a0.

Cowart, Lisa. 2009. Analyzing estuarine shoreline change in coastal North Carolina. Greenville, N.C., East Carolina University, M.S. thesis, 83 p.

Craft, Christopher, Jonathan Clough, Jeff Ehman, Samantha Joye, Richard Park, Steve Pennings, Hongyu Guo, et al. 2009. Forecasting the effects of accelerated sea-level rise on tidal marsh ecosystem services. *Frontiers in Ecology and the Environment* 7, 73–78. doi:10.1890/070219.

Currin, Carolyn A, W. Scott Chappell, and Anne Deaton. 2010. Developing alternative shoreline armoring strategies: the living shoreline approach in North Carolina. *in* Shipman, Hugh, Megan N Dethier, Guy Gelfenbaum, Kurt L Fresh, Richard S Dinicola, eds., 2010, Puget Sound Shorelines and the Impacts of Armoring—Proceedings of a State of the Science Workshop, May 2009: U.S. Geological Survey Scientific Investigations Report 2010-5254, p. 91-102

Davis, Jenny L., Carolyn A. Currin, Colleen O'Brien, Craig Raffenburg, and Amanda Davis. 2015. Living Shorelines: Coastal Resilience with a Blue Carbon Benefit. *PLoS ONE* 10, e0142595. doi:10.1371/journal.pone.0142595.

Duarte, Carlos M., Jack J. Middelburg, and Nina Caraco. 2005. Major role of marine vegetation on the oceanic carbon cycle. *Biogeosciences* 2, 1–8.

Duarte, Carlos M., William C. Dennison, Robert J. W. Orth, and Tim J. B. Carruthers. 2008. The Charisma of Coastal Ecosystems: Addressing the Imbalance. *Estuaries and Coasts* 31, 233–238. doi:10.1007/s12237-008-9038-7.

Fagherazzi, S., G. Mariotti, P. L. Wiberg, and K. J. McGlathery. 2013. Marsh collapse does not require sea level rise. *Oceanography* 26, 70–77. doi:10.5670/oceanog.2011.65.

Fagherazzi, Sergio, Matthew L Kirwan, Simon M Mudd, Glenn R Guntenspergen, Stijn Temmerman, John M Rybczyk, Enrique Reyes, Chris Craft, and Jonathan Clough. 2012. Numerical models of salt marsh evolution: Ecological, geormorphic, and climatic factors. *Review of Geophysics* 50, 1–28. doi:10.1029/2011RG000359.1

Fodrie, F. Joel, Antonio B. Rodriguez, Christopher J. Baillie, Michelle C. Brodeur, Sara E. Coleman, Rachel K. Gittman, Danielle a. Keller, et al. 2014. Classic paradigms in a novel environment: inserting food web and productivity lessons from rocky shores and saltmarshes into biogenic reef restoration. Edited by Shelley Arnott. *Journal of Applied Ecology* 51, 1314–1325. doi:10.1111/1365-2664.12276.

Gedan, Keryn B., Matthew L. Kirwan, Eric Wolanski, Edward B. Barbier, and Brian R. Silliman. 2011. The present and future role of coastal wetland vegetation in protecting shorelines: Answering recent challenges to the paradigm. *Climatic Change* 106, 7–29. doi:10.1007/s10584-010-0003-7.

Gittman, Rachel K., Alyssa M. Popowich, John F. Bruno, and Charles H. Peterson. 2014. Marshes with and without sills protect estuarine shorelines from erosion better than bulkheads during a Category 1 hurricane. *Ocean and Coastal Management* 102, 94–102. doi:10.1016/j.ocecoaman.2014.09.016.

Grabowski, Jonathan H., A. Randall Hughes, David L. Kimbro, and Margaret A. Dolan. 2005. How Habitat Setting Influences Restored Oyster Reef Communities. *Ecology* 86, 1926–1935. doi:10.1890/04-0690.

Grabowski, Jonathan H, and Charles H Peterson. 2007. Restoring oyster reefs to recover ecosystem services. In *Ecosystem engineers: concepts, theory and applications*, ed. K. Cuddington, James E. Byers, W. G. Wilson, and A. Hastings, 281–298. Amsterdam, Netherlands: Elsevier Academic Press.

Green, Mark A, George G Waldbusser, Shannon L Reilly, Karla Emerson, and Scott O'Donnell. 2009. Death by dissolution: Sediment saturation state as a mortality factor for juvenile bivalves. *Limnology and Oceanography* 54, 1037–1047.

Grizzle, Raymond E., Richard Langan, W. Huntting Howell, and W Huntting Howell. 1992. Growth responses of suspension-feeding bivalve molluscs to changes in water flow: differences between siphonate and nonsiphonate taxa. *Journal of Experimental Marine Biology and Ecology* 162, 213–228. doi:10.1016/0022-0981(92)90202-L.

Halpern, Benjamin S., Brian R. Silliman, Julian D. Olden, John F. Bruno, and Mark D. Bertness. 2007. Incorporating positive interactions in aquatic restoration and conservation. *Frontiers in Ecology and the Environment* 5, 153–160. doi:10.1890/1540-9295(2007)5.

Housego, Rachel M., and Johanna H. Rosman. 2015. A model for understanding the effects of sediment dynamics on oyster reef development. *Estuaries and Coasts* 39, 495–509. doi:10.1007/s12237-015-9998-3.

Irlandi, E. A., and M. K. Crawford. 1997. Habitat linkages: the effect of intertidal saltmarshes and adjacent subtidal habitats on abundance, movement, and growth of an estuarine fish. *Oecologia* 110, 222–230.

Jordan-Cooley, William C., Romuald N. Lipcius, Leah B. Shaw, Jian Shen, and Junping Shi. 2011. Bistability in a differential equation model of oyster reef height and sediment accumulation. *Journal of Theoretical Biology* 289, 1–11. doi:10.1016/j.jtbi.2011.08.013.

Kennish, Michael J. 2001. Coastal salt marsh systems in the U.S.: A review of anthropogenic impacts. *Journal of Coastal Research* 17, 731–748.

Kirwan, Matthew L., Glenn R. Guntenspergen, Andrea D'Alpaos, James T. Morris, Simon M. Mudd, and Stijn Temmerman. 2010. Limits on the adaptability of coastal marshes to rising sea level. *Geophysical Research Letters* 37, L23401. doi:10.1029/2010GL045489.

Kirwan, Matthew L., Stijn Temmerman, Emily E. Skeehan, Glenn R. Guntenspergen, and Sergio Faghe. 2016. Overestimation of marsh vulnerability to sea level rise. *Nature Climate Change* 6, 253–260. doi:10.1038/nclimate2909.

Knutson, Paul L, Robert A Brochu, and William N See. 1982. Wave dampening in *Spartina alterniflora* marshes. *Wetlands* 2, 87–104.

Kraeuter, John N., Susan Ford, and Meagan Cummings. 2007. Oyster growth analysis: A comparison of methods. *Journal of Shellfish Research* 26, 479–491.

Lenihan, Hunter S. 1999. Physical-biological coupling on oyster reefs: How habitat structure influences individual performance. *Ecological Monographs* 69, 251–275. doi:10.1890/0012-9615(1999)069[0251:PBCOOR]2.0.CO;2.

Lenihan, Hunter S., Charles H. Peterson, and Jennifer M. Allen. 1996. Does flow speed also have a direct effect on growth of active suspension-feeders: an experimental test on oysters. *Limnology and Oceanography* 41, 1359–1366. doi:10.4319/lo.1996.41.6.1359.

Lenihan, H. S. 1999. Physical-biological coupling on oyster reefs: how habitat structure influences individual performance. *Ecological Monographs*, *69*(3), 251–275.

Leonard, Lynn A., and Alexander L. Croft. 2006. The effect of standing biomass on flow velocity and turbulence in *Spartina alterniflora* canopies. *Estuarine, Coastal and Shelf Science* 69, 325–336. doi:10.1016/j.ecss.2006.05.004.

Lewis, David and Lisa A. Eby. 2002. Spatially heterogeneous refugia and predation risk in intertidal salt marshes. *Oikos* 96, 119–129.

Lotze, Heike K., Hunter S. Lenihan, Bruce J. Bourque, Roger H. Bradbury, Richard G. Cooke, Matthew C. Kay, Susan M. Kidwell, Michael X. Kirby, Charles H. Peterson, and Jeremy B. C. Jackson. 2006. Depletion, degradation, and recovery potential of estuaries and coastal seas. *Science* 312, 1806–9. doi:10.1126/science.1128035.

MacKenzie, Clyde L. 1981. Biotic potential and environmental resistance in the American oyster (*Crassostrea virginica*) in Long Island Sound. *Aquaculture* 22, 229–268.

Mann, Roger, and Eric N. Powell. 2007. Why oyster restoration goals in the Chesapeake Bay are not and probably cannot be achieved. *Journal of Shellfish Research* 26, 905–917.

Mariotti, Giulio, and Sergio Fagherazzi. 2010. A numerical model for the coupled long-term evolution of salt marshes and tidal flats. *Journal of Geophysical Research: Earth Surface* 115, 1–15. doi:10.1029/2009JF001326.

Mattheus, Christopher R., Antonio B. Rodriguez, Brent A. McKee, and Carolyn A. Currin. 2010. Impact of land-use change and hard structures on the evolution of fringing marsh shorelines. *Estuarine, Coastal and Shelf Science* 88, 365–376. doi:10.1016/j.ecss.2010.04.016.

Milbrandt, E.C., M. Thompson, L.D. Coen, R.E. Grizzle, and K. Ward. 2015. A multiple habitat restoration strategy in a semi-enclosed Florida embayment, combining hydrologic restoration, mangrove propagule plantings and oyster substrate additions. *Ecological Engineering* 83, 394–404. doi:10.1016/j.ecoleng.2015.06.043.

Möller, Iris. 2006. Quantifying saltmarsh vegetation and its effect on wave height dissipation: Results from a UK East coast saltmarsh. *Estuarine, Coastal and Shelf Science* 69, 337–351. doi:10.1016/j.ecss.2006.05.003.

Möller, Iris, Matthias Kudella, Franziska Rupprecht, Tom Spencer, Maike Paul, Bregje K. van Wesenbeeck, Guido Wolters, et al. 2014. Wave attenuation over coastal salt marshes under storm surge conditions. *Nature Geoscience* 7, 727–731. doi:10.1038/ngeo2251.

Morris, James T., P. V. Sundareshwar, Christopher T. Nietch, Bjorn Kjerfve, and D. R. Cahoon. 2002. Responses of coastal wetlands to rising sea level. *Ecology* 83, 2869–2877. doi:10.1890/0012-9658(2002)083[2869:ROCWTR]2.0.CO;2.

Murray, Brian C, Linwood Pendleton, W. Aaron Jenkins, and Samantha Sifleet. 2011. *Green Payments for Blue Carbon Economic Incentives for Protecting Threatened Coastal Habitats*. Durham.

Nicholls, R. J., P. P. Wong, V. Burkett, J. Codignotto, J. Hay, R. McLean, S. Ragoonaden, and C. D. Woodroffe. 2007. Coastal systems and low-lying areas. In *Climate Change 2007: impacts, adaptation and vulnerability. Contribution of Working Group II to the fourth assessment report of the Intergovernmental Panel on Climate Change*, ed. M. L. Parry, O.

F. Canziani, J. P. Palutikof, P. J. van der Linden, and C. E. Hanson, 315–356. Cambridge, UK: Cambridge University Press.

Peterson, Charles H., and Romauld N. Lipcius. 2003. Conceptual progress towards predicting quantitative ecosystem benefits of ecological restorations. *Marine Ecology Progress Series* 264, 297–307. doi:10.3354/meps264297.

Peterson, G. W., and R. E. Turner. 1994. The value of salt marsh edge vs interior as a habitat for fish and decapod crustaceans in a Louisiana tidal marsh. *Estuaries* 17, 235. doi:10.2307/1352573.

Powell, Eric N., Kathryn A. Ashton-Alcox, and John N. Kraeuter. 2006. How long does oyster shell last on an oyster reef? *Estuarine, Coastal and Shelf Science* 69, 531–542. doi:10.1016/j.ecss.2006.05.014.

Powell, Eric N., John M. Klinck, Kathryn Ashton-Alcox, Eileen E. Hofmann, and Jason Morson. 2012. The rise and fall of *Crassostrea virginica* oyster reefs: The role of disease and fishing in their demise and a vignette on their management. *Journal of Marine Research* 70, 505–558. doi:10.1357/002224012802851878.

Reed, Denise J. 1995. The response of coastal marshes to sea-level rise: Survival or submergence? *Earth Surface Processes and Landforms* 20, 39–48. doi:10.1002/esp.3290200105.

Reimer, Paula J., Edouard Bard, Alex Bayliss, J. Warren Beck, Paul G. Blackwell, Christopher Bronk Ramsey, Caitlin E. Buck, Hai Cheng, R. Lawrence Edwards, Michael Friedrich, Pieter M. Grootes, Thomas P. Guilderson, Haflidi Haflidason, Irka Hajdas, Christine Hatté, Timothy J. Heaton, Dirk L. Hoffmann, Alan G. Hogg, Konrad A. Hughen, K. Felix Kaiser, Bernd Kromer, Sturt W. Manning, Mu Niu, Ron W. Reimer, David A. Richards, E. Marian Scott, John R. Southon, Richard A. Staff, Christian S. M. Turney, Johannes van der Plicht. 2013. IntCal13 and Marine13 Radiocarbon Age Calibration Curves 0–50,000 Years cal BP. *Radiocarbon* 55, 1869-1887

Ridge, Justin T., Antonio B. Rodriguez, F. Joel Fodrie, Niels L. Lindquist, Michelle C. Brodeur, Sara E. Coleman, Jonathan H. Grabowski, and Ethan J. Theuerkauf. 2015. Maximizing oyster-reef growth supports green infrastructure with accelerating sea-level rise. *Scientific Reports* 5, 14785. doi:10.1038/srep14785.

Rodriguez, Antonio B, F Joel Fodrie, Justin T Ridge, Niels L Lindquist, Ethan J Theuerkauf, Sara E Coleman, Jonathan H Grabowski, et al. 2014. Oyster reefs can outpace sea-level rise. *Nature Climate Change* 4, 493–497. doi:10.1038/NCLIMATE2216.

Schulte, David M, Russell P Burke, and Romuald N Lipcius. 2009. Unprecedented restoration of a native oyster metapopulation. *Science* 325, 1124–8. doi:10.1126/science.1176516.

Sharma, Shailesh, Joshua Goff, Just Cebrian, and Carl Ferraro. 2016a. A hybrid shoreline stabilization technique: Impact of modified intertidal reefs on marsh expansion and nekton

habitat in the northern Gulf of Mexico. *Ecological Engineering* 90, 352–360. doi:10.1016/j.ecoleng.2016.02.003.

Sharma, Shailesh, Joshua Goff, Ryan M. Moody, Dorothy Byron, Kenneth L. Heck, Sean P. Powers, Carl Ferraro, and Just Cebrian. 2016b. Do restored oyster reefs benefit seagrasses? An experimental study in the Northern Gulf of Mexico. *Restoration Ecology* doi:10.1111/rec.12329.

Solomon, Joshua a., Melinda J. Donnelly, and Linda J. Walterst. 2014. Effects of Sea Level Rise on the Intertidal Oyster Crassostrea Virginica by Field Experiments. *Journal of Coastal Research* 68, 57–64. doi:10.2112/SI68-008.1.

Stuiver, Minze, and Paula J. Reimer. 1993. Extended ^{14}C database and revised CALIB 3.0 ^{14}C age calibration program. *Radiocarbon* 35, 215-230

Syvitski, James P. M., Albert J. Kettner, Irina Overeem, Eric W. H. Hutton, Mark T. Hannon, G. Robert Brakenridge, John Day, et al. 2009. Sinking deltas due to human activities. *Nature Geoscience* 2, 681–686. doi:10.1038/ngeo629.

Taylor, Jaclyn, and David Bushek. 2008. Intertidal oyster reefs can persist and function in a temperate North American Atlantic estuary. *Marine Ecology Progress Series* 361, 301–306. doi:10.3354/meps07429.

Theuerkauf, Ethan J., J. Drew Stephens, Justin T. Ridge, F. Joel Fodrie, and Antonio B. Rodriguez. 2015. Carbon export from fringing saltmarsh shoreline erosion overwhelms carbon storage across a critical width threshold. *Estuarine, Coastal and Shelf Science* 164, 367–378. doi:10.1016/j.ecss.2015.08.001.

Theuerkauf, Seth J, David B Eggleston, Brandon J Puckett, and Kathrynlynn W Theuerkauf. 2016. Wave exposure structures oyster distribution on natural intertidal reefs, but not on hardened shorelines. *Estuaries and Coasts*. doi:10.1007/s12237-016-0153-6.

U.S. Army Corps of Engineers. 1976. Morehead City Harbor, North Carolina. General Design Memo. Dept Army, Wilmington District, Wilmington, North Carolina.

Walles, Brenda, F. Joel Fodrie, Sil Nieuwhof, Oliver J. D. Jewell, Peter M. J. Herman, and Tom Ysebaert. 2016. Guidelines for evaluating performance of oyster habitat restoration should include tidal emersion: reply to Baggett et al. *Restoration Ecology* 24, 4–7. doi:10.1111/rec.12328.

Ware, John R., Stephen V. Smith, and Marjorie L. Reaka-Kudla. 1992. Coral reefs: sources or sinks of atmospheric CO_2? *Coral Reefs* 11, 127–130. doi:10.1007/BF00255465.

Zu Ermgassen, Philine S. E., Mark D. Spalding, Brady Blake, Loren D. Coen, Brett Dumbauld, Steve Geiger, Jonathan H. Grabowski, et al. 2012. Historical ecology with real numbers: past and present extent and biomass of an imperilled estuarine habitat. *Proceedings of the Royal Society / Biological Sciences* 279, 3393–3400. doi:10.1098/rspb.2012.0313.

CHAPTER 3: EVIDENCE OF EXCEPTIONAL OYSTER-REEF RESILIENCE TO FLUCTUATIONS IN SEA LEVEL[3]

3.1. Introduction

Climate change poses a significant threat to ecosystems across the globe with pronounced impacts to biogeography, manifesting most prominently at the edges of species ranges, near an organism's threshold tolerance to physicochemical or biotic controls. Changes to the environment along these boundaries could result in a variety of outcomes including species adaptations (Hoffman & Sgro 2011), changes to phenology (Edwards & Richardson 2004, Poloczanska *et al.,* 2013), range shifts (Davis & Shaw 2001; Chen *et al.,* 2011; Poloczanska *et al.,* 2013), community and trophic restructuring (Walther *et al.,* 2002, Edwards and Richardson 2004), and even localized extinction (Colwell *et al.,* 2008; Pinsky *et al.,* 2013). The magnitude of these responses will depend on an organism's sensitivity to the suite of environmental factors that may be undergoing change or the resultant altered biotic relationships, the rate at which the system is changing (Ackerly *et al.,* 2010), and the reaction time of the species to adapt.

The response and reaction time of various organisms to climate fluctuations is highly specific among different taxa. Conditions detrimental to fitness may occur if there is a notable lag in community response to climate alterations, as seen with forest communities and temperature (Bertrand *et al.,* 2011), or a species unable to shift correspondingly to the vector and acceleration at which an environmental variable, like temperature or average rainfall, is changing (Zhu *et al.,* 2011; Dobrowski *et al.,* 2013; Burrows *et al.,* 2014). The nature of environmental

[3] At time of dissertation submission, this chapter is currently under review in *Global Change Biology*.

shifts across geographic space means mobile organisms can respond more readily by migrating (Pinsky *et al.,* 2013), whereas sessile organisms must rely on adaptation, propagation and habitat modification to maintain their populations (Bertrand *et al.,* 2011). As many communities depend on the persistence of habitat-forming foundation species, it is crucial that these sessile ecosystem engineers keep pace with climate changes to sustain habitat area and quality.

Biogenic habitats are experiencing environmental change in a variety of forms, including temperature, precipitation/desertification, ocean acidification, and sea-level rise (SLR); all of which vary in rate geographically and can interact to cause complex responses in ecological communities as populations react differently (Tingley *et al.,* 2012). While many of these climatic factors shift laterally across a geographic space, SLR also presents change in the vertical, which is particularly important for developed coastal areas where infrastructure prevents upland migration. Intertidal and shallow-subtidal biogenic habitats exist in a narrow elevation range due to a combination of biophysical intolerance and interspecific interactions (Paine *et al.,* 1971; Bertness & Ellison 1987; Fodrie *et al.,* 2014). Fluctuations in sea level can represent a dramatic change to species that are relegated to intertidal zones, like saltmarshes and mangroves, because it changes the inundation time during a tidal cycle. The change in sea level may be significant compared to the overall range of elevations the organisms occupy. If these foundation species cannot maintain their surface elevations compared to relative SLR (RSLR, the combination of eustatic sea-level rise and local shifts to continental crust), they will become imperiled by the stress of saltwater submergence, which could result in a loss of their supported communities and associated ecosystem services (Kirwan & Megonigal 2013; Lovelock *et al.,* 2015).

While sea level along the coast of the United States is generally rising 2-6 mm yr^{-1}, it fluctuates significantly from year to year, seasonally, and even on shorter timescales (weeks to months). These changes can range from 15-20 cm interannually with the most dramatic being greater than 30 cm (Morris et al. 2001, NOAA 2009, Sea Level Trends, NOAA Tides & Currents). Some of this variation is due to seasonal temperature and wind climate, but pronounced deviations may also arise with the complex interconnectivity of the North Atlantic Oscillations (NAO), prolonged or frequent storm activity, and sea-level anomalies linked to the strength of the Gulf Stream (Kolker & Hameed 2007; Sweet *et al.,* 2009; Ezer *et al.,* 2013; Goddard *et al.,* 2015; Ezer 2016). Losada *et al.* (2013) demonstrated that interannual shifts in sea level in other areas of the Atlantic Ocean can be on the order of 4-12 cm, with ENSO induced sea level shifts exceeding historical RSLR and an increased frequency in sea-level extremes occurring in recent decades. Short-term elevations in sea level are responsible for more frequent flooding along the U.S. East Coast (Ezer & Atkinson 2014) and increased coastal erosion (Theuerkauf *et al.,* 2014). These fluctuations in sea level may have a marked impact on coastal and estuarine habitats as their regularity and longevity are expected to increase (Ezer & Atkinson 2014).

The persistence of biogenic habitats, along with the critical services they provide to ecosystems and coastal infrastructure, is uncertain in the face of accelerated RSLR. Vegetated habitats (saltmarshes, mangroves, and seagrasses) alter their surface elevations through passive trapping of sediment from the water column, accumulation of annual aboveground biomass, and by augmenting belowground biomass forcing the sediment surface upwards (Morris *et al.,* 2002). Habitats constructed by invertebrates (e.g., coral reefs, oyster reefs, worm reefs) rely on individual growth and gregarious settlement to maintain their placement in suitable conditions,

with multiple generations building on one another. Given the range of accretion rates exhibited by these ecosystem engineers (Cahoon *et al.*,2006; Baustian *et al.*, 2012; Bhomia *et al.*, 2015; Perry *et al.*, 2015; Sasmito *et al.*, 2016), many will maintain their relative position with moderate rates of RSLR, while higher rates of RSLR may result in massive loss of coastal habitats along large geographic stretches due to drowning and compression against coastal infrastructure (Pontee 2013).

Oyster reefs are ubiquitous features within temperate and subtropical estuaries, spanning from the intertidal to subtidal zones depending on salinity and climate (Baggett *et al.*, 2015; Walles *et al.*, 2016). While oysters provide many important benefits to the ecosystem, populations are recovering from decimation during the last century (Beck *et al.*, 2011). Previous work examining intertidal oyster-reef growth indicates that constructed *Crassostrea virginica* reefs have a relatively high growth capacity compared to other coastal habitats (Rodriguez *et al.*, 2014), far outpacing any predicted rate of RSLR. However, growth rates are highly variable across reef-elevation gradients due to stress associated with exposure (desiccation) and submergence (competition and predation), with the reef crest and base exhibiting stunted or lack of growth (critical exposure boundaries) and the sides growing at the highest rate (optimal growth zone [OGZ], Ridge *et al.*, 2015) (Fig. 3.1). In the lower portions of estuaries, where salinities are typically greater than 30 ppt, *C. virginica* reefs cannot persist in the subtidal zone due to overwhelming predation and competition by species that are intolerant to exposure (Powers *et al.*, 2009, Fodrie *et al.*, 2014), indicating that transitioning from intertidal to subtidal conditions will place reefs that cannot keep pace with rising seas in peril (Ridge *et al.*, 2015). While oyster-reef growth patterns are well constrained over decadal scales, their sensitivity to changing sea levels over monthly to yearly timeframes is still relatively unknown. Considering

the degree to which sea level can fluctuate from weeks to months, understanding how the critical boundaries and OGZ will shift in response is necessary information for proper timing and siting of oyster restoration projects as well as assessing how future trends of RSLR will affect reef persistence, which in many estuaries is the only available hard substrate.

3.2. Materials and Methods

3.2.1. Study area

This study was conducted using *C. virginica* oyster reefs located in the Rachel Carson Research Reserve (North Carolina National Estuarine Research Reserve, NCNERR), Back Sound, North Carolina, USA (all reefs are within 2 km of 34.693007°N, 76.621709°W, see Fig. 3.2a). The area is comprised of channelized sandflats and marsh islands (*Spartina alterniflora).* Tides are semidiurnal with a mean range of 0.9 m and mean sea level at -0.03 m (all elevations reported in the North American Vertical Datum of 1988 [NAVD88]). Oyster reefs are predominantly intertidal in areas around Back Sound, occurring along marsh shorelines (fringing) or isolated on sandflats (patch).

3.2.2. Study design

Our study included an assortment of reefs of different ages (grouped into three "generations") ranging from 2 years to a century old (Fig. 3.2b). Constructed reefs ranged from 5-10 m in diameter, similar in size to many natural reefs in our study area, while the natural reef included in this study was one of the larger reefs locally, approximately 15 x 50 m (width x length). Constructed reefs began as mounds of loose, recycled oyster shell (cultch shell) measuring 3 x 5 x 0.15 m (width x length x height), followed by natural recruitment of oyster larvae from the estuary. Growth (cm yr^{-1}) of three reefs constructed over a decade prior (Grabowski *et al.*, 2005, hereafter "decade-old reefs"), including one reef constructed in 1997

and two in 2000, was measured from Spring 2010 to Spring 2012, and from Spring 2012 to Spring 2015 (Table 3.1, Fig. 3.3a). Growth of eleven reefs constructed in 2011 (hereafter "young reefs") and scanned each subsequent winter was measured over nearly a 1-year period in 2012 and nearly a 1-year period in 2013 (Table 3.1, Fig. 3.3a). Finally, growth of one natural reef nearly 100 years old (based on old nautical maps, hereafter "centennial reef") was calculated from 2012 to 2014 and from 2014 to 2015 (Table 3.1, Fig. 3.3a).

To examine fine-scale growth across oyster reefs, terrestrial lidar (Riegl LMSZ210ii laser scanner) was used to image reefs (Fig. 3.4). Reef-mapping with lidar required dry weather and a low spring tide, providing only a narrow operating window to scan a reef, which typically took an hour. As such, it sometimes required several days to several months to acquire all the scans of each reef generation, particularly in the case of the young reefs, which were numerous and widely separated (denoted by the bar widths in Fig. 3.3a). Within each reef generation, we collected scans during the same season and normalized the data to annual rates to avoid uneven seasonal influences across the time steps. The combination of RiSCAN Pro (Riegl) and Merrick Advanced Remote Sensing (MARS 7.1) software packages were used to extract ground points, which were then gridded (5-cm grid spacing) in Surfer 13 (Golden Software) using the Kriging algorithm to create digital elevation models (DEMs). Consecutive DEMs were subtracted, the resulting elevation change was linked to the corresponding grid-cell elevation from the initial DEM and those linked data were binned to determine average vertical change at 2-cm elevation bins across a reef (Fig. 3.4). Total volume change for each elevation bin was then calculated by multiplying the grid cell area (25 cm^2) by the total number of grid cells and average vertical change within a particular elevation bin. A portion of the centennial reef was excluded from the

growth analysis due to signs of heavy disturbance from harvesting and boat impacts along the adjacent tidal channel.

(MSL) data from a NOAA tide gauge (NOAA Tides & Currents Station ID: 8656483, Beaufort, North Carolina) located approximately 5 km northeast of the reefs. We used VDatum 3.6 (NOAA/NOS Vertical Datum Transformation) to transform monthly MSL data into elevations in the North American Vertical Datum of 1988 (NAVD88). Average sea level during scan periods was then calculated for each time step. Six-minute water level data were also queried from the Beaufort tide gauge and used to construct elevation-exposure histograms to predict the OGZ elevation range for each scan comparison. Local water salinity and temperature recorded in Back Sound by the North Carolina Coastal Reserves (North Carolina National Estuarine Research Reserve) during the study period were also examined by month to elucidate if patterns in reef growth were tied to changes in water quality. Using JMP v12 (SAS 2015), regression analyses were run on monthly mean water temperatures and salinity during the overall scan period (June 2010 – June 2015) to determine any trends in water quality beyond regular seasonal fluctuations. Additionally, data were transformed (cube transformation) to meet assumptions for parametric analysis and a series of t-tests were run to compare monthly mean water temperatures and salinities between scan periods within each reef generation.

3.3. Results

3.3.1. Water level and quality

Monthly MSL data from 2009 to 2015 indicate that sea level in the study area was -0.028 ± 0.062 m NAVD88 (mean ± standard deviation) (Fig. 3.3b). Prior to the start of scanning, the study area experienced prolonged levels of high water from frequent sea-level anomalies during the fall and winter of 2009-2010 that persisted for five months (Theuerkauf *et al.*, 2014). The

sea-level peak in 2009 corresponds to the November Mid-Atlantic nor'easter that spawned from the remnants of Hurricane Ida (deemed Nor'Ida). This peak in sea level was followed by relatively low water during 2010 and 2011. Prolonged periods of elevated monthly sea levels (above mean longer than 3 consecutive months) occurred during 2012, 2014, and 2015 (Fig. 3.3b, Table 3.2).

Water temperature consistently fluctuated seasonally during the study period (Fig. 3.3c), and mean monthly temperatures ranged from 5-30 °C with no significant trend during the study period (R^2 = -0.02, $F_{1,57}$ = 0.99, p = 0.33). Furthermore, all comparisons of water temperatures between scan periods within reef generations did not yield significant differences (Tables 3.2, Appendix 3.1). Overall, salinity declined during the study period (R^2 = 0.17, $F_{1,56}$ = 11.1, p = 0.0015). Prior to the first scan period, the area experienced a distinct drop in salinity with high water associated with Nor'Ida (winter 2009-2010). Subsequent drops in salinity occurred periodically during the scan periods, with the most pronounced declines coinciding with high water in late 2014 and low water in early 2015 (Fig. 3.3c). Comparisons of salinity between scan periods indicated significant decreases in salinity across time steps in both decade-old and young reefs, but only marginal significance (if $\alpha = 0.1$) in the centennial reef (Table 3.2, Appendix 3.1).

3.3.2. Reef growth

For the decade-old reefs, average sea level between the two periods increased approximately 4 cm from -0.053 m NAVD88 (averaged through Spring 2010-Spring 2012) to -0.016 m NAVD88 (average through Spring 2012-Spring 2015) (Fig 3.5a,b), with prolonged higher water during the warm seasons (April through September) of 2012 (0.004 m NAVD88) and 2014 (0.032 m NAVD88). Initial elevations (2010-2012) of the OGZ on decade-old reefs were positioned between -0.15 m and -0.30 m NAVD88 with growth peaking at 2 cm yr^{-1} (Fig.

3.5b, Table 3.2). From 2012 to 2015, the maximum-growth rate on these reefs remained at 2 cm yr^{-1}, but the zone of high growth expanded 34%, spanning the elevations from -0.05 m to -0.49 m NAVD88. The upper critical no-growth boundary, or growth ceiling, increased in elevation from -0.07 m to 0.05 m NAVD88, while the lower critical exposure boundary was not evident in the second time step, indicating growth over the entire reef surface. Greatest volume increases occurred within the OGZ during both time steps, yielding an average of nearly 0.04 m^3 yr^{-1} (Fig. 3.5c). Minor reef volume loss occurred at the reef crests during both time periods at nearly -0.01 m^3 yr^{-1}. The base of the decade-old reefs lost volume (-0.02 m^3 yr^{-1}) during the first time step, but regained it over the second (0.03 m^3 yr^{-1}).

Mean annual sea level during the 2012 and 2013 scan periods for the young reefs dropped 2.6 cm, from -0.017 m NAVD88 (averaged through Winter 2012-Winter 2013) to -0.043 m NAVD88 (averaged through Winter 2013-Winter 2014) (Fig. 3.6a). Over the course of 2012, young reefs experienced a maximum growth rate of 3.6 cm yr^{-1} at -0.23 m NAVD88 (Fig. 3.6b, Table 3.2). The following year, the OGZ shifted to a lower elevation with greatest growth (6.7 cm yr^{-1}) at -0.25 m NAVD88. These young reefs lack both the lower and upper critical exposure boundaries because they occupy shallower substrates than the decade-old reefs and have also not yet grown to sea level (i.e. filling the accommodation space). In terms of volume change, the young reefs accumulated the most volume at the base of the OGZ during each time step, increasing from 0.1 m^3 yr^{-1} to almost 0.3 m^3 yr^{-1} between the two time periods, a magnitude greater volume gain than the decade-old reefs (Fig. 3.6c)

With the centennial reef, mean sea levels over the two time periods increased 3.9 cm, from -0.021 m NAVD88 (averaged through June 2012-June 2014) to 0.018 m NAVD88 (averaged through June 2014-June 2015) (Fig. 3.7a). During the first time step (average sea

level), the centennial reef only exhibited growth between the elevations of -0.41 m to -0.09 m NAVD88, with losses of 2 cm yr^{-1} on top of the reef (Fig. 3.7b), and maximum growth (2.9 cm yr^{-1}) at -0.29 m NAVD88 (Table 3.2). The second time step (high sea level) revealed accretion over the entire elevation gradient as the OGZ shifted higher with maximum growth (4.4 cm yr^{-1}) at 0.01 m NAVD88. While sea levels and the predicted OGZ raised 4 cm in elevation, the upper growth boundary experienced an increase from -0.09 m to 0.13 m NAVD88 (22 cm). We also did not capture a lower critical boundary where growth dropped near zero, which is likely not resolvable because this reef extended below the water line during low tide. Reef volume gain during the first time step hovered just below 0.1 m^3 yr^{-1} within the OGZ (Fig. 3.7c). In contrast, the second time step had increasing volume change beginning in the OGZ and peaking (1.0 m^3 yr^{-1}) just above MSL.

3.4. Discussion

Changes in reef morphology and reef-wide growth were tightly aligned with month-to-year patterns in sea level (Figs. 3.5-7, Table 3.2). The magnitude and direction of these interannual fluctuations in sea level coincided with similarly scaled growth and erosion that manifested along reef profiles. When compared to other intertidal or shallow subtidal habitats such as salt marsh and mangrove (Cahoon *et al.,* 2006; Baustian *et al.,* 2012; Bhomia *et al.,* 2015; Perry *et al.,* 2015; Sasmito *et al.,* 2016), surface accretion across all reef generations exceeded the rates of accretion in other coastal biogenic habitats. Additionally, the predicted OGZ and growth ceiling, based on sea level during each scan-period, paralleled general growth trends across reefs of all ages, further supporting its use as a management tool in oyster reef conservation and restoration.

Variations in water quality did not appear to have a strong influence on reef growth, but fluctuations in salinity may be responsible for nonconformities in the expected growth pattern. Water temperatures over the entire study period did not display dramatic deviations that would explain differences in growth between years (Fig. 3.3c). Overall temperatures varied about a degree Celsius or less between scan periods, having cooler temperatures during the second time steps. Cooler temperatures would be associated with less growth in *C. virginica* (Dame 1972), which is contrary to our results, indicating that temperatures had little effect on how growth manifested on reefs. In contrast, salinity decreased throughout the entire study period, which could have impacted how growth manifested in deeper portions of the reef profiles. *C. virginica* is robust to fluctuations in salinity, and the range (15-36 ppt) is not outside of the Eastern oyster's tolerance (Shumway 1996). Salinities below 25 ppt may actually be more conducive for oyster growth, especially in subtidal waters (Walles *et al.*, 2016) where fresher water may hinder predators (e.g., gastropods) and competitors (e.g., macroalgae), which could explain high growth below the OGZ on the decade-old reefs after periods of pronounced lower salinity. Our study was not designed as a controlled experiment to control for a suite of abiotic and biotic factors. However, changes to biotic or abiotic influences, other than salinity, should generally impact the magnitude of growth profiles, rather than shifting growth curves upward or downward as we observed. For instance, increased thermal stress or disease should decrease the magnitude of a growth curve overall but not change the elevations associated with growth. The exceptions to this response would be those processes dictated by tidal-exposure stressors (e.g., desiccation, predation, competition, etc.), which shift correspondingly with sea level, reinforcing sea level as the primary control (and certainly the most parsimonious based on the available data).

3.4.1. Decade-old reefs

Distinct patterns of growth were exhibited by the decade-old reefs during the two sampling timeframes (Fig. 3.5) coinciding with shifts in sea level. The initial OGZ occurred in the mid-low intertidal with these reefs showing erosion above -0.07 m. Although the reefs extended above MSL (-0.03 m NAVD88) during the first time step, they predominantly experienced erosion across their plateaus between 2010 and 2012. Erosion was most likely the response of these reefs returning to equilibrium after a year of high water preceding the first scan (Fig. 3.3b). This would have temporarily increased the growth ceiling before waters returned to a lower stand, exposing the reef crest to higher desiccation stress and potentially greater foraging by avian predators, resulting in oyster mortality. Thus, it appears that while oysters cement together to create a solid reef matrix, oyster mortality within the taphonomically active zone (layer of living oysters) due to overexposure could compromise the outer reef structure, making it more susceptible to erosional forces. A similar process has been documented on coral reefs during extreme low tides (Anthony and Kerswell 2007), and it vertically mirrors dieback of marshes in response to long-term over inundation creating highly reduced soils (Koch *et al.,* 1990). We could also have witnessed a natural process of compaction within the reef. As multiple generations of oysters continue to build on one another, the structure of the reef matrix likely condenses and fills the empty cavities of once living oysters. During years of average or higher water, this process is likely compensated by oyster growth on the reef surface, and therefore only manifests as loss during periods of protracted low water.

For the decade-old reefs, mean sea level increased 3.7 cm between the two time steps with prolonged higher water during the winter of 2014-2015, which corresponds to increased growth at higher elevations on the reef as both the OGZ and growth ceiling shifted upwards (Fig. 3.5). Extended high water can benefit a reef by providing increased accommodation space, or

the space available for deposition that is usually controlled by sea level. This temporary increase in accommodation space is similar to how short (monthly) periods of high water have been shown to positively impact marsh communities (Morris *et al.*, 1990). While the average maximum growth remained at 2 cm yr^{-1}, the overall distribution of this growth encompassed nearly the entire elevation range of the reefs between 2012 and 2015. As there was not a drop in sea level during the time period that would have corresponded to growth lower on the reef than the initial OGZ, it remains to be determined why the lower reef elevations exhibited the same amount of accretion. It could be related to decreased poaching of oysters on the reef at this time; the lower edges of intertidal reefs are generally less consolidated, making it easier to harvest oysters. Lower reef growth could also be a trend linked to reef maturity, as older reefs have been shown to have greater densities of adult oysters at depth (Ridge *et al.*, 2015). It is also possible that prolonged periods of decreased salinity during the 2014-2015 winter could be responsible for some of the deeper-reef growth witnessed. Brackish water favors subtidal reef growth (Walles *et al.*, 2016) as it inhibits competition and predation. Therefore, the pronounced drops in salinity during the winter and spring of 2014-2015 could have fostered oyster growth in the shallow subtidal.

3.4.2. Young reefs

Elevations of growth maximums on young reefs also paralleled changes in sea levels (Fig. 3.6). Sea levels during 2012 were higher than the initial time step for the decade-old reefs, which resulted in an elevated OGZ. When sea levels dropped 2 cm in 2013, maximum growth also occurred 2 cm lower, doubling the average accretion rate while also increasing growth along deeper areas of these reefs. Young reefs appear to have the strongest response to sea-level changes, but this could be a result of our scan-period resolution isolating narrow time frames

with fairly distinct trends in sea level. Areas of the young reefs exhibited growth as high as 8-11 cm yr^{-1} after their construction in 2011 (Rodriguez *et al.,* 2014). The sustained high average growth across these reefs indicates they will only require 4-6 years to occupy the accommodation space and reach MSL. Volume changes on young reefs are an order of magnitude greater than the decade-old reefs because of the greater surface area located within the OGZ coupled with a much higher vertical accretion rate. This pattern of growth, two to three times greater than the decade-old reefs, follows the modeled maturation of other intertidal habitats like marshes, which experience rapid growth during immaturity that asymptotes at the rate of RSLR at maturity (Allen 1990; Jennings *et al.,* 1995).

3.4.3. Centennial reef

Growth changes on the centennial reef over the study period behaved comparably to patterns displayed by the other study reefs (Fig. 3.7). Peak growth during the initial time step occurred at the base of the predicted OGZ. Similar to the decade-old reefs, the centennial reef experienced erosion at elevations above -0.07 during a period of relatively low water (2013). However, the higher water of 2014-2015 yielded 4 cm yr^{-1} accretion in previously eroded areas at or above MSL, which manifests as a comparably large increase in volume across the reef plateau. This growth rate (4 cm yr^{-1}) is equivalent to the 3.9 cm jump in average sea levels over the two time intervals and is also comparable to the rapid growths displayed by the young reefs. Thus, mature reefs not only follow the intertidal oyster-reef-growth paradigm, they also have the capacity to respond just as rapidly to changes in sea level as immature reefs. This would indicate that mature oyster reefs are not confined to nearly asymptotic growth at the rate of RSLR like that of other coastal habitats. Considering the clarity in response of the centennial reef to the relatively confined sea level trend in 2014-2015, it is possible that we could have measured a

similar response on the decade-old reefs if we had isolated a smaller window of time. Instead, the growth response of the decade-old reefs is diluted across three years of fluctuating sea level.

Growth on the centennial reef was measured at higher elevations than the other reefs included in this study. This reef is much larger than the constructed reefs, and we may be witnessing a certain degree of facilitation (Bruno *et al.*, 2003) within the oyster population, similar to the Northern Acorn Barnacles of the New England rocky intertidal (Bertness 1989), due to thermal buffering and reduced desiccation stress. In fact, each time the centennial reef was sampled there remained ponds of water on the reef's plateau during low tide (appear as dark spots on the reef in Fig. 3.2b). Presence of these ponds shows that the reef is fairly non-porous, retaining water at higher elevations throughout a tidal cycle. This would indicate that, while the OGZ magnitude of large natural reefs corresponds to shifts in sea level, the elevations at which the OGZ manifests may behave differently as a reef matures and expands.

3.4.4. Resilience to sea level fluctuations

Oyster reefs appear to be in dynamic equilibrium with sea level. Like other intertidal habitats, decadal or longer measurements of mature reef surface-elevation changes would show they track RSLR (DeAlteris 1988). However, unlike other habitats, annual rates of change in reef vertical relief could be ± 5 cm depending on relative sea levels. Prolonged shifts in sea level cause different reef elevations to essentially turn off or on, akin to a phenomenon present in coral reefs (Perry and Smithers 2011) but operating at a much greater magnitude. Rapid coral reef vertical accretion is on the order of 0.5 to 0.9 cm yr^{-1} during reef turn-on (Perry and Smithers 2011), while oyster reefs can achieve greater than 2 cm yr^{-1} regardless of maturity. Therefore, oyster reefs, despite being sessile organisms, are well adapted for tracking this particular climate velocity vector as long as the environment remains estuarine. It should be noted that this

outstanding vertical accretion has only been measured on intertidal oyster reefs, and subtidal oyster reef accretion may not respond to fluctuations in sea level. Existing in the intertidal zone mediates the impact of biotic interactions and near bottom hypoxia, to which subtidal reefs are exposed (Lenihan 1999), allowing for growth to be dictated primarily by sea level and aerial exposure regime assuming no disease or degraded water quality.

The ubiquity of this response across oyster-reef ages is a testament to their resilience to RSLR as well as their utility and longevity for stabilizing shorelines, likely reducing the potential impacts of the coastal squeeze (Pontee 2013). This work supports the value of using the OGZ for intertidal oyster population management (Ridge et al. 2015), being an effective predictive tool for oyster reef growth patterns. Use of the OGZ will prove highly valuable in restoration projects, particularly the implementation of green infrastructure like living shorelines that incorporate oyster breakwaters. However, there remains a need to measure oyster reef lateral expansion and adjacent benthic-sediment modification processes. These measurements will help establish whether or not oyster reefs will build landward as they track SLR or eventually create reef islands. Similar to wetland upland transgression with RSLR (Kirwan *et al.*, 2016), this process will depend on the ability of oysters to expand up the littoral slope (Ridge *et al.*, 2016). Considering the outstanding vertical growth captured in this study, the primary limiting factor would appear to be the rate of transgression (i.e., expansion up slope) at a particular shoreline.

This study presents evidence that intertidal oyster reefs are highly responsive to short term fluctuations in local sea level even at maturation. When compared to other coastal habitats and their capacities for RSLR response, oyster reefs are unparalleled in their ability to maintain surface elevation with changing sea level. Greatest recorded rates of surface elevation change in intertidal and shallow subtidal systems like marshes, mangroves, and corals are below 1-2 cm yr^{-}

[1] excluding storm related allochthonous sedimentation (Baustian *et al.*, 2012; Bhomia *et al.*, 2015; Perry *et al.*, 2015; Sasmito *et al.*, 2016). Overall, this research further solidifies that oyster reefs are resilient habitats that will become increasingly important in estuarine systems with changing sea level.

Table 3.1 Reef name sorted by type, average area scanned for each reef type, and date of each terrestrial laser scan mapping.

Reef Name	Mean Area (m^2)	Scan 1	Scan 2	Scan 3
Decade-Old	**52.8**			
MF2-1997		June 2010	July 2012	May 2015
MF1-2000		June 2010	July 2012	May 2015
MF2-2000		April 2010	July 2012	May 2015
Young	**39.1**			
1L5		Dec 2011	Dec 2012	Feb 2014
1L6		Dec 2011	Jan 2013	March 2014
1S5		Dec 2011	Jan 2013	March 2014
1S6		Dec 2011	Dec 2012	Feb 2014
2L5		Oct 2011	Jan 2013	Jan 2014
2L6		March 2012	Jan 2013	Jan 2014
2S5		-	Jan 2013	Jan 2014
2S6		March 2012	Jan 2013	Jan 2014
3L5		Oct 2011	Jan 2013	Feb 2014
3S5		Oct 2011	Jan 2013	Feb 2014
4S5		Jan 2012	Jan 2013	March 2014
Centennial	**222.5**			
CI-1		June 2012	June 2014	June 2015

Table 3.2 Summary of peak growth, sea level, temperature, and salinity for each time step by reef generation. The elevation change in growth peak occurrence and sea level between each period is also included.

Reef Type	Time Step	Elevation of Growth Peak (cm)†	Mean Sea Level (cm)†	Mean Temperature (ºC)	Mean Salinity (ppt)	Peak Growth (cm yr^{-1})	Δ Growth Peak Elevation (cm)	Δ Sea Level (cm)
Decade-old	1	-17	-5.3	19.7	31.8	1.90	+8.0	+3.7
	2	-9	-1.6	18.6	*29.6	1.72		
Young	1	-23	-1.7	19.7	32.4	3.68	-2.0	-2.6
	2	-25	-4.3	18.2	*29.7	6.67		
Centennial	1	-29	-2.1	18.8	30.6	2.89	+30.0	+3.9
	2	1	1.8	18.5	27.7	4.36		

† Elevations reference North American Vertical Datum of 1988

* Significant difference ($P < 0.05$) from previous time step.

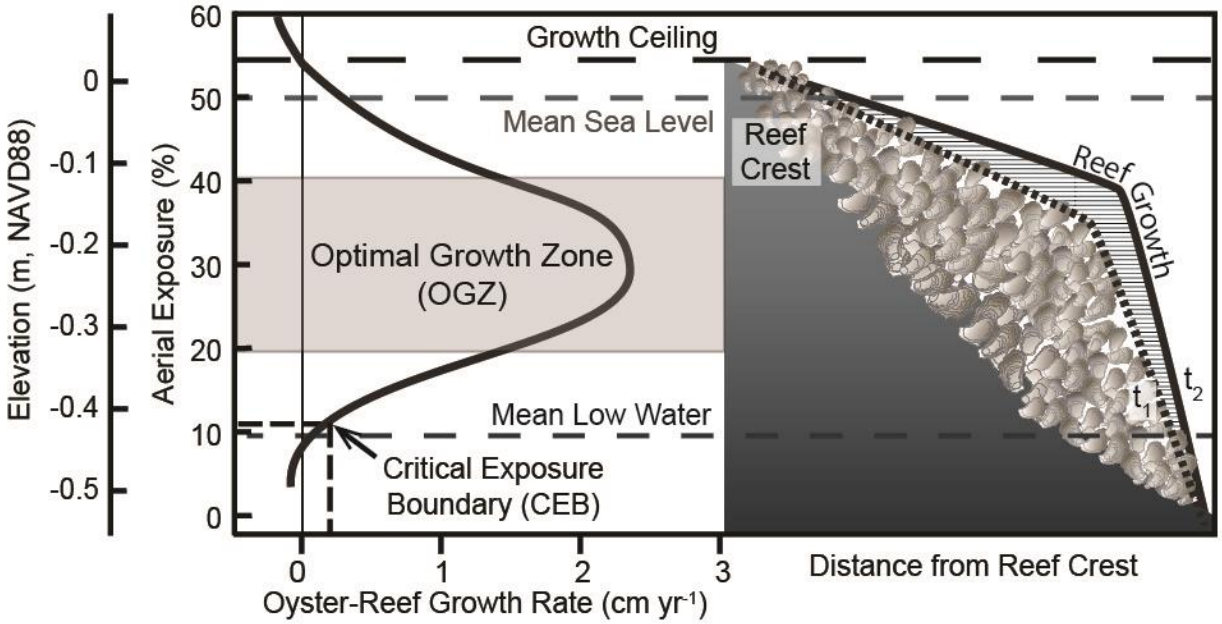

Figure 3.1 Reef growth conceptual model adapted from Ridge *et al.* (2015) that predicts oyster reef growth rate with aerial (tidal) exposure. Relevant elevations in NAVD88 are provided for aerial exposures (%) for the Cape Lookout region of North Carolina. The lower critical exposure boundary occurs where oyster reef growth equals the rate of RSLR, shifting correspondingly as RSLR changes. Oyster reef growth is illustrated (right panel) across a hypothetical reef-elevation profile using dotted (time 1) and solid (time 2) profile lines.

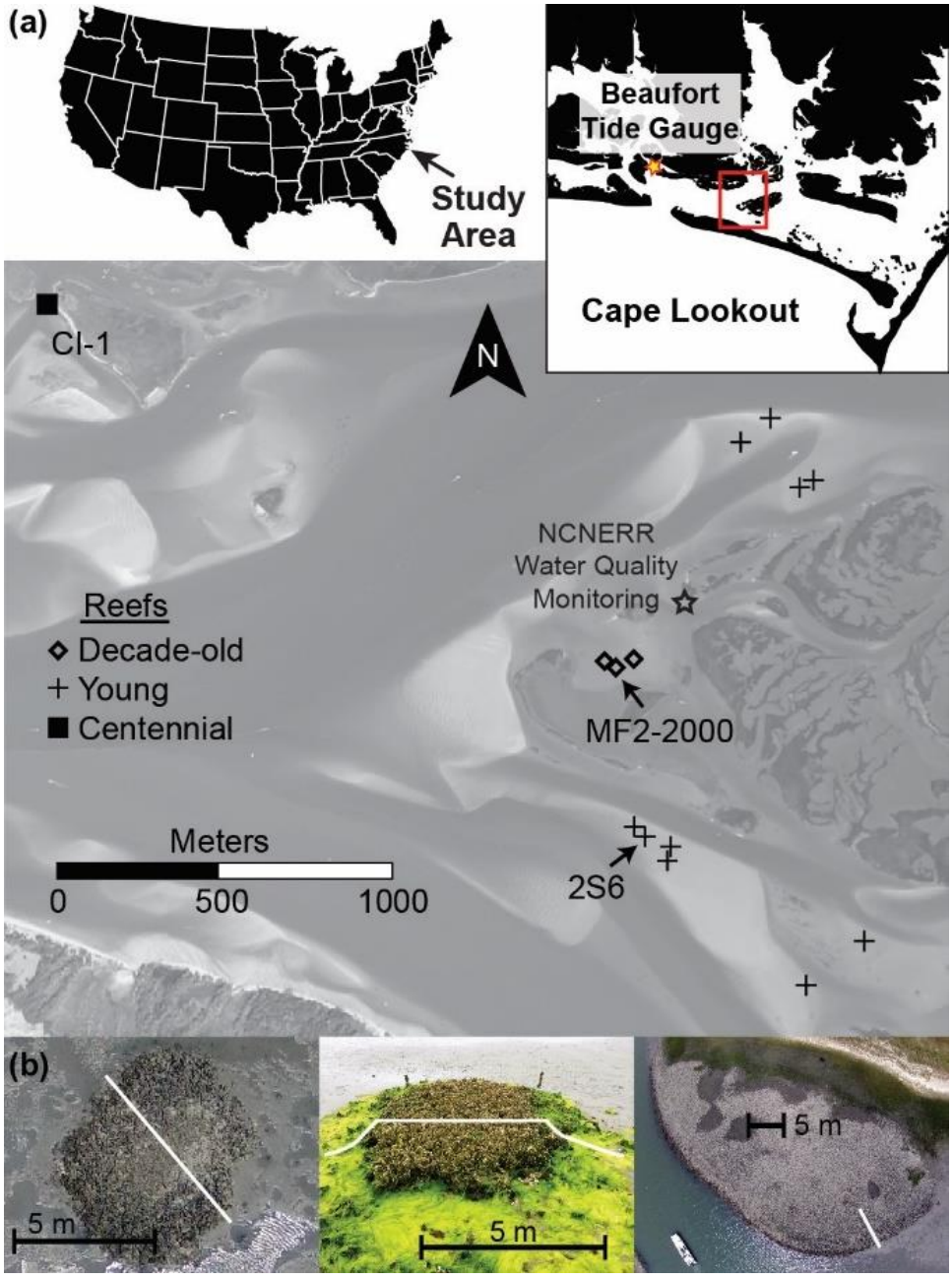

Figure 3.2 Study area map of Back Sound, North Carolina. (a) All reefs are located within the Rachel Carson Research Reserve (NC Coastal Reserves/National Estuarine Research Reserves) in Beaufort, NC. (b) Examples of the three generations of reefs samples, decade-old (left, constructed in 1997 and 2000), young (middle, constructed in 2011), and centennial (right, natural). White bars represent transects for elevation profiles presented in Figure 3.5. Black bars are included for scale.

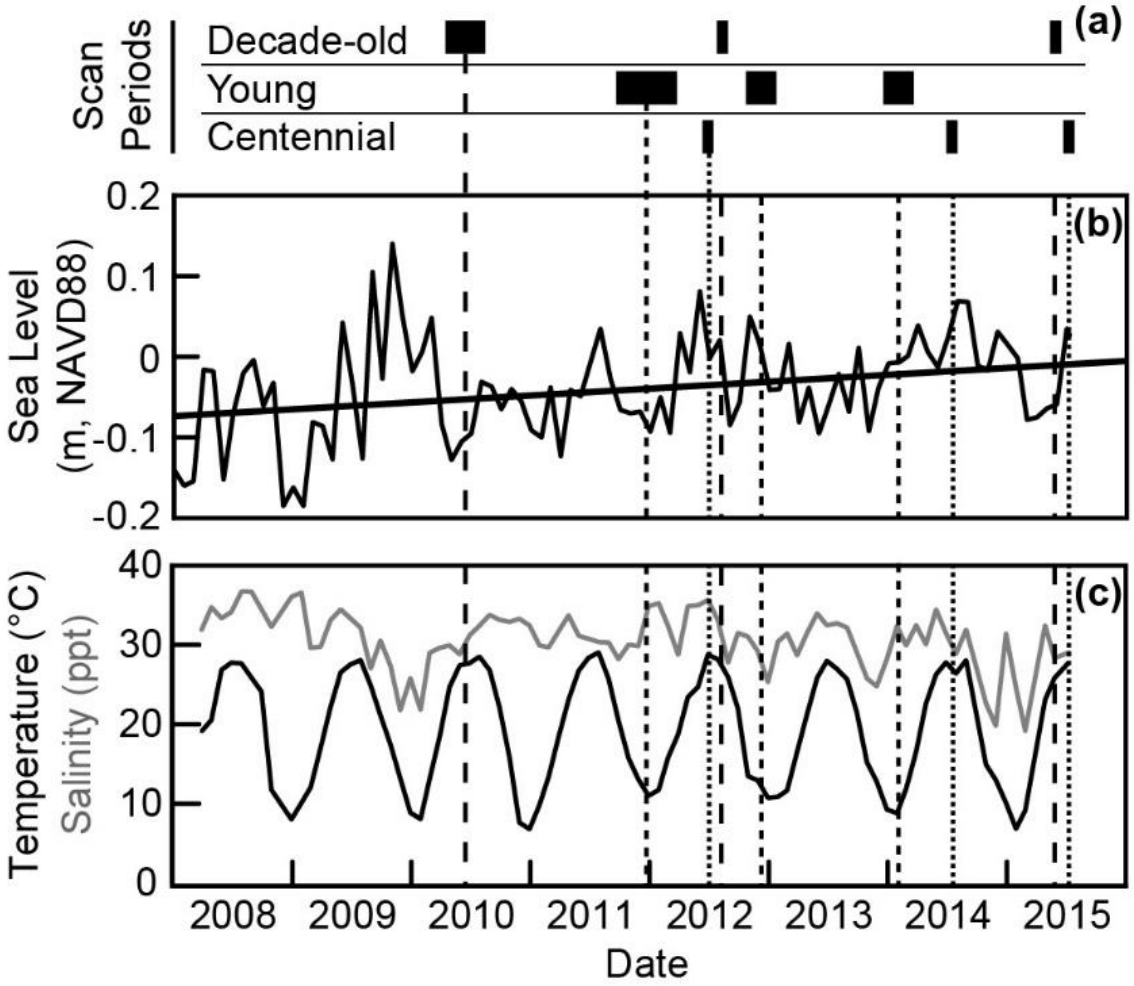

Figure 3.3 Timeline of reef scans obtained for each reef generation with water level and quality over study period. (a) Width of bars indicates the length of time to obtain scans during each sampling period. Each reef generation scanning period is denoted by a unique dashed line through the rest of the figure. See Table 3.1 for additional information. (b) Monthly mean sea level data from the NOAA Tide Gauge in Beaufort (Station ID 8656483). Data are reported as elevations (m NAVD88), and the linear trend of the sea level data is plotted. (c) Mean monthly water temperature (°C, black line) and salinity (ppt, gray line) obtained at the Rachel Carson Research Reserve (NCNERR).

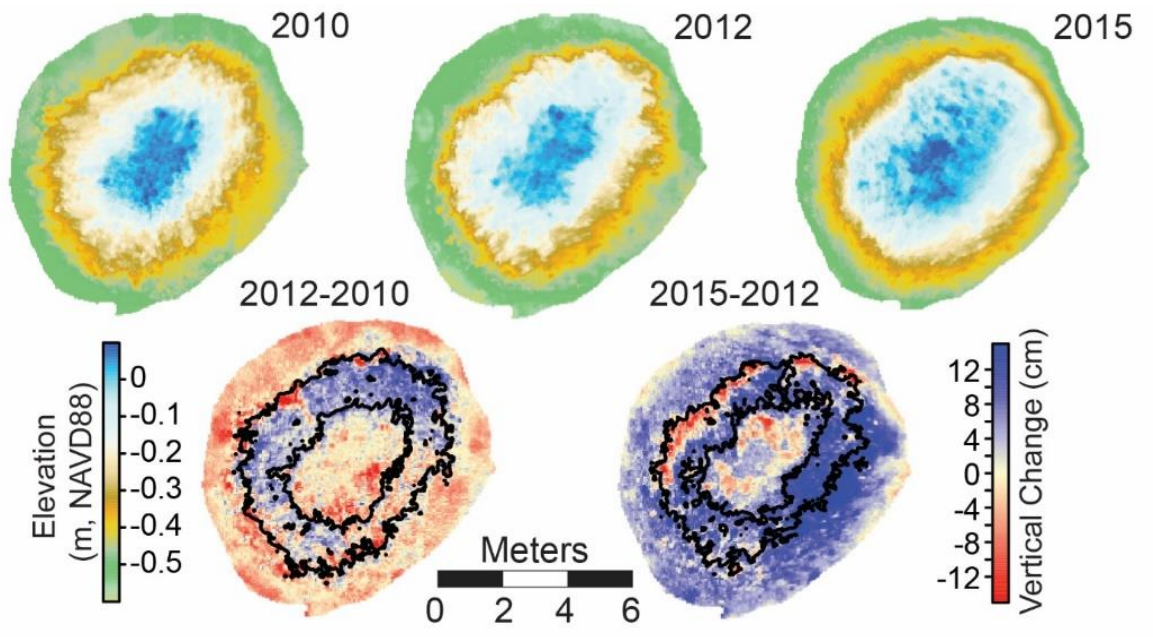

Figure 3.4 Digital elevation models and subsequent subtraction maps from the decade-old reef MF2-2000. The reef was mapped with terrestrial lidar in 2010 (April), 2012 (July), and 2015 (May). Black contours on the subtraction maps represent the boundaries of the OGZ (20-40% aerial exposure) referencing elevations from 2010 and 2012 (initial scans) respectively. Fluctuations in sea level from 2009 to 2015 were examined using monthly mean sea level

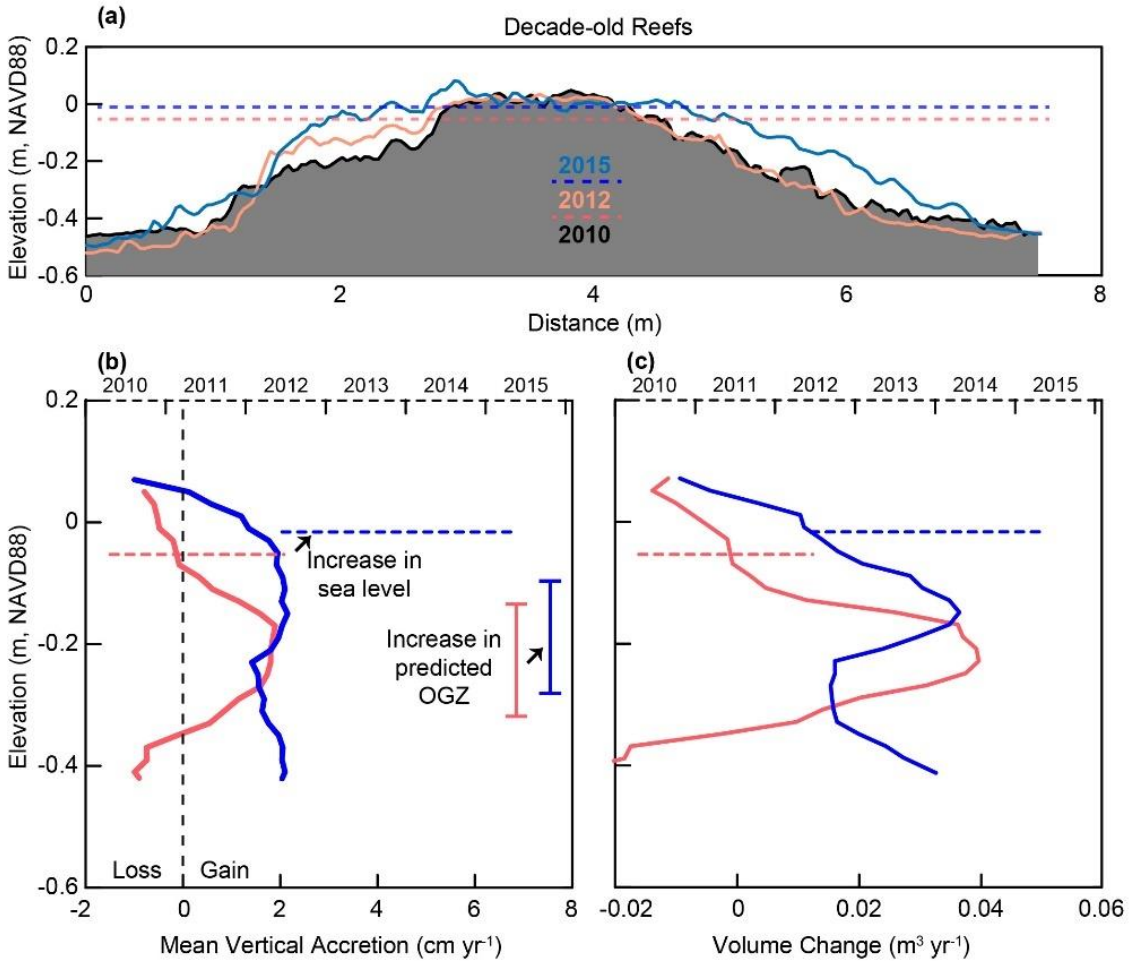

Figure 3.5 Growth of decade-old reef reefs constructed in 1997 (n = 1) and 2000 (n = 2) scanned in 2010, 2012, and 2015. (a) Vertical profiles of MF2-2000 during each scan with average sea levels between each scan period (dashed lines). (b) Mean vertical accretion rates by elevation (solid lines) and mean relative sea levels (dashed horizontal lines) during the scan time steps. Light red and dark blue bracketed bars represent the predicted optimal growth zone (OGZ) based on water level data for relevant scan periods. (c) Reef volume change at each elevation (solid lines) with mean sea level data (dashed lines).

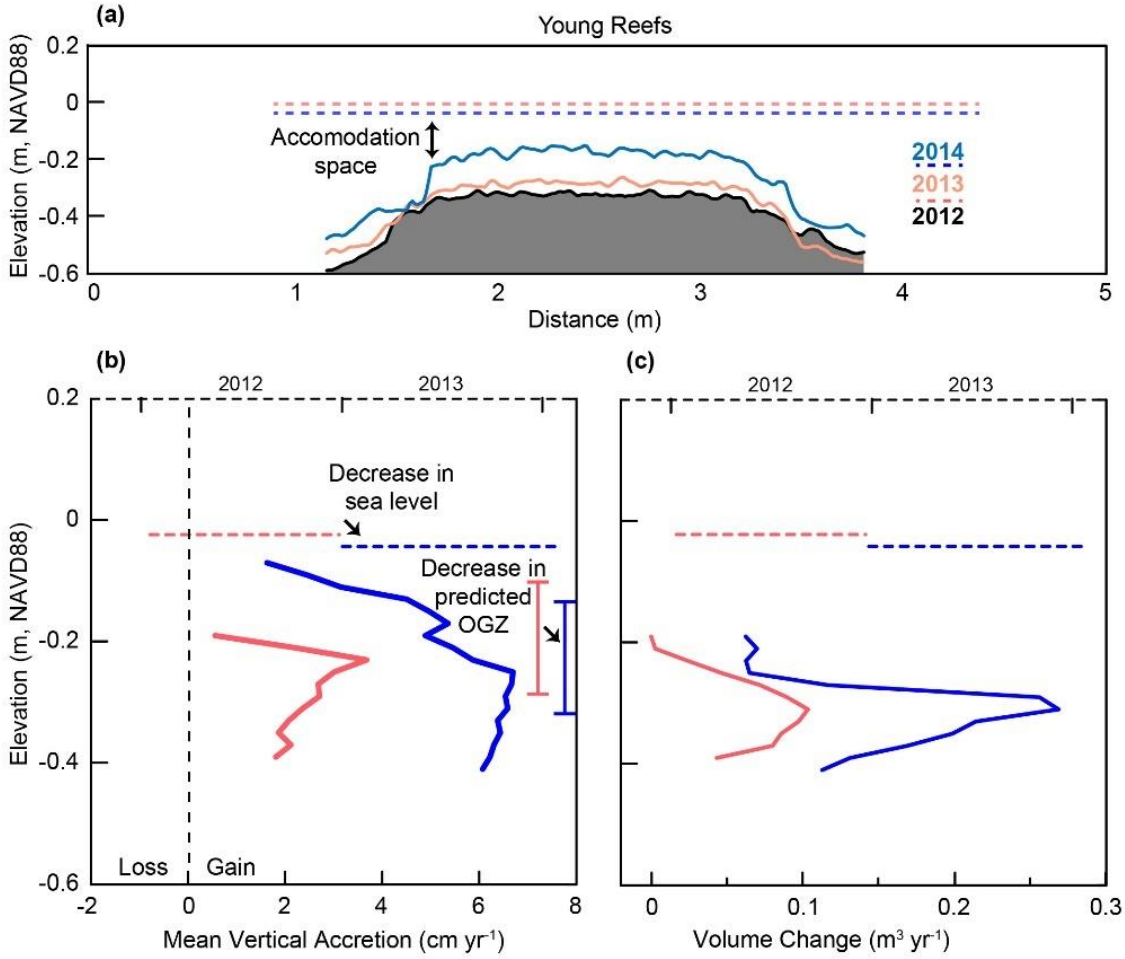

Figure 3.6 Growth of young reefs constructed in 2011 (n = 10) measured at the beginning of 2012, 2013 and 2014. (a) Vertical profiles of reef 2S6 during each scan with average sea levels between each scan period (dashed lines). (b) Mean vertical accretion rates by elevation (solid lines) and mean relative sea levels (dashed horizontal lines) during the scan time steps. Light red and dark blue bracketed bars represent the predicted optimal growth zone (OGZ) based on sea level data for relevant scan periods. (c) Reef volume change at each elevation (solid lines) with mean sea level data (dashed lines).

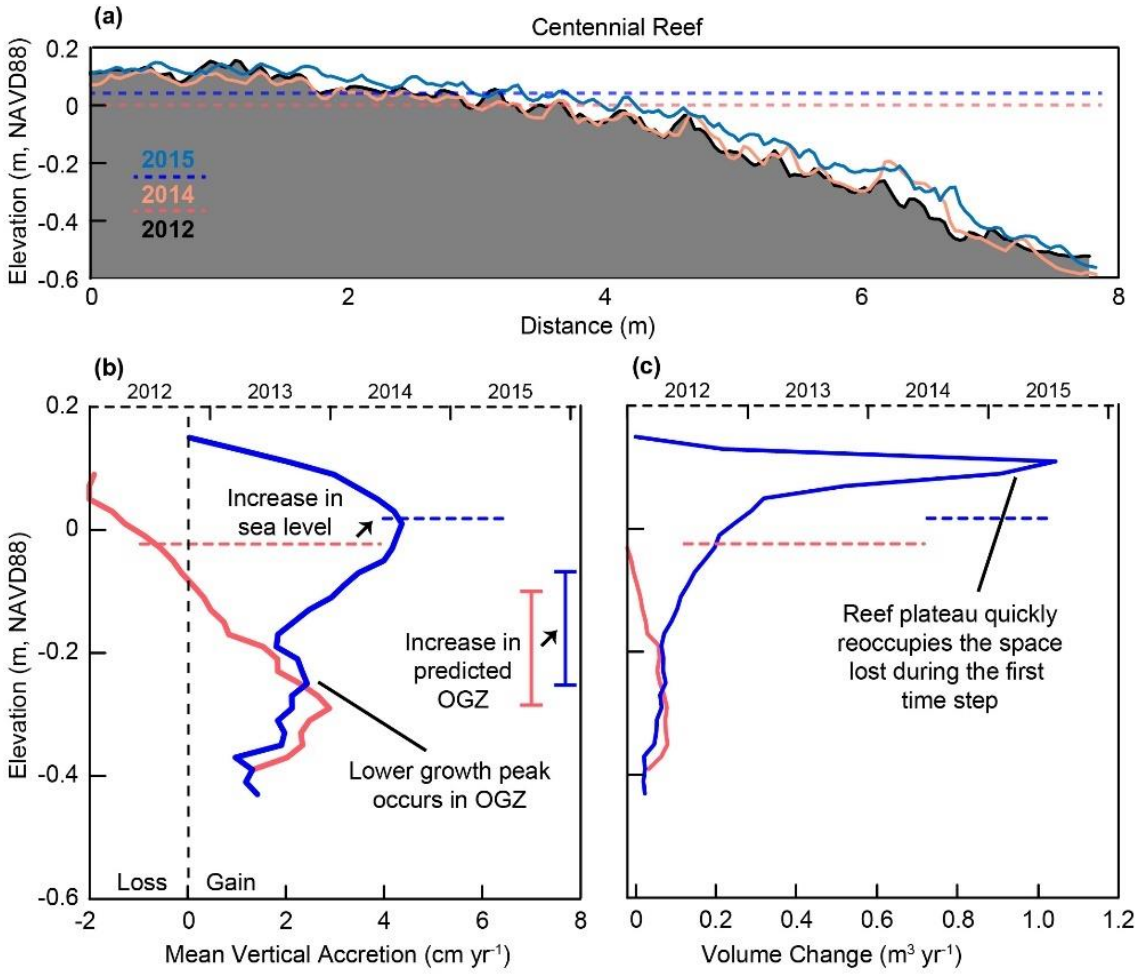

Figure 3.7 Growth of the natural, centennial reef scanned in 2012, 2014, and 2015. (a) Vertical profiles of reef CI-1 during each scan with average sea levels between each scan period (dashed lines). (b) Mean vertical accretion rates by elevation (solid lines) and mean relative sea levels (dashed horizontal lines) during the scan time steps. Light red and dark blue bracketed bars represent the predicted optimal growth zone (OGZ) based on sea level data for relevant scan periods. (c) Reef volume change at each elevation (solid lines) with mean sea level data (dashed lines).

REFERENCES

Ackerly DD, Loarie SR, Cornwell WK, Weiss SB, Hamilton H, Branciforte R, Kraft NJB (2010) The geography of climate change: Implications for conservation biogeography. *Diversity and Distributions*, 16, 476–487.

Allen JRL (1990) Constraints on measurement of sea-level movements from salt-marsh accretion rates. *Journal of the Geological Society*, 147, 5–7.

Anthony KRN, Kerswell AP (2007) Coral mortality following extreme low tides and high solar radiation. *Marine Biology*, 151, 1623–1631.

Baggett LP, Powers SP, Brumbaugh RD *et al.* (2015) Guidelines for evaluating performance of oyster habitat restoration. *Restoration Ecology*, 23, 737–745.

Baustian JJ, Mendelssohn IA, Hester MW (2012) Vegetation's importance in regulating surface elevation in a coastal salt marsh facing elevated rates of sea level rise. *Global Change Biology*, 18, 3377–3382.

Beck MW, Brumbaugh RD, Airoldi L *et al.* (2011) Oyster Reefs at Risk and Recommendations for Conservation, Restoration, and Management. *BioScience*, 61, 107–116.

Bertness MD (1989) Intraspecific Competition and Facilitation in a Northern Acorn Barnacle Population. *Ecology*, 70, 257–268.

Bertness MD, Ellison AM (1987) Determinants of Pattern in a New England Salt Marsh Plant Community. *Ecological Monographs*, 57, 129–147.

Bertrand R, Lenoir J, Piedallu C *et al.* (2011) Changes in plant community composition lag behind climate warming in lowland forests. *Nature*, 479, 517–20.

Bhomia RK, Inglett PW, Reddy KR (2015) Soil and phosphorus accretion rates in sub-tropical wetlands: Everglades Stormwater Treatment Areas as a case example. *Science of The Total Environment*, 533, 297–306.

Bruno JF, Stachowicz JJ, Bertness MD (2003) Inclusion of facilitation into ecological theory. *Trends in Ecology and Evolution*, 18, 119–125.

Burrows MT, Schoeman DS, Richardson AJ *et al.* (2014) Geographical limits to species-range shifts are suggested by climate velocity. *Nature*, 507, 492–5.

Cahoon DR, Hensel PF, Spencer T, Reed DJ, McKee KL, Saintilan N (2006) Coastal Wetland Vulnerability to Relative Sea-Level Rise:Wetland Elevation Trends and Process Controls. In: *Wetlands and Natural Resource Management: Ecological Studies*, Vol. 190 (eds Verhoeven JTA, Beltman B, Bobbink R, Whigham DF), pp. 271–292. Springer.

Chen I-C, Hill JK, Ohlemüller R, Roy DB, Thomas CD (2011) Rapid range shifts of species associated with high levels of climate warming. *Science*, 333, 1024–1026.

Colwell RK, Brehm G, Cardelus CL, Gilman AC, Longino JT (2008) Global warming, elevational range shifts, and lowland biotic attrition in the wet tropics. *Science*, 322, 258–261.

Dame, RF. (1972) The ecological energies of growth, respiration and assimilation in the intertidal American oyster Crassostrea virginica. *Marine Biology* 17, 243–250.

Davis RG, Shaw MB (2001) Range shifts and adaptive responses to quaternary climate change. *Science*, 292, 673–679.

DeAlteris JT (1988) The Geomorphic Development of Wreck Shoal, a Subtidal Oyster Reef of the James River, Virginia. *Estuaries*, 11, 240–249.

Dobrowski SZ, Abatzoglou J, Swanson AK, Greenberg JA, Mynsberge AR, Holden ZA, Schwartz MK (2013) The climate velocity of the contiguous United States during the 20th century. *Global Change Biology*, 19, 241–251.

Edwards M, Richardson AJ (2004) Impact of climate change on marine pelagic phenology and trophic mismatch. *Nature*, 430, 881–884.

Ezer T (2016) Can the Gulf Stream induce coherent short-term fluctuations in sea level along the US East Coast? A modeling study. *Ocean Dynamics*, 66, 207–220.

Ezer T, Atkinson LP, Corlett WB, Blanco JL (2013) Gulf Stream's induced sea level rise and variability along the U.S. mid-Atlantic coast. *Journal of Geophysical Research: Oceans*, 118, 685–697.

Fodrie FJ, Rodriguez AB, Baillie CJ *et al.* (2014) Classic paradigms in a novel environment: inserting food web and productivity lessons from rocky shores and saltmarshes into biogenic reef restoration (ed Arnott S). *Journal of Applied Ecology*, 51, 1314–1325.

Grabowski JH, Hughes AR, Kimbro DL, Dolan MA (2005) How Habitat Setting Influences Restored Oyster Reef Communities. *Ecology*, 86, 1926–1935.

Hoffmann AA, Sgro CM (2011) Climate change and evolutionary adaptation. *Nature*, 470, 479–485.

Jennings SC, Carter RWG, Orford JD (1995) Implications for sea-level research of salt marsh and mudflat accretionary processes along paraglacial barrier coasts. *Marine Geology*, 124, 129–136.

Kirwan ML, Temmerman S, Skeehan EE, Guntenspergen GR, Fagherazzi S (2009) Overestimation of marsh vulnerability to sea level rise. *Nature Climate Change*, 6, 253–260.

Kirwan ML, Megonigal JP (2013) Tidal wetland stability in the face of human impacts and sea-level rise. *Nature*, 504, 53–60.

Koch MS, Mendelssohn IA., Mckee KL (1990) Mechanism for the hydrogen sulfide-induced growth limitation in wetland macrophytes. *Limnology and Oceanography*, 35, 399–408.

Kolker AS, Hameed S (2007) Meteorologically driven trends in sea level rise. *Journal of Geophyiscal Research Letters*, 34, 1–7.

Lenihan HS (1999) Physical-biological coupling on oyster reefs: How habitat structure influences individual performance. *Ecological Monographs*, 69, 251–275.

Lovelock CE, Cahoon DR, Friess DA *et al.* (2015) The vulnerability of Indo-Pacific mangrove forests to sea-level rise. *Nature*, 526, 559-U217.

Morris JT, Kjerfve B, Dean JM (1990) Dependence of estuarine productivity on anomalies in mean sea level. *Limnology and Oceanography*, 35, 926–930.

Paine RT (1971) A Short-Term Experimental Investigation of Resource Partitioning in a New Zealand Rocky Intertidal Habitat. *Ecology*, 52, 1096–1106.

Perry CT, Murphy GN, Graham NAJ, Wilson SK, Januchowski-Hartley FA, East HK (2015) Remote coral reefs can sustain high growth potential and may match future sea-level trends. *Scientific Reports*, 5, 18289.

Perry CT, Smithers SG (2011) Cycles of coral reef "turn-on", rapid growth and "turn-off" over the past 8500 years: A context for understanding modern ecological states and trajectories. *Global Change Biology*, 17, 76–86.

Pinsky ML, Worm B, Fogarty MJ, Sarmiento JL, Levin SA (2013) Marine taxa track local climate velocities. *Science*, 341, 1239–1242.

Poloczanska ES, Brown CJ, Sydeman WJ *et al.* (2013) Global imprint of climate change on marine life. *Nature Climate Change*, 3, 919–925.

Pontee N (2013) Defining coastal squeeze: A discussion. *Ocean and Coastal Management*, 84, 1–4.

Ridge JT, Rodriguez AB, Fodrie FJ *et al.* (2015) Maximizing oyster-reef growth supports green infrastructure with accelerating sea-level rise. *Scientific Reports*, 5, 14785.

Ridge, JT., Rodriguez, AB, Fodrie, FJ (2016). Salt Marsh and Fringing Oyster Reef Transgression in a Shallow Temperate Estuary: Implications for Restoration, Conservation and Blue Carbon. *Estuaries and Coasts*. 1–15. doi:10.1007/s12237-016-0196-8.

Rodriguez AB, Fodrie FJ, Ridge JT *et al.* (2014) Oyster reefs can outpace sea-level rise. *Nature Climate Change*, 4, 493–497.

Sasmito SD, Murdiyarso D, Friess DA, Kurnianto S (2016) Can mangroves keep pace with contemporary sea level rise? A global data review. *Wetlands Ecology and Management*, 24, 263–278.

Shumway SE (1996) Natural Environmental Factors. In: *The eastern oyster, Crassostrea virginica*, 1st edn (eds Kennedy VS, Newell RIE, Able AF), pp. 467–513. Maryland Sea Grant College, College Park, Maryland.

Sweet W, Zervas C, Gill S (2009) *Elevated East Coast Sea Level Anomaly: June - July 2009*. 40 pp.

Theuerkauf EJ, Rodriguez AB, Fegley SR, Luettich RA (2014) Sea level anomalies exacerbate beach erosion. *Geophysical Research Letters*, 41, 5139–5147.

Tingley MW, Koo MS, Moritz C, Rush AC, Beissinger SR (2012) The push and pull of climate change causes heterogeneous shifts in avian elevational ranges. *Global Change Biology*, 18, 3279–3290.

Walles B, Fodrie FJ, Nieuwhof S, Jewell OJD, Herman PMJ, Ysebaert T (2016) Guidelines for evaluating performance of oyster habitat restoration should include tidal emersion: reply to Baggett *et al. Restoration Ecology*, 24, 4–7.

Walther GR, Post E, Convey P *et al.* (2002) Ecological responses to recent climate change. *Nature*, 416, 389–395.

Zhu K, Woodall CW, Clark JS (2012) Failure to migrate: Lack of tree range expansion in response to climate change. *Global Change Biology*, 18, 1042–1052.

CHAPTER 4: CHANGES IN COMPOSITION AS OYSTER REEFS CATCH-UP AND KEEP-UP WITH SEA-LEVEL RISE

4.1. Introduction

With a vast majority of the natural world being impacted by human activity, it is difficult to determine baseline ecosystem health and performance for assessing conservation and restoration success, especially in the face of climate change. Many studies that use current reference sites as benchmarks may already be biased by an overall altered environment as the ecological baseline has shifted (Pauly 1995, Jackson et al. 2011). To create reference criteria, many researchers are delving into the past through historical ecology and conservation paleobiology to understand how ecosystems and organisms have evolved with the progression of human society and a fluctuating climate (Dietl and Flessa 2011, Rick and Lockwood 2013, Dietl et al. 2015). These methods have been used across terrestrial and marine ecosystems, and help differentiate impacts to ecosystem function from both human influence and climatic changes (see reviews in Rick and Lockwood 2013; Dietl et al. 2015).

Studies have explored long-term trends in shellfish mollusc populations related to anthropogenic changes. Shell middens (domestic waste dump sites) store valuable information on historical and prehistorical harvesting pressure and impact on mollusks (Erlandson et al. 2008, Harding et al. 2008, Dame 2009, Klein and Steele 2013, Rick et al. 2016), and there is evidence of a resilient response in bivalves to changing water quality (e.g., eutrophication, drought) prior to the industrial revolution (Kirby and Miller 2005, Harding et al. 2010, Rick et al. 2016). Oysters represent a highly valuable estuarine habitat (Grabowski et al. 2012) that has

experienced global decimation over the last century through overfishing, water quality changes, and disease (Beck et al. 2011). Their extirpation in some areas, like Australia, has caused a complete loss of ecological baseline that makes restoration progress more difficult (Alleway and Connell 2015). Investigations of oyster shell middens have been used to infer impacts to estuarine water quality and disease vulnerability through population removal (Dame 2009, Mann et al. 2009a;b), with the exacerbation of these effects from climate-related increases in water temperatures (Harding et al. 2008). These studies have provided a window into oyster-population trends but are confounded by the inherent bias of harvesting practices and cannot directly address reef-scale response to climatic and anthropogenic alterations to the estuarine environment.

Similar to other reef-building organisms, oyster reefs are self-accreting with younger generations growing atop older. This process creates structural complexity and promotes deposition within the reef matrix, trapping allogenic and biofiltered seston (feces and pseudofeces) below the taphonomically active zone (region of living oysters overlying the reef core sediment, Bahr and Lanier 1981; Figure 4.1). This accretion provides a well-preserved chronology of reef growth and evolution in addition to a record of environmental conditions throughout the reef's lifespan (DeAlteris 1988, Perry et al. 2012, Stathakopoulus et al. 2015, Rick et al. 2016). DeAlteris (1988) used excavations of the Wreck Shoal oyster reef to determine that growth and development of the reef was directly tied to sea-level rise (SLR) and the migration of the James River (Virginia) estuary. Just as coral reefs exhibit catch-up and keep-up phases of reef growth linked to SLR (Neumann and Macintyre 1985), oyster reefs likely experience the same phenomenon (Figure 4.1), which is supported by the rapid growth witnessed on constructed reefs (8-11 cm yr^{-1}, Rodriguez et al. 2014) that is minimized when reef crests

reach sea level (< 1 cm yr^{-1}, Ridge et al. 2015). Some oyster reefs, however, have also been found to enter a give-up phase, unable to keep up with SLR, leading to their eventual demise and burial (see examples in Simms et al. 2008, Troiani et al. 2011, Mattheus et al. 2014). Understanding the conditions resulting in reef give-up is invaluable for conservation and restoration consideration and our ability to evaluate how alterations to the system might impact ecosystem development and function (Kidwell 2015).

A thorough examination of oyster reef fossil records could help elucidate if reef development has changed through time in response to environmental changes, such as SLR and estuarine water quality. In addition to capturing reef growth patterns, fossil records can explore changes in sedimentary composition, which may include organic carbon burial and implications for estuarine fluctuations, as well as shell production and preservation, important for shell budgets and estuarine chemistry (Powell et al. 2012, Waldbusser et al. 2013). This study empirically explored oyster-reef growth and composition over reef lifetimes and across multiple ages from prehistoric reefs to extant-natural reefs and recently-constructed reefs. Reef growth was evaluated within the context of sea level, comparing reef position and growth rates with sea-level curves to assess if oysters follow the catch-up/keep-up paradigm. Reef composition, in the form of shell production and sedimentary composition (grain size and organic carbon content), was measured throughout reef histories and placed within the growth-model framework to determine if reefs of different ages are developing similarly.

4.2. Methods

Extant oyster reefs (*Crassostrea virginica*) were located in Back Sound and the North River Estuary in the Cape Lookout region of North Carolina, USA (Figure 4.2). Ancient, buried reefs were originally found by Mattheus et al. (2014) in the North River and Newport River

Estuaries. Back Sound experiences a semi-diurnal tide (~0.9 m tide range) with mean sea level (MSL) occurring at -0.03 m (all elevations reported in the North American Vertical Datum of 1988 [NAVD88]). Extant oyster reefs are almost exclusively intertidal in these areas with some subtidal oyster beds existing up river.

We examined the growth models and composition of oyster reefs of varying ages, from recently (~5 ya) and decade-old constructed reefs to natural reefs originating over 100 ya as well as ancient reefs buried in mud for more than 1,000 years (Table 4.1). Constructed reefs began as cultch shell reefs, using recycled oyster shell to foster natural recruitment and development. All extant reefs, except some of the constructed reefs, have plateaus at elevations just above MSL and natural reefs ranged from 2x to 40x larger in area than the constructed reefs (15-80 m^2). Vertical cores (~10-cm diameter aluminum pipe) were taken through each reef, and surface elevations recorded with a Trimble RTK GPS. Elevations for the ancient, buried reef cores were estimated based on depth to sediment interface and the water level at time of extraction obtained from the nearby tide gauge (Station 8656483, NOAA Tides and Currents, Beaufort, NC).

4.2.1. Reef growth and sea level

Growth of extant natural oyster reefs was estimated using an endpoint method, obtaining a radiocarbon date from the umbo of an articulated shell (both valves present) sampled at the base of each reef and using the collection date of the core for the age of the reef top. Accretion and growth of ancient reefs were assessed by creating a chronostratigraphy using 4-5 radiocarbon dates from articulated oysters distributed throughout the reef core. Shells were analyzed for radiocarbon by the National Ocean Sciences Accelerator Mass Spectrometry (NOSAMS) Facility at the Woods Hole Oceanographic Institution. Radiocarbon results were calibrated to calendar years using CALIB 7.1 (Reimer et al. 2013, Stuiver et al. 2016), the

atmospheric correction curve and a radiocarbon-dated oyster shell collected in 1948 from Back Sound, NC to establish the local reservoir age (420 ± 20 calibrated years before present [Cal yr BP], Stuiver and Polach 1977). Dates are reported as years before present (BP), where present is 1950 Common Era (CE). Growth of constructed reefs was measured by dividing the vertical distance from the reef surface to the cultch shell (construction material) by the duration in years between reef construction and core collection.

We matched reef position and growth to sea level using the elevations of the radiocarbon dated oyster shells compared to both local tide gauge data and sea level reconstructions. Monthly mean sea-level data were queried from the NOAA tide gauge in Beaufort, NC (Station 8656483) from -25 to -65 yr BP (1975-2015 CE). The sea level reconstruction for North Carolina (Kemp et al. 2011) was used to relate sea level from -25 to 2070 yr BP (1975 CE back to 120 BCE, Before Common Era;). Beyond 2070 yr BP, we used relative SLR (RSLR) rates for North Carolina determined by Engelhart and Horton (2012) to extrapolate sea level, which were 0.9 mm yr^{-1} from 2070 yr BP to 4000 yr BP and then 1.7 mm yr^{-1} from 4000 yr BP to 8000 yr BP.

4.2.2. Reef composition

Compositional changes within the reef matrix were examined through gain size, organic carbon content, and shell production. Reef cores were divided into 5-cm sections (405.37 cm^3 sample volume), then shell material and sediment were separated by wet sieving (2 mm sieve), dried at 60 °C, weighed for shell content and prepared for grain size and carbon analyses. Shell volumes were estimated based on the density of calcium carbonate (2.71 g cm^{-3}) and converted to shell production using relevant growth models. Grain size was measured using a Cilas 1180 laser particle size analyzer that produces a grain-size distribution from 0.04 to 2000 µm divided

into 100 bins (24 bins <4 µm [Clay]; 31 bins <63 µm [Silt]; 45 bins <2,000 µm [Sand]). Resultant histograms were translated into grain-size maps for each core using relative percentages.

Depositional habitats trap sediments from adjacent environments, and we assessed the connectivity of these reefs to nearby sources through time by analyzing the sediment grain size throughout each core. To visualize how reef maturation impacts connectivity between adjacent sandflats and reef sedimentation, we conducted a regression analysis to determine if the percent of sand stored within natural reefs was dependent on the overall vertical distance from the reef base. Data transformations were applied to both percent sand (Log10) and distance from reef base (Square Root) to meet assumptions for parametric analysis.

Sedimentary organic carbon was measured in cores using both CHN and Loss on Ignition (LOI) methods. For most cores, multiple samples were selected down core for CHN analysis to create a rough carbon profile. CHN was conducted using a Perkins-Elmer CHN Analyzer with samples being acid fumed to remove inorganic carbon. Many of these samples were also run through LOI, conducted by combusting sediments at 550 °C for 4 h, to obtain an oyster-reef specific correction for true percent organic carbon from percent organic matter ($y_{CHN} = 0.457[x_{LOI}]$, $R^2 = 0.68$, Appendix 4.1), similar to Craft et al. (1991). Remaining core samples (not run for CHN) were processed for LOI and the calibration applied. Carbon burial rates were then determined using the sediment component for each core section and pertinent growth-model estimate for each reef.

To further assess reef functioning through time, we examined the sediment organic carbon trend with distance from the reef base as well as the relationship between organic carbon, mean grain size, and shell content within distinct samples (as a proxy for reef productivity at the

time). Sediment organic carbon was regressed with relative height from the reef base using the natural reefs sampled in Back Sound, and carbon data were Log10 transformed. Shell content, mean grain size, and percent organic carbon stored within all natural reefs were explored through a series of correlations using multiple samples from each core. We divided the dataset into extant natural and ancient reef subsets and used a series of Spearman rank correlations because the data did not meet the assumptions for parametric testing.

4.3. Results

4.3.1. Reef growth and sea level

Both ancient reefs formed above organic-rich sediment layers that were dated in Mattheus et al. (2014) to be 5844-5890 Cal yr BP (North River) and 5387-5424 Cal yr BP (Newport River). These layers are likely terrestrial paleosols or *Juncus roemerianus* saltmarsh, given their higher depletion of ^{13}C, $\delta^{13}C$ values between -25 to -28 are representative of C3 plant carbon fixation (Kohn 2010). Overall, ancient-reef thickness was 2.29 m (North River) and 1.05 m (Newport River), and these reefs were buried under 1.11 m and 2.22 m of riverine sediment, respectively (Table 4.1).

Radiocarbon dates from all of the ancient reefs were placed in stratigraphic position (Table 4.1, Figure 4.3 and Appendix 4.2), and dates from the base of the ancient reefs indicate that they formed around the same time. The North River ancient reef formed at approximately -5.145 m NAVD88 around 4430 Cal yr BP. The Newport River ancient reef originated near -4.585 m NAVD88 around 4265 Cal yr BP. The North River reef existed for nearly 2,500 years, while the Newport River reef lasted 1,000 years. Sea level during this stretch of time (4430-4265 Cal yr BP) was estimated to be -5.01 to -4.74 m NAVD88 (± 0.6 m, Engelhart and Horton 2012). This would place the North River ancient reef just below sea level at the time of origin

and the Newport River reef just above; however, the Newport River reef's position is unlikely given the growth ceiling exhibited by extant reefs (Ridge et al. 2015) and is probably an artifact of our core elevation calculation at that site. Growth and accretion rates calculated for all radiocarbon time steps in both ancient reef cores range from 0.47 mm yr^{-1} to 1.6 mm yr^{-1} (Table 4.1).

The extant natural reefs ranged from 0.4 m to 1.05 m in thickness above a sand substrate or eroded marsh sediment. Radiocarbon dates from the base of the extant natural reefs range from 185 Cal yr BP to modern (later than 1950 CE; Table 4.1). Sea level during this time frame rose from -0.47 to -0.19 m NAVD88 (~1.5 mm yr^{-1}), indicating reefs originated from -0.4 to -0.2 m below sea level at the time. Using the endpoint method from date of origin to core collection, extant natural reefs had growth rates between 4-5 mm yr^{-1}.

Constructed reefs ranged from 0.15 m to 0.35 m in thickness above the cultch shell layer. All of the constructed reefs were created on sandflats around mean low water with the base of the reefs (above the cultch shell material) beginning at -0.35 to -0.4 m NAVD88. Mean sea level from 1997 to 2011 increased from 0 to 0.06 m NAVD88, rising 3.9 mm yr^{-1}. From date of construction to core collection, reef accretion spanned 1.25 cm yr^{-1} to 5 cm yr^{-1}.

4.3.2. Reef composition

Shell weight within all reef strata increased from 50 g per 5-cm core sample at the base to 150-250 g throughout the rest of the core (Figure 4.3), composed mostly of oyster (*C. virginica*) with less than 10% of other molluscan shells that included mud snails (*Ilyanassa obsoleta*), hard clams (*Mercenaria mercenaria*), and scorched mussels (*Brachidontes exustus*). Greatest shell masses were recorded within the constructed reefs. Silt or sand beds (5-10 cm thick) with little to no shell (< 50 g) were present within several of the ancient and extant-natural reefs and these

beds are interpreted to represent periods when the reef was buried. The North River ancient reef experienced three periods of burial and resurgence (Figure 4.3) while growth of the Newport River ancient reef remained uninterrupted by periods of burial during its lifetime (Appendix 4.2). The extant natural reefs MMBB1, CI-1, and CI-6 each experienced one burial period (Appendix 4.2).

Ancient reefs have silt-dominated sediment within the reef matrix (Figure 4.3). The living natural reefs all exhibited a fining upwards trend in grain size from the base, with less sand accumulating over time and transitioning to silt-dominated sediment at the base of the TAZ. This is supported by the regression analysis, where the percent of sand within a core sample had a significant, negative linear relationship ($F_{(1,83)} = 25.17$, $R^2 = 0.39$, $p < 0.001$) with the distance from the reef base (Figure 4.4A). Many of the constructed reefs also exhibited this fining-upwards pattern, but several were dominated by sandy sediment throughout.

Percent organic carbon within reef sediments typically ranged from 1-6%. The carbon stock (g C_{org} m^{-2}) of each reef was calculated and scaled with the reef ages (Table 4.1). For better comparison, these values were converted into a carbon inventory for a given meter of core for each reef (Figure 4.4B). Sediment organic carbon of the extant natural reefs exhibited a significant, positive trend ($F_{(1,42)} = 53.34$, $R^2 = 0.64$, $p < 0.0001$) with height from the reef base (Figure 4.4C).

Correlations displayed significant relationships between sediment organic carbon, percent shell, and mean grain size (Table 4.2 and Figure 4.4D-F). Of the ancient and extant natural reef datasets, all reefs showed a significant positive correlation between percent shell and percent organic carbon in core samples. Percent organic carbon exhibited strong negative correlations with mean grain size in all reefs. When percent shell and mean grain size were compared, reefs

displayed weak but significant correlations, with the ancient reefs having the weakest relationship.

4.4. Discussion

4.4.1. Reef growth and sea level

Growth on reefs, when using the endpoint method from the radiocarbon chronology, is generally much higher on extant natural reefs (4-5 mm yr^{-1}) than the ancient reefs (<2 mm yr^{-1}). This difference is likely due to the greater rate of relative SLR (RSLR) over the past century (2.1 mm yr^{-1}, Kemp et al. 2011) compared to SLR when the ancient reefs were growing (0.9-1.7 mm yr^{-1}, Engelhart and Horton 2012, Kopp et al. 2014). Several factors support that the ancient reefs initially occupied an intertidal setting, including the consistent narrow shell morphology, similar to the shell morphology of current intertidal oysters (Bahr and Lanier 1981), as well as the fact that the ancient reefs are in direct contact with underlying terrestrial or high marsh sediment. Additionally, when all radiocarbon dates from ancient and extant natural reefs are plotted with their respective elevations, we find a linear trend ($R^2 = 0.96$) of 0.95 mm yr^{-1} that matches the sea level curve until its acceleration in the last millennium (Figure 4.5A). According to Engelhart and Horton (2012), RSLR slowed from 1.7 mm yr^{-1} to 0.9 mm yr^{-1} around 4000 yr BP in southern North Carolina. This is mirrored in growth rates of both ancient reefs that formed during the higher SLR rate, with slower accretion occurring after the SLR deceleration (Table 4.1, Figure 4.2). This means the ancient reefs were accreting at the same rate as RSLR, paralleling the growth pattern exhibited by coral reefs tracking sea level, termed keep-up phase by Neumann and Macintyre (1985). Based on the reef chronology, it appears that the North River ancient reef could have entered a catch-up phase (Neumann and Macintyre 1985), growth rate exceeded SLR, when its vertical accretion accelerated to 1.3 mm yr^{-1} while RSLR was

estimated to be 0.9 mm yr^{-1}. This greater accretion period is marked by the presence of the major sand layer and likely underestimates the growth rate of the reef because of the lag time before the substrate could be recolonized by oysters (source of radiocarbon dating material). Alternating periods of increased and reduced accretion could indicate hiatuses where the bottom surface, either reef or sand, was not accreting with rising sea level, possibly the result of an erosional event or non-deposition following a sediment pulse. The most recent date from the ancient reefs was well below sea level (Figure 4.5A), potentially signifying the transition of these reefs into a give-up phase (Neumann and Macintyre 1985), where growth is below the rate of RSLR. Both of the ancient reefs either transitioned into give-up phases or encountered a significant change to the estuary that resulted in their demise and burial.

Work done by Berelson and Heron (1985) indicates that, since 4800 yr BP, an inlet (perhaps Beaufort Inlet) was twice present through present-day Shackleford Banks across from the mouth of the North River and is likely responsible for the deltaic formation of Middle Marsh in Back Sound. The presence of this inlet probably changed the estuarine dynamics (salinity and temperature) of the North River, possibly increasing the habitability of the area for intertidal reefs and promoting the formation of the ancient reef. This is comparable to conclusions by DeAlteris (1988) where migration of the James River estuary with SLR provided suitable salinity conditions for the Wreck Shoal oyster reef to develop. Variations in inlet exchange may have contributed to the burial periods present in the North River core, and the eventual burial of the reef may be linked to the closing or migration of the inlet, which would also dramatically alter the estuarine dynamics of the system. Alternatively, if changing conditions slowed reef growth to become more subtidal, a period of increased salinity would allow marine predators, competitors, and bioeroders to further reduce the reef to a breaking point. Similarly, a study

examining the history of Bogue Banks has shown the oldest dune ridges date back 3330 Cal yr BP (Timmons et al. 2010), signifying island development at this time could have impacted ocean exchange with the estuaries and reduced the suitability of the Newport River. We may be able to further elucidate changes to estuarine dynamics if we processed the shells through elemental analysis. As oyster shell has been shown to maintain isotopic equilibrium with their environments during calcification (Surge et al. 2001), it is possible the shell chemistry maintained a record of these salinity fluctuations. Given that recent research has revealed how robust oyster reefs can be to changes in sea level (Rodriguez et al. 2014, Ridge et al. 2015), their capacity for growth may be overwhelmed by pronounced change to water quality (e.g., salinity, eutrophication), which is likely a major contributor to the continued decline and failure of subtidal reefs along the North Carolina and Virginia coasts (Kirby and Miller 2005, Powers et al. 2009).

Growth on the extant natural reefs is far outpaced by the constructed reefs, nearly a magnitude greater (1-5 cm yr^{-1}), which matches short-term (< 5 year) measurements of constructed oyster-reef growth in this study area (Rodriguez et al. 2014, Ridge et al. 2015, Ridge et al. 2016). In all likelihood, the extant natural reefs initially experienced accelerated growth equivalent to the constructed reefs until they caught up to MSL (catch-up phase). As the height of the reef approached the growth ceiling, rates of oyster-reef accretion subsequently slowed to the rate of RSLR (Rodriguez et al. 2014, Ridge et al. 2015), entering a keep-up phase. During the keep-up phase, maximum growth shifts to the reef flanks for lateral expansion (Rodriguez et al. 2014), similar to highstand shedding in carbonate platforms (Schlager et al. 1994). The extant natural reefs originated between 0.2 m to 0.4 m below MSL (Figure 4.5B). Mean low water occurs between -0.4 m to -0.45 m for this area and represents the lower critical boundary for

oyster growth in lower estuaries (Ridge et al. 2015), indicating that these reefs were intertidal at formation. Endpoint calculations of extant natural reef accretions (4-5 mm yr^{-1}) are much higher than the rate of RSLR, which would suggest they are in a state of catch-up. However, sustained growth at this rate would actually place reefs above sea level for part of the last century (see endpoint lines in Figure 4.5B), and it is much more likely that these reefs grew rapidly to sea level (catch-up) and then tracked sea level (keep-up) for the past two centuries (Figure 4.5B). It may be possible to better define this growth pattern by reconstructing reef chronologies using excess ^{210}Pb profiles if the reef core keeps sediment relatively undisturbed. Regardless, we can assume that these reefs did not just reach sea level prior to this study, and have been tracking RSLR for a majority of the past two centuries. Likewise, growth in the constructed reefs (MF2-97 and MF2-00) that have plateaued at sea level was calculated at 2.6-3.8 cm yr^{-1} (endpoint) and is being skewed higher by the rapid growth these reefs experienced in their first decade, probably mirroring the 5 cm yr^{-1} growth of the youngest constructed reef. This is strong evidence that extant reefs did in fact grow rapidly at inception, which would change the calculated rates of shell production and sediment accretions based on modified reef chronologies using the catch-up/keep-up model (Figure 4.5B).

4.4.2. Reef composition

The internal composition of oyster reefs appeared quite similar among different generations but dependent upon maturity and possibly estuarine setting. In terms of grain size, ancient reefs had uniformly silt-dominated sediment within the reef pore space, but extant reefs show a transition from sandy sediment to silt-dominated as the reef grew, with some constructed reefs still undergoing this transition. This appears to be a consequence of the reefs connectivity to adjacent environments (e.g., sandflat) that eventually disconnects at a certain maturity (i.e.,

reef height), which was also seen in Ridge et al. (2016). Variability in the regression of distance from reef base and % sand that occurs at lower reef heights would indicate there are more factors determining sand content within the reef pore space that become less important as the reef grows vertically (Figure 4.4A). Once disconnected, the reef is almost exclusively sourcing pore sediment from ambient and biofiltered deposition out of the water column. While there was a weak correlation between shell content and mean grain size, regression analysis (Fig 4A) indicated that we should expect this grain size transition to be complete when the reef exceeds 0.5 m in height within our study area. Thus, grain size differences seem less associated with reef productivity and more linked to overall reef height. As this trend appears across all of our natural reefs and the mature constructed reefs, it is consistent through time and has not been impacted by environmental changes over the last two centuries. This height is equivalent to half the local tidal range, and therefore this expected transition height may differ in areas with different tidal ranges. This switch in sediment composition makes it easy to define distinct sand layers (seen most prominently in the CI-1, CI-6, and MMBB1 cores, Appendix 4.2) that are likely related to large storm events, where the reef was temporarily reconnected to the adjacent environment and then recovered. The uniformity of the two ancient reefs being silt-dominated may imply that these reefs originated in the middle or upper estuary, being heavily influenced by finer riverine sediment compared to the sandier sediments of the lower estuary. Placing these reefs farther up estuary would also support that changes to inlet dynamics at the estuary mouth would be more impactful to water quality, potentially dropping salinity to less ideal conditions and increasing suspended sediment load as the turbidity maximum migrates down river.

Both organic carbon content and shell content within oyster reefs display similar trends across all reefs sampled (Figure 4.3). Generally, as soon as the reef begins to grow there is an

immediate increase in organic-carbon content of the sediments. When reefs mature, the pore sediment becomes finer as it disconnects from coarser adjacent environments and switches to water-column sourced deposition. Sediment-organic carbon correlates well with increases in shell content, assumed to be a proxy for reef productivity, likely due to the combination of higher filtration capacity and subsequent biodeposition through feces and pseudofeces (Figure 4.4). Sediment-organic carbon increases as grain size decreases, which is due to the reef becoming disconnected from adjacent environments and increasing retention of fine-grained sediment due to flow reduction from greater oyster density and structural complexity (Figure 4.4). Because we already see equivalent carbon values in the constructed reefs, the time for a reef to begin efficiently trapping carbonaceous sediments within the pore space requires less than a decade.

Some variability in the overall organic-carbon content of the reefs becomes noticeable when examining the carbon inventories (Figure 4.4B). Correlations between shell content, mean grain size, and carbon indicate that this variability seems tied to location (Figure 4.2). As these reefs occur in disparate areas of the estuary, the sediment trends could be impacted by distance from the head of the estuaries. The ancient reefs occur closest to river outlets, where sandflats in wave-dominated estuaries typically do not exist (Dalrymple et al. 2012). As a result of this setting, those reefs have an overall finer sediment, and a sharper relationship in grain size and carbon than the extant natural reefs. In contrast both sets of reefs show a similar, direct relationship between percent shell and carbon. Thus, while shell content and grain size may be decent proxies for how carbon-rich a reef may be, the estuarine location must be considered to gauge where they fall on the spectrum.

The North River ancient reef has the greatest carbon inventory, being the oldest and longest lived, but its carbon accumulation rate pales in comparison to the constructed reefs, as

does the natural reefs, when using the endpoint method for reef chronology. However, when we frame these reefs within the catch-up and keep-up model of reef growth (Figure 4.5B), we find the rates of carbon accumulation become much more comparable. In fact, organic carbon accumulation (g m^{-2} yr^{-1}) divides into two distinct groupings based on reef phase (Figure 4.6A). We also capture how the natural reefs and some of the constructed reefs have transitioned or are in the process of transitioning to the keep-up phase. Rates of oyster reef organic carbon accumulation (115 ± 37.2 g m^{-2} yr^{-1}, Mean ± SD) in the catch-up phase fall on the lower end of the saltmarsh carbon accumulation spectrum (*Distichlis* marsh: 107.5 g m^{-2} yr^{-1}, Ouyang and Lee 2014), but are actually greater than some nearby saltmarsh carbon accumulation rates (10-15 g m^{-2} yr^{-1}, Theuerkauf et al. 2015). However, carbon accumulation rates of extant natural reefs within the keep-up phase (5.1 ± 2.6 g m^{-2} yr^{-1}) are far below what saltmarshes sustain but overlap with carbon accumulation rates displayed by the ancient reefs (2.6 ± 1.6 g m^{-2} yr^{-1}). The section of the North River ancient reef that could be considered in a catch-up phase, mentioned previously, displays some of the higher carbon accumulation rates of the ancient reefs, but is still not as high as the extant natural keep-up reefs. Consequently, driven by greater rates of RSLR, current living reefs appear to be accumulating carbon more rapidly than the ancient reefs and are significant carbon burial spots during their initial stages, nonetheless this is minimized when they reach MSL. It should be noted that the carbon content of the pore sediment is not a complete representation of a reef's full carbon budget, as it excludes the complex dynamic of inorganic carbon exchange during shell formation.

Similar to carbon burial, shell production also forms distinct groupings using the catch-up/keep-up growth model (Figure 4.6B). Shell production in extant reefs is an order of magnitude greater during the catch-up phase (1.9 ± 0.56 L m^{-2} yr^{-1}) than the keep-up phase

(0.072 ± 0.029 L m^{-2} yr^{-1}). Shell production in the natural reefs in the keep-up phase is still greater than the ancient reefs (0.031 ± 0.016 L m^{-2} yr^{-1}), but similar to some of the oldest (deepest) sections of the ancient reefs. This is likely due to reef growth response to relative rates of SLR for each of these reef sections, with the oldest portions of the ancient reefs having greater growth during a SLR rate (1.7 mm yr^{-1}, Engelhart and Horton 2012) that is closer to the rate of RSLR over the past century (2.1 mm yr^{-1}, Kemp et al. 2011). Contrary to the carbon accumulations and despite shell production being generally high in the catch-up phase of living reefs, the potential catch-up phase of the North River ancient reef has relatively low shell production. Shell preservation across generations appears to be high as there are not large differences in calculated shell production from constructed to natural (immature, catch-up) and from natural (mature, keep-up) to ancient that are not attributable to relative accretion rates. Indeed, both carbon accumulation and shell production appear to be enhanced by the anthropogenically modified SLR of the last century compared to prehistoric rates. Therefore, SLR has continued to act as the dominant control over oyster reef growth and influenced composition, while other changes to these estuaries in the last two centuries have not significantly impacted intertidal reefs.

4.5. Conclusion

This study has provided evidence that oyster reefs have consistent patterns in SLR-driven growth, shell production, and sedimentary composition over the past four millennia. Reef growth is strongly linked to sea level, exhibiting catch-up and keep-up phases with SLR. During catch-up phase both organic carbon accumulation and shell production are enhanced but greatly reduced when the reef shifts to a keep-up phase. The transition of ancient reefs to a give-up phase suggests that significant loss of extant reefs could result from pronounced changes to the

estuarine system (water quality), anthropogenic disturbance/modification and/or catastrophic events (e.g., storms). These results highlight the fragility of reefs growing at the edge of this balance; as we continue to develop along our coasts, special attention must be given to how we are modifying estuarine dynamics through altered river flow and inlet maintenance, which could change the suitability of large areas for oyster-reef growth. While SLR may actually enhance growth in some locations as estuarine gradients shift, climatic changes (e.g., precipitation, storm-driven alterations) may cause other areas to become more susceptible to transitioning to a give-up phase, especially with the added stress of harvesting pressure.

Table 4.1 Details of each oyster reef cored for growth and compositional analysis. Origin year for each constructed reef is included in the reef name. Number associated with each reef is for use with the study map (Figure 4.2). Core elevations for ancient reefs are estimations based on depth of sediment-water interface compared to local water level data at time of collection.

#	Reef	Type	Location	Reef Thickness (cm)	Core Elevation (m NAVD88)	Reef Base Elevation (m NAVD88)	Carbon Analysis	Radiocarbon Sample Depth Interval (cm from top)	Calibrated ^{14}C Age† (yr BP ± 1σ)	Estimated accretion rate (cm yr^{-1})
1	NR-12-01	Ancient	North River	229	-1.5	-5.145	CHN	117-122	1819 ± 25	0.066
								157-162	2663 ± 27	0.047
								222-227	3161 ± 36.5	0.131
								272-277	4057 ± 20	0.056
								312-317	4430 ± 10.5	0.107
2	NPR-14-01	Ancient	Newport River	105	-1.7**	-4.585	CHN	288-293	3240 ± 30.5	0.090
								323-328	3866 ± 73	0.056
								343-348	4057 ± 41.5	0.157
								383-388	4265 ± 114	0.144
3	SB-13-02	Natural	Back Sound	70	0.07	-0.656	CHN	70-75	157 ± 6.5	0.478
4	CI-1	Natural	Back Sound	73	0.01	-0.702	CHN	70-73	179 ± 17	0.399
5	CI-6	Natural	Back Sound	60	0.00	-0.560	CHN	85-90	185 ± 20	0.487
6	MM2	Natural	Back Sound	40	-0.18	-0.871	CHN	35-40	Modern	0.577‡
7	MMNATBB1	Natural	Back Sound	105	0.03	-0.995	CHN, LOI			-
8	MF2-1997	Constructed	Back Sound	35	0.01	-0.365	CHN			2.68
9	MF2-2000	Constructed	Back Sound	35	0.03	-0.398	CHN			3.86
10	SM4-1997	Constructed	Back Sound	15	-0.26	-0.436	CHN			1.25
11	SG3-2000	Constructed	Back Sound	20	-0.19	-0.362	CHN			1.59
12	2S6 (2011)	Constructed	Back Sound	25	-0.12	-0.346	LOI			5.00

† yr Before Present is relative to Present being 1950 CE

‡ Growth rate of MM2 is a conservative estimate based on oldest possible origin within Modern age (1950 CE). Growth rates of constructed reefs is based on year of construction.

Table 4.2 Spearman rank correlation results comparing percent shell, mean grain size, and percent carbon in ancient and natural reef core samples separated by age. Correlations are displayed in Figure 4.3.

	Shell % x Carbon %		Grain Size x Carbon %		Shell % x Grain Size	
Reefs	**Spearman ρ**	***P*-value**	**Spearman ρ**	***P*-value**	**Spearman ρ**	***P*-value**
Ancient	0.72	< 0.0001	-0.81	< 0.0001	-0.40	0.007
Extant natural	0.67	< 0.0001	-0.76	< 0.0001	-0.47	< 0.0001

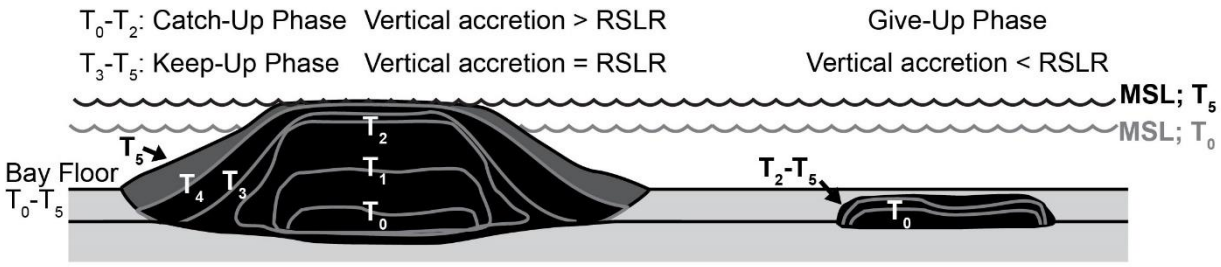

Figure 4.1 Conceptual model of oyster reef growth with relative sea level rise. Figure is modified from Rodriguez et al. (2014) considering catch-up, keep-up, and give-up phases suggested for coral reefs by Neumann and Macintyre (1985).

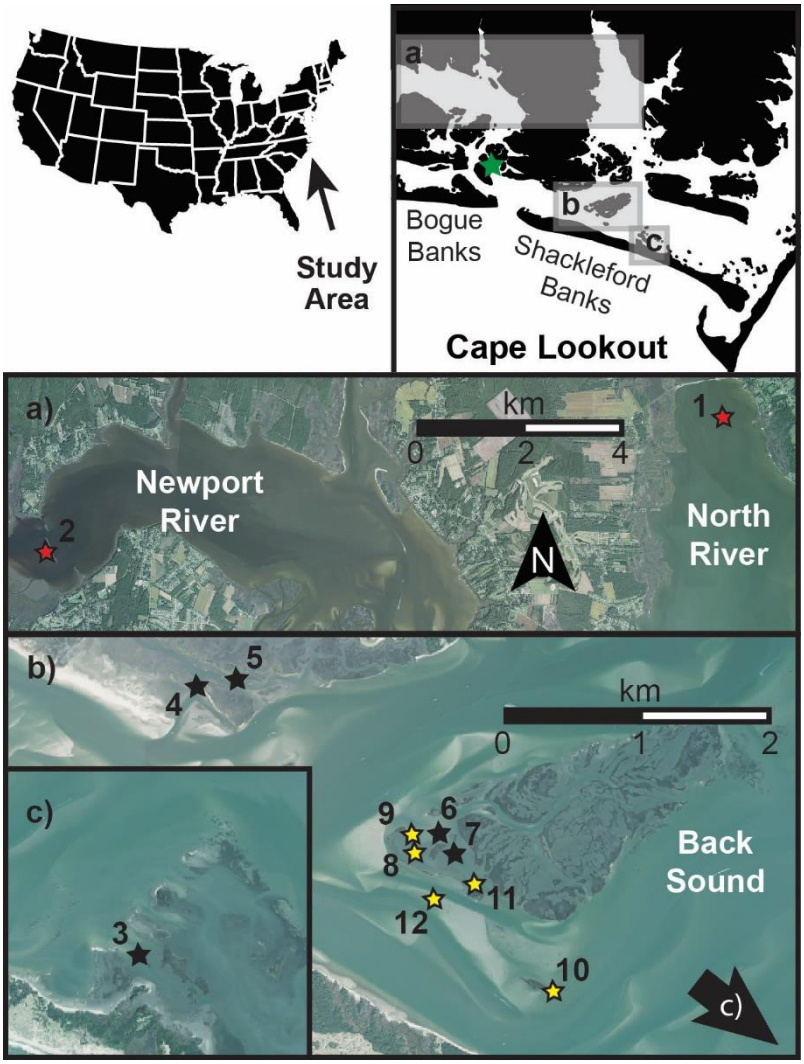

Figure 4.2 Map of the study area in the Cape Lookout area of North Carolina. Reef cores were obtained from Back Sound, North River, and Newport River. Stars indicate the type of reef samples: ancient (red), extant natural (black), constructed (yellow). Numbers refer to each reef on Table 1. Green star denotes the location of the NOAA Tide Gauge (Station ID: 8656483, Beaufort, NC).

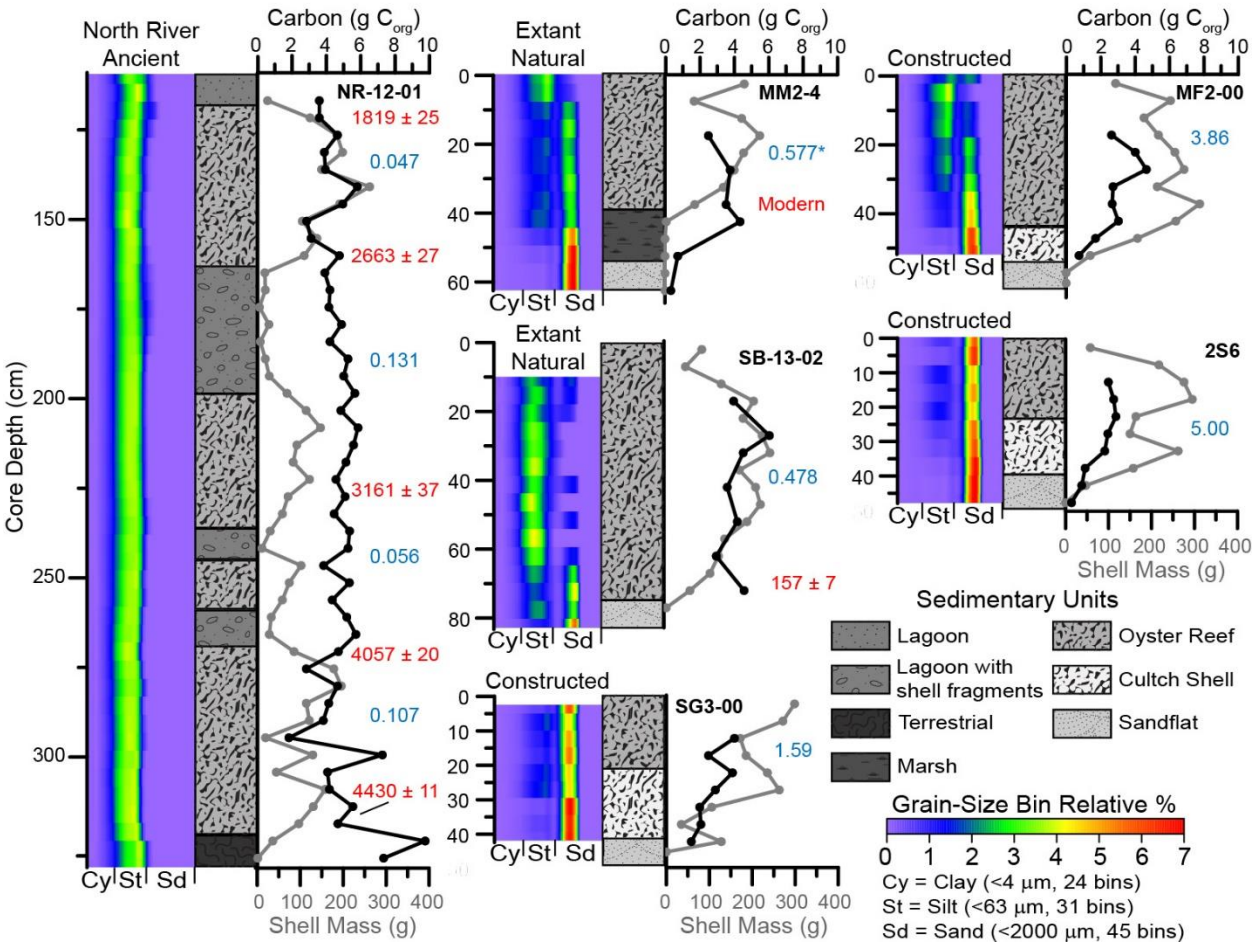

Figure 4.3 Core data from select sampled oyster reefs including grain size distribution maps, descriptions (sedimentary units), organic carbon and shell mass profiles. Carbon (black lines) and shell mass (gray lines) values are for distinct core sample volumes (405.37 cm^3). Dates obtained from radiocarbon analysis are presented in red as calibrated years before present (yr BP), where the present is defined as 1950. Accretion rates (cm yr^{-1}, endpoint method, blue numbers) are placed in stratigraphic position between radiocarbon dates within the ancient reef and for the entire cores of the extant natural and constructed reefs.

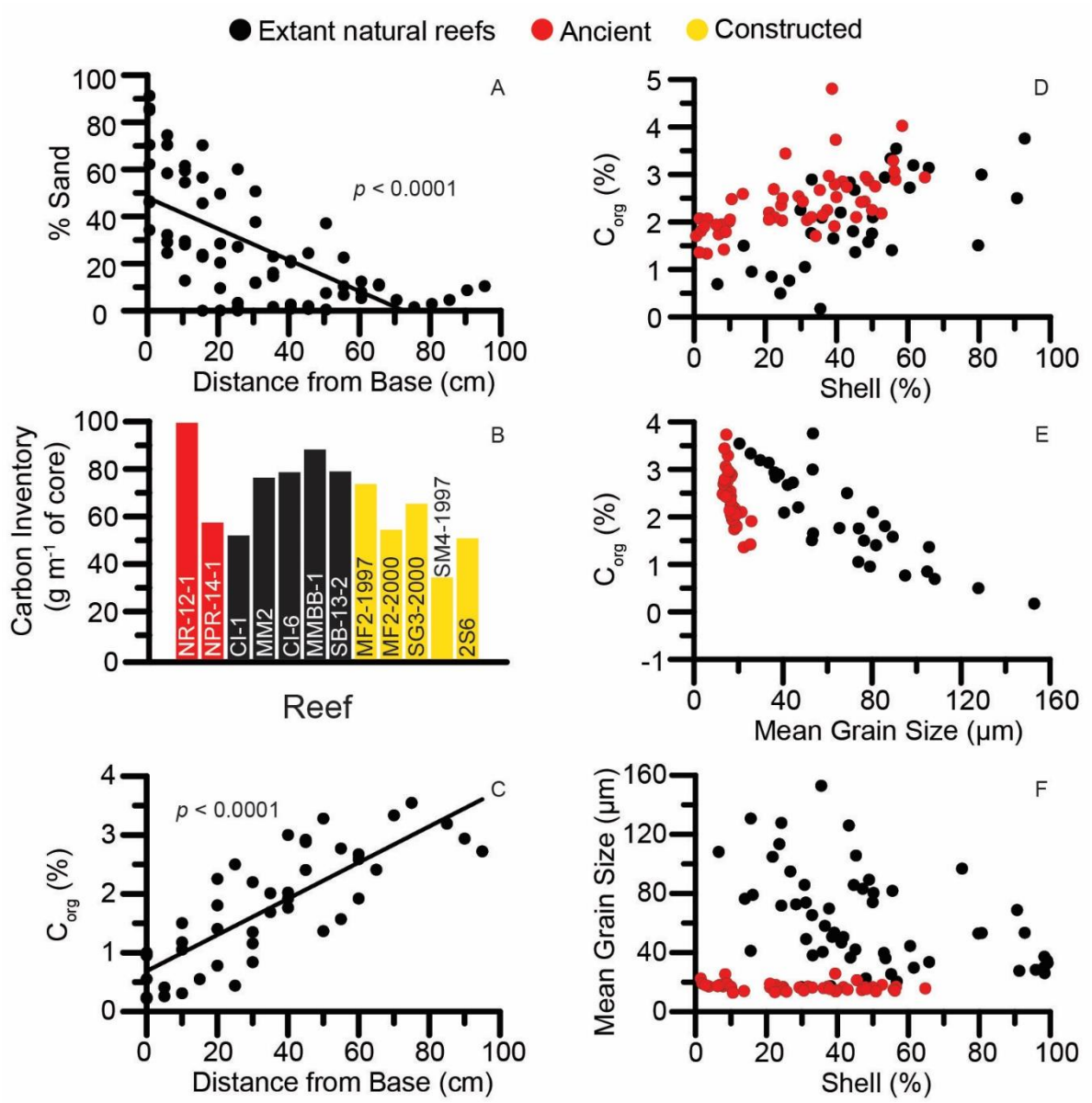

Figure 4.4 Sedimentary comparisons across and among natural and constructed reefs. A) Regression of percent sand in pore sediment compared to the distance of core sample from the base of the natural reefs. B) Carbon inventory of each reef normalized to a meter of core. Colors correspond to age or geographic location of reefs: red (ancient), black (extant natural reefs), and yellow (constructed). C) Regression of percent organic carbon with distance from reef base. D,E,F) Correlations among percent shell, mean grain size, and percent organic carbon by reef age.

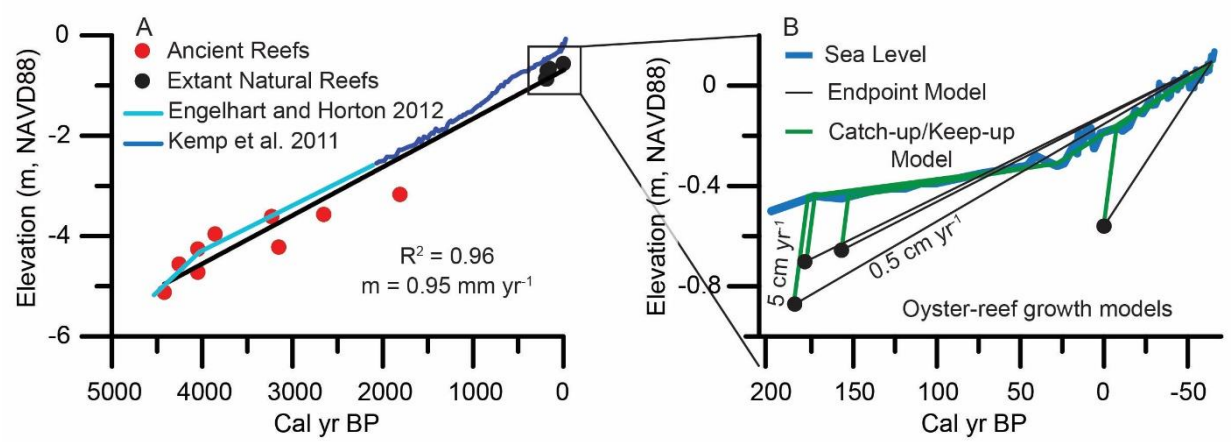

Figure 4.5 Reef origin and sea level reconstructions. A) Regression of reef base elevations by radiocarbon date. Local sea level curve is also plotted (blue line, data from Kemp et al. 2011; light blue line, sea level extrapolation using Engelhart and Horton 2012). B) Oyster-reef growth models considering the endpoint method and the catch-up/keep-up model applied to the extant natural reefs.

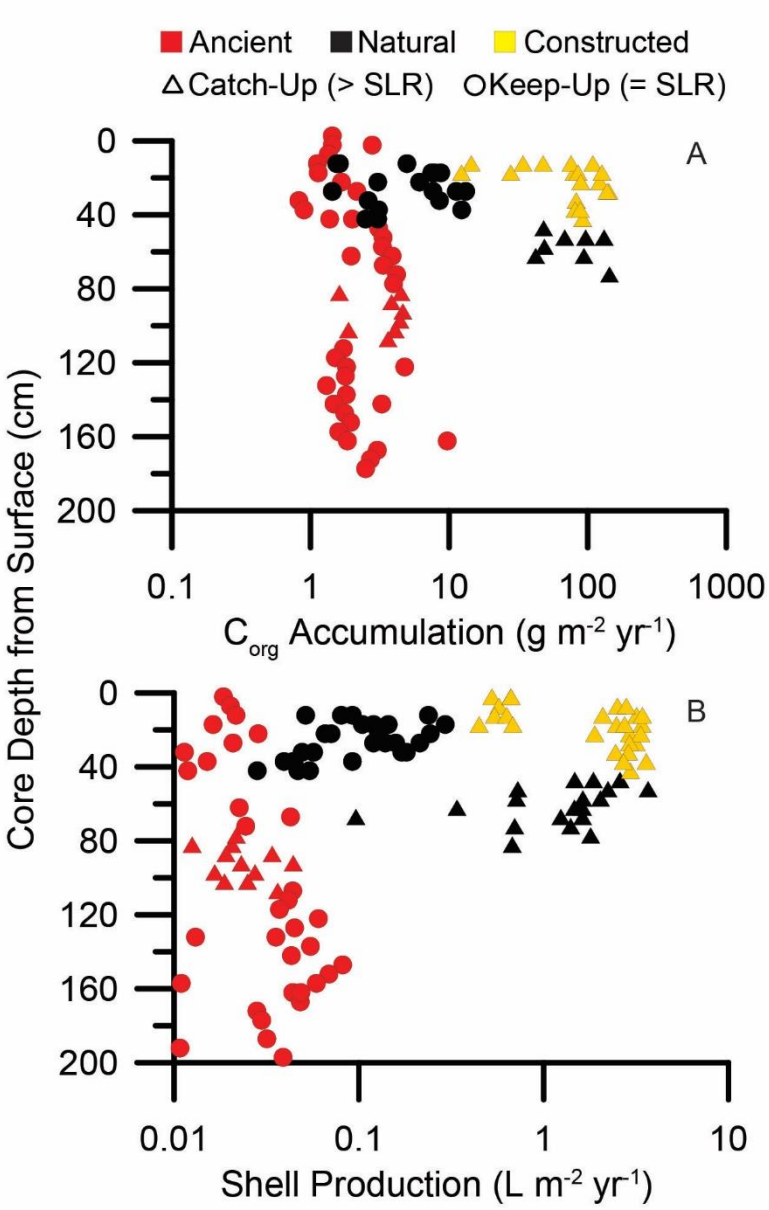

Figure 4.6 Carbon accumulation and shell production based on a catch-up and keep-up reef growth model for different reef generations. Volume of shell is calculated from the shell mass of a 5-cm core sample (405.37 cm^3 sample volume) using the density of calcium carbonate. Both x-axes are presented in a log scale.

REFERENCES

Alleway, Heidi K., and Sean D. Connell. 2015. Loss of an ecological baseline through the eradication of oyster reefs from coastal ecosystems and human memory. *Conservation Biology* 29, 795–804. doi:10.1111/cobi.12452.

Beck, Michael W., Robert D. Brumbaugh, Laura Airoldi, Alvar Carranza, Loren D. Coen, Christine Crawford, Omar Defeo, et al. 2011. Oyster Reefs at Risk and Recommendations for Conservation, Restoration, and Management. *BioScience* 61, 107–116. doi:10.1525/bio.2011.61.2.5.

Berelson, William M., and S. Duncan Jr Heron. 1985. Correlations between Holocene flood tidal delta and barrier island inlet fill sequences: Back Sound-Shackleford Banks, North Carolina. *Sedimentology* 32, 215–222. doi:10.1111/j.1365-3091.1985.tb00504.x.

Craft, C. B., E. D. Seneca, and S. W. Broome. 1991. Loss on ignition and kjeldahl digestion for estimating organic carbon and total nitrogen in estuarine marsh soils: Calibration with dry combustion. *Estuaries* 14, 175–179. doi:10.1007/BF02689350.

Cronin, T. M., K. Hayo, R. C. Thunell, G. S. Dwyer, C. Saenger, and D. A. Willard. 2010. The Medieval Climate Anomaly and Little Ice Age in Chesapeake Bay and the North Atlantic Ocean. *Palaeogeography, Palaeoclimatology, Palaeoecology* 297, 299–310. doi:10.1016/j.palaeo.2010.08.009.

Dalrymple, R. W., Mackay, D. A., Ichaso, A. A., & Choi, K. S. 2012. Processes, Morphodynamics, and Facies of Tide-Dominated Estuaries. In R. A. Davis & R. W. Dalrymple (Eds.), *Principles of Tidal Sedimentology* (pp. 1–621). Springer Science+Business Media. doi:10.1007/978-94-007-0123-6

Dame, Richard F. 2009. Shifting Through Time: Oysters and Shell Rings in Past and Present Southeastern Estuaries. *Journal of Shellfish Research* 28, 425–430. doi:10.2983/035.028.0301.

DeAlteris, Joseph T. 1988. The Geomorphic Development of Wreck Shoal, a Subtidal Oyster Reef of the James River, Virginia. *Estuaries* 11, 240–249. doi:10.2307/1352010.

Dietl, Gregory P., and Karl W. Flessa. 2011. Conservation paleobiology: Putting the dead to work. *Trends in Ecology and Evolution* 26, 30–37. doi:10.1016/j.tree.2010.09.010.

Dietl, Gregory P, Susan M Kidwell, Mark Brenner, David A Burney, Karl W Flessa, Stephen T Jackson, and Paul L Koch. 2015. Conservation Paleobiology: Leveraging Knowledge of the Past to Inform Conservation and Restoration. *Annu. Rev. Earth Planet. Sci* 43, 79–103. doi:10.1146/annurev-earth-040610-133349.

Engelhart, Simon E., and Benjamin P. Horton. 2012. Holocene sea level database for the Atlantic coast of the United States. *Quaternary Science Reviews* 54, 12–25. doi:10.1016/j.quascirev.2011.09.013.

Engelhart, Simon E., Benjamin P. Horton, Bruce C. Douglas, W. Richard Peltier, and Torbjörn E. Törnqvist. 2009. Spatial variability of late Holocene and 20th century sea-level rise along the Atlantic coast of the United States. *Geology* 37, 1115–1118. doi:10.1130/G30360A.1.

Erlandson, Jon M., Torben C. Rick, Todd J. Braje, Alexis Steinberg, and René L. Vellanoweth. 2008. Human impacts on ancient shellfish: a 10,000 year record from San Miguel Island, California. *Journal of Archaeological Science* 35, 2144–2152. doi:10.1016/j.jas.2008.01.014.

Grabowski, Jonathan H, Robert D Brumbaugh, Robert F Conrad, Andrew G Keeler, J James, Charles H Peterson, Michael F Piehler, P Sean, and Ashley R Smyth. 2012. Economic Valuation of Ecosystem Services Provided by Oyster Reefs. *BioScience* 62, 900–909. doi:10.1525/bio.2012.62.10.10.

Harding, Juliana M, Roger Mann, and Melissa J Southworth. 2008. Shell Length-at-age Relationships in James River, Virginia, Oysters (Crassostrea virginica) Collected Four Centuries Apart. *Journal of Shellfish Research* 27, 1109–1115. doi:10.2983/0730-8000-27.5.1109.

Harding, Juliana M, Howard J Spero, Roger Mann, Gregory S Herbert, and Jennifer L Sliko. 2010. Reconstructing early 17th century estuarine drought conditions from Jamestown oysters. *Proceedings of the National Academy of Sciences of the United States of America* 107, 10549–10554. doi:10.1073/pnas.1001052107.

Horton, B. P., W. R. Peltier, S. J. Culver, R. Drummond, S. E. Engelhart, A. C. Kemp, D. Mallinson, et al. 2009. Holocene sea-level changes along the North Carolina Coastline and their implications for glacial isostatic adjustment models. *Quaternary Science Reviews* 28, 1725–1736. doi:10.1016/j.quascirev.2009.02.002.

Jackson, J. B. C., K. A. Alexander, and E. Sala, editors. 2011. Shifting baselines: the past and the future of ocean fisheries. Island Press, New York in Rick, Torben C., and Rowan Lockwood. 2013. Integrating Paleobiology, Archeology, and History to Inform Biological Conservation. *Conservation Biology* 27, 45–54. doi:10.1111/j.1523-1739.2012.01920.x.

Kemp, Andrew C., Christopher E. Bernhardt, Benjamin P. Horton, Robert E. Kopp, Christopher H. Vane, W. Richard Peltier, Andrea D. Hawkes, Jeffrey P. Donnelly, Andrew C. Parnell, and Niamh Cahill. 2014. Late Holocene sea- and land-level change on the U.S. southeastern Atlantic coast. *Marine Geology* 357, 90–100. doi:10.1016/j.margeo.2014.07.010.

Kemp, Andrew C, Benjamin P Horton, Jeffrey P Donnelly, Michael E Mann, Martin Vermeer, and Stefan Rahmstorf. 2011. Climate related sea-level variations over the past two millennia. *Proceedings of the National Academy of Sciences of the United States of America* 108, 11017–22. doi:10.1073/pnas.1015619108.

Kidwell, S M. 2015. Biology in the Anthropocene: Challenges and insights from young fossil records. *Proceedings of the National Academy of Sciences of the United States of America* 112, 4922–4929. doi:10.1073/pnas.1403660112.

Kidwell, Susan M. 2009. Evaluating human modification of shallow marine ecosystems: Mismatch in composition of molluscan living and time-averaged death assemblages. *Conservation Paleobiology: Using the Past to Manage for the Future* 15, 113–31.

Kirby, Michael X., and Henry M. Miller. 2005. Response of a benthic suspension feeder (Crassostrea virginica Gmelin) to three centuries of anthropogenic eutrophication in Chesapeake Bay. *Estuarine, Coastal and Shelf Science* 62, 679–689. doi:10.1016/j.ecss.2004.10.004.

Klein, Richard G, and Teresa E Steele. 2013. Archaeological shellfish size and later human evolution in Africa. *Proceedings of the National Academy of Sciences of the United States of America* 110, 10910–5. doi:10.1073/pnas.1304750110.

Kohn, Matthew J. 2010. Carbon isotope compositions of terrestrial C3 plants as indicators of (paleo)ecology and (paleo)climate. *Proceedings of the National Academy of Sciences of the United States of America* 107, 19691–5. doi:10.1073/pnas.1004933107.

Kopp, Robert E., Benjamin P. Horton, Andrew C. Kemp, and Claudia Tebaldi. 2015. Past and future sea-level rise along the coast of North Carolina, USA. *Climatic Change* 132, 693–707. doi:10.1007/s10584-015-1451-x.

Mann, Roger, Juliana M. Harding, and Melissa J. Southworth. 2009. Reconstructing pre-colonial oyster demographics in the Chesapeake Bay, USA. *Estuarine, Coastal and Shelf Science* 85, 217–222. doi:10.1016/j.ecss.2009.08.004.

Mann, Roger, Melissa Southworth, Juliana M Harding, and James A Wesson. 2009. Population Studies of the Native Eastern Oyster, Crassostrea virginica , (Gmelin , 1791) in the James River , Virginia , USA. *Journal of Shellfish Research* 28, 193–220.

Mattheus, Christopher R., and Antonio B. Rodriguez. 2014. Controls on Lower-Coastal-Plain Valley Morphology and Fill Architecture. *Journal of Sedimentary Research* 84, 314–325. doi:http://dx.doi.org/10.2110/jsr.2014.30.

Neumann, A. C. and Macintyre, Ian G. 1985. Reef Response of Sea Level Rise: Keep-up, Catch-up or Give-up. In: Gabrie, C., Toffart, J. L. and Salvat, B., *Proceedings of the Fifth International Coral Reef Congress, Tahiti, 27 May-1 June 1985: Volume 3, Symposia and seminars (A).* Moorea, French Polynesia: Antenne Museum-EPHE, pp.105-110.

Ouyang, X., and S. Y. Lee. 2014. Updated estimates of carbon accumulation rates in coastal marsh sediments. *Biogeosciences* 11, 5057–5071. doi:10.5194/bg-11-5057-2014.

Pauly, D. 1995. Anecdotes and the Shifting Base-Line Syndrome of Fisheries. *Trends in Ecology & Evolution* 10, 430. doi:10.1016/s0169-5347(00)89171-5.

Perry, C. T., S. G. Smithers, P. Gulliver, and N. K. Browne. 2012. Evidence of very rapid reef accretion and reef growth under high turbidity and terrigenous sedimentation. *Geology* 40, 719–722. doi:10.1130/G33261.1.

Powell, Eric N., Kathryn A. Ashton-Alcox, and John N. Kraeuter. 2006. How long does oyster shell last on an oyster reef? *Estuarine, Coastal and Shelf Science* 69, 531–542. doi:10.1016/j.ecss.2006.05.014.

Powell, Eric N., John M. Klinck, Kathryn Ashton-Alcox, Eileen E. Hofmann, and Jason Morson. 2012. The rise and fall of Crassostrea virginica oyster reefs: The role of disease and fishing in their demise and a vignette on their management. *Journal of Marine Research* 70, 505–558. doi:10.1357/002224012802851878.

Powers, S. P., C. H. Peterson, J. H. Grabowski, and H. S. Lenihan. 2009. Success of constructed oyster reefs in no-harvest sanctuaries: implications for restoration. *Marine Ecology Progress Series* 389, 159–170. doi:10.3354/meps08164.

Reimer, Paula J, Mike G L Baillie, Edouard Bard, Alex Bayliss, J Warren Beck, Chanda J H Bertrand, Paul G Blackwell, et al. 2004. INTCAL04 Terrestrial radiocarbon age calibration, 0-26 cal kyr BP. *Radiocarbon* 46, 0–26.

Rick, Torben C., and Rowan Lockwood. 2013. Integrating Paleobiology, Archeology, and History to Inform Biological Conservation. *Conservation Biology* 27, 45–54. doi:10.1111/j.1523-1739.2012.01920.x.

Rick, Torben C., Leslie A. Reeder-Myers, Courtney A. Hofman, Denise Breitburg, Rowan Lockwood, Gregory Henkes, Lisa Kellogg, et al. 2016. Millennial-scale sustainability of the Chesapeake Bay Native American oyster fishery. *Proceedings of the National Academy of Sciences* 113, 201600019. doi:10.1073/pnas.1600019113.

Ridge, Justin T., Antonio B. Rodriguez, and F. Joel Fodrie. 2016. Salt Marsh and Fringing Oyster Reef Transgression in a Shallow Temperate Estuary: Implications for Restoration, Conservation and Blue Carbon. *Estuaries and Coasts*. 1–15. doi:10.1007/s12237-016-0196-8.

Ridge, Justin T., Antonio B. Rodriguez, F. Joel Fodrie, Niels L. Lindquist, Michelle C. Brodeur, Sara E. Coleman, Jonathan H. Grabowski, and Ethan J. Theuerkauf. 2015. Maximizing oyster-reef growth supports green infrastructure with accelerating sea-level rise. *Scientific Reports* 5, 14785. doi:10.1038/srep14785.

Rodriguez, Antonio B, F Joel Fodrie, Justin T Ridge, Niels L Lindquist, Ethan J Theuerkauf, Sara E Coleman, Jonathan H Grabowski, et al. 2014. Oyster reefs can outpace sea-level rise. *Nature Climate Change* 4, 493–497. doi:10.1038/NCLIMATE2216.

Simms, A.R., Anderson, J.B., Rodriguez, A.B. and Taviani, M., 2008. Mechanisms controlling environmental change within an estuary: Corpus Christi Bay, Texas, USA. *Geological Society of America Special Papers*, *443*, pp.121-146.

Soniat, Thomas M., Nathan Cooper, Eric N. Powell, John M. Klinck, Mahdi Abdelguerfi, Shengru Tu, Roger Mann, and Patrick D. Banks. 2014. Estimating Sustainable Harvests of Eastern Oysters, Crassostrea virginica. *Journal of Shellfish Research* 33. National Shellfisheries Association, 381–394. doi:10.2983/035.033.0207.

Stathakopoulos, A., and B. M. Riegl. 2015. Accretion history of mid-Holocene coral reefs from the southeast Florida continental reef tract, USA. *Coral Reefs* 34, 173–187. doi:10.1007/s00338-014-1233-3.

Stuiver, M., & Polach, H. A. 1977. Reporting of 14C Data. *Radiocarbon*, 19(3), 355–363.

Stuiver, Minze, Paula J. Reimer, and Thomas F. Braziunas. 1998. High-Precision Radiocarbon Age Calibration for Terrestrial and Marine Samples. *Radiocarbon* 40, 1127–1151. doi:10.2458/azu_js_rc.v40i3.3786.

Surge, D., K. C. Lohmann, and David L. Dettman. 2001. Controls on isotopic chemistry of the American oyster, Crassostrea virginica: Implications for growth patterns. *Palaeogeography, Palaeoclimatology, Palaeoecology* 172, 283–296. doi:10.1016/S0031-0182(01)00303-0.

Theuerkauf, Ethan J., J. Drew Stephens, Justin T. Ridge, F. Joel Fodrie, and Antonio B. Rodriguez. 2015. Carbon export from fringing saltmarsh shoreline erosion overwhelms carbon storage across a critical width threshold. *Estuarine, Coastal and Shelf Science* 164, 367–378. doi:10.1016/j.ecss.2015.08.001.

Thomas, Kenneth D. 2015. Molluscs emergent, Part II: Themes and trends in the scientific investigation of molluscs and their shells as past human resources. *Journal of Archaeological Science* 56, 159–167. doi:10.1016/j.jas.2015.01.015.

Timmons, Emily A., Antonio B. Rodriguez, Christopher R. Mattheus, and Regina DeWitt. 2010. Transition of a regressive to a transgressive barrier island due to back-barrier erosion, increased storminess, and low sediment supply: Bogue Banks, North Carolina, USA. *Marine Geology* 278, 100–114. doi:10.1016/j.margeo.2010.09.006.

Troiani, B T, A R Simms, T Dellapenna, E Piper, and Y Yokoyama. 2011. The importance of sea-level and climate change , including changing wind energy , on the evolution of a coastal estuary : Copano Bay , Texas. *Marine Geology* 280, 1–19. doi:10.1016/j.margeo.2010.10.003.

Waldbusser, George G., Eric N. Powell, and Roger Mann. 2013. Ecosystem effects of shell aggregations and cycling in coastal waters: An example of Chesapeake Bay oyster reefs. *Ecology* 94, 895–903. doi:10.1890/12-1179.1.

Waldbusser, George G., Ryan A. Steenson, and Mark A. Green. 2011. Oyster Shell Dissolution Rates in Estuarine Waters: Effects of pH and Shell Legacy. *Journal of Shellfish Research* 30, 659–669. doi:10.2983/035.030.0308.

Walles, Brenda, Roger Mann, Tom Ysebaert, Karin Troost, Peter M J Herman, and Aad C. Smaal. 2015. Demography of the ecosystem engineer Crassostrea gigas, related to vertical reef accretion and reef persistence. *Estuarine, Coastal and Shelf Science* 154. 224–233. doi:10.1016/j.ecss.2015.01.006.

Willard, Debra A., Thomas M. Cronin, and Stacey Verardo. 2003. Late-Holocene climate and ecosystem history from Chesapeake Bay sediment cores, USA. *The Holocene* 13, 201–214. doi:10.1191/0959683603hl607rp.

APPENDIX 1.1 EXAMPLE PROFILES FROM THREE STUDY REEFS

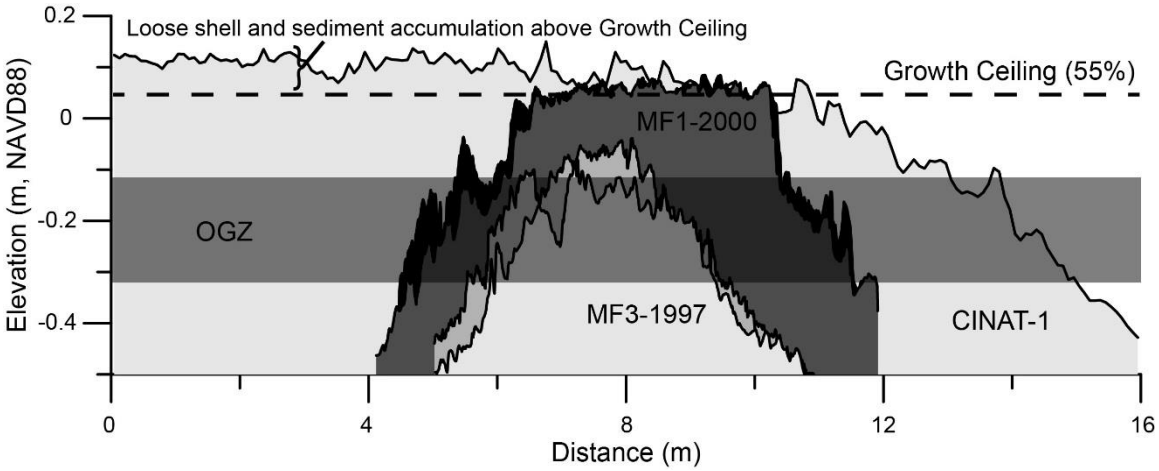

Reefs form plateaus around 55% aerial exposure. The optimal-growth zone (OGZ), occurring between 20-40% aerial exposure is highlighted. Profiles from MF3-1997 and MF1-2000 are from reef scans taken in 2010 (lighter) and 2012 (darker). CINAT-1 is a natural fringing reef.

APPENDIX 1.2 MAP OF STUDY AREA IN BACK SOUND, NORTH CAROLINA

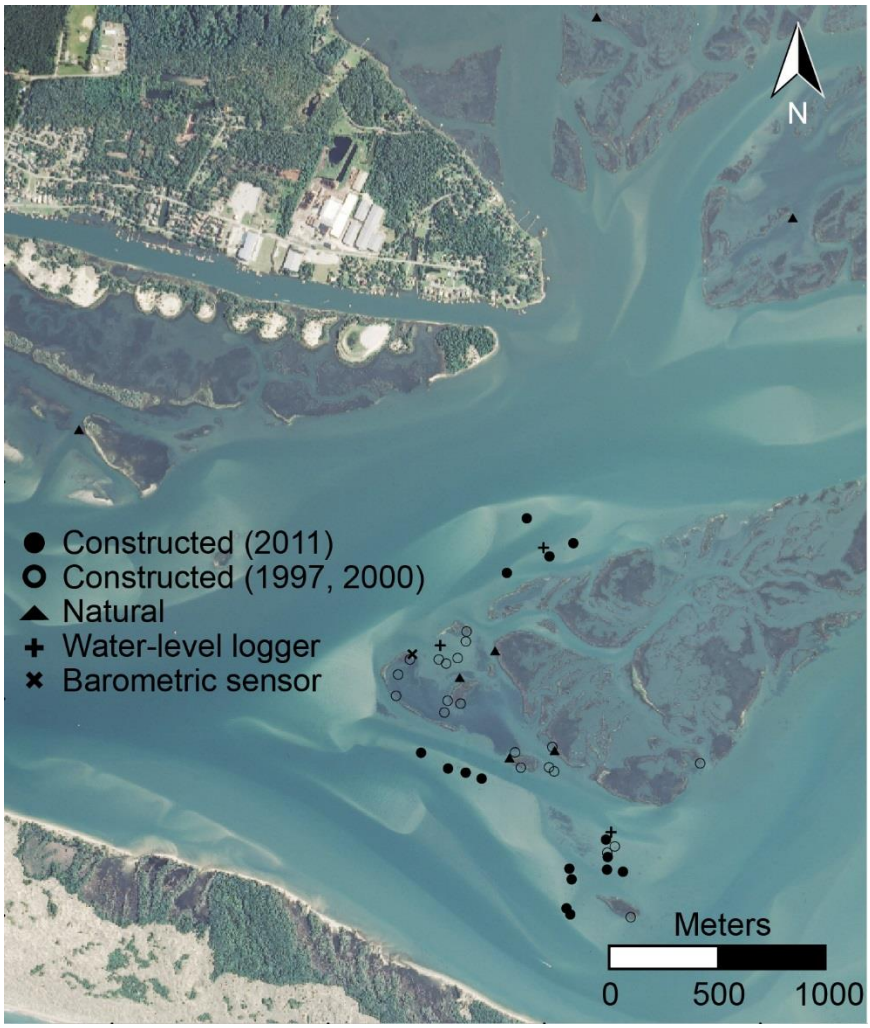

Sampled reefs and locations of water-level loggers are indicated. Map created with Surfer® 11 (Golden Software) and Adobe® Illustrator (Adobe Systems) using aerial imagery from the United States Department of Agriculture National Agriculture Imagery Program.

APPENDIX 1.3 EXPANDED GROWTH-TIDAL HEIGHT MODEL

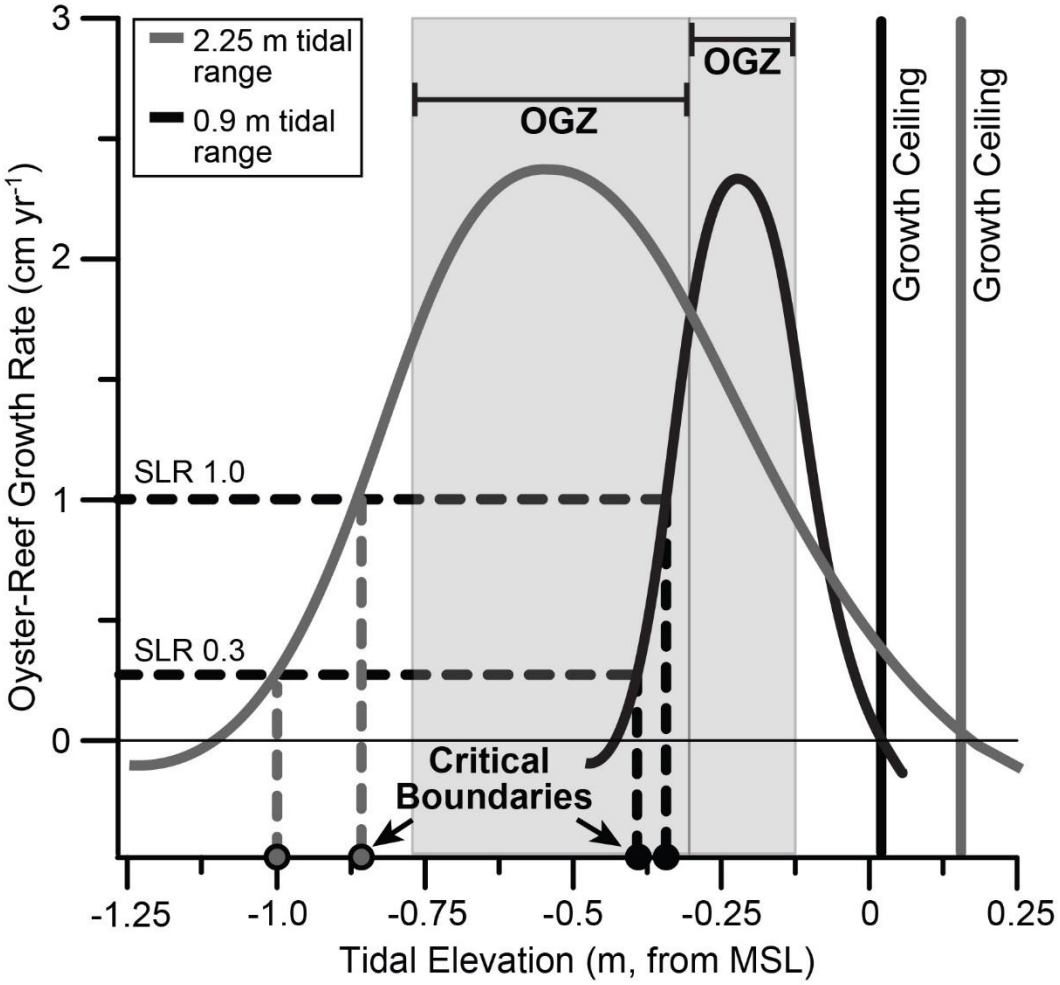

Including a greater tidal range (2.25 m), model illustrates a larger OGZ (bounded by 20-40% aerial exposure) but greater loss of suitable substrate elevations above the critical exposure boundary with a SLR-rate acceleration from 0.3 to 1.0 cm yr^{-1}. Growth rates are approximate.

APPENDIX 1.4 SAMPLE BREAKDOWN OF STUDY REEFS

Reef locations (UTM), type, and sampling conducted of all oyster reefs within the study.

Reef name	Easting	Northing	Reef Type	Scan	GPS Grid	Density
Decade-old Reefs						
MF1-1997	351637	3840264	Patch	X		X
MF1-2000	351599	3840188	Patch	X		X
MF2-1997	351512	3840181	Patch	X		X
MF2-2000	351546	3840162	Patch	X		X
MF3-1997	352022	3839684	Patch	X		X
MF4-2000	352326	3839319	Patch	X		X
MF3-2000	352046	3839665	Patch			X
MF4-1997	352291	3839290	Patch			X
SG1-1997	351553	3839991	Fringing			X
SG1-2000	351613	3839977	Fringing			X
SG2-1997	351378	3840181	Fringing			X
SG2-2000	351314	3840013	Fringing			X
SG3-1997	352037	3839777	Fringing			X
SG3-2000	351865	3839752	Fringing			X
SG4-2000	352721	3839702	Fringing			X
SM1-1997	351640	3840310	Fringing			X
SM3-1997	351892	3839682	Fringing			X
SM4-1997	352400	3838992	Fringing			X
SUB2	351538	3839937	Patch			X
SUBSG	351324	3840112	Patch			X
2011 Reefs						
1S5	352134	3840717	Patch		X	
1S6	351919	3840832	Patch		X	
1S75	352024	3840657	Patch		X	
1S9	351827	3840581	Patch		X	
2S5	351710	3839631	Patch		X	
2S6	351636	3839659	Patch		X	
2S75	351555	3839678	Patch		X	
2S9	351430	3839751	Patch		X	
3S5	352116	3839216	Patch		X	
3S6	352126	3839167	Patch		X	
3S75	352120	3839005	Patch		X	
3S9	352102	3839033	Patch		X	
4S5	352285	3839350	Patch		X	
4S6	352293	3839270	Patch		X	
4S75	352364	3839202	Patch		X	
4S9	352290	3839211	Patch		X	
Natural Reefs						
NRM_NAT2	353150	3842219	Fringing			X
NRM_NAT1	352242	3843145	Fringing			X
ClNAT-1	349847	3841242	Fringing			X
MMNAT1	351839	3839727	Fringing			X
MMNAT2	351609	3840098	Fringing			X
MMNAT3	352048	3839761	Fringing			X
MMNAT4	351772	3840221	Fringing			X

APPENDIX 2.1 STEM DENSITY AND HEIGHT DATA FROM MARSH SITES WITH AND WITHOUT OYSTER REEFS ADJACENT

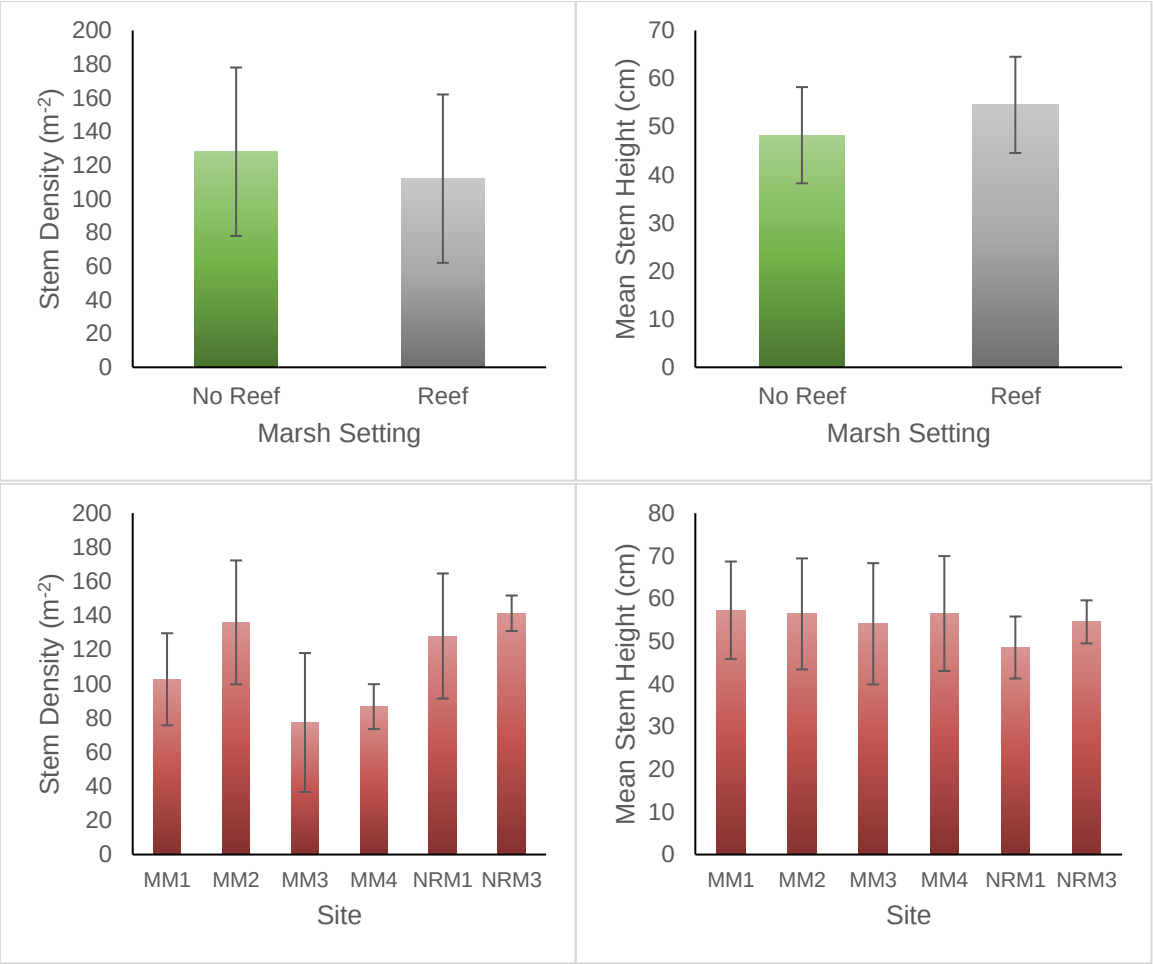

Lower panels examine differences just among sites with reefs.

APPENDIX 2.2 CROSS SECTIONS FROM NORTH RIVER MARSH AND CARROT ISLAND WITH CORES LABELED

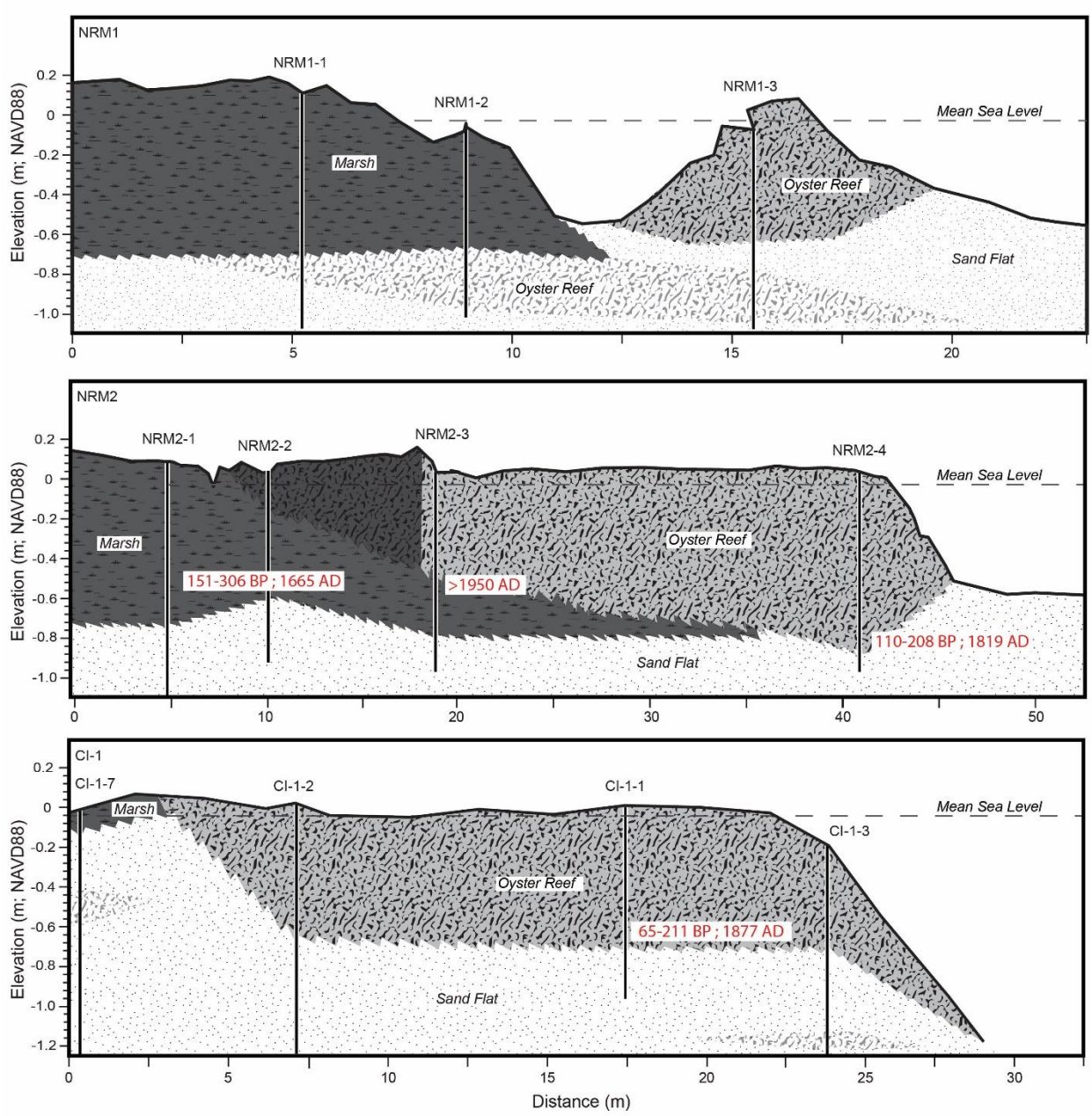

Radiocarbon dates are labeled in red from relative depths sampled.

APPENDIX 2.3 CORES AND SECTION SHELL PHOTOS FROM SIX CONSTRUCTED REEFS LABELED BY DATE OF ORIGIN

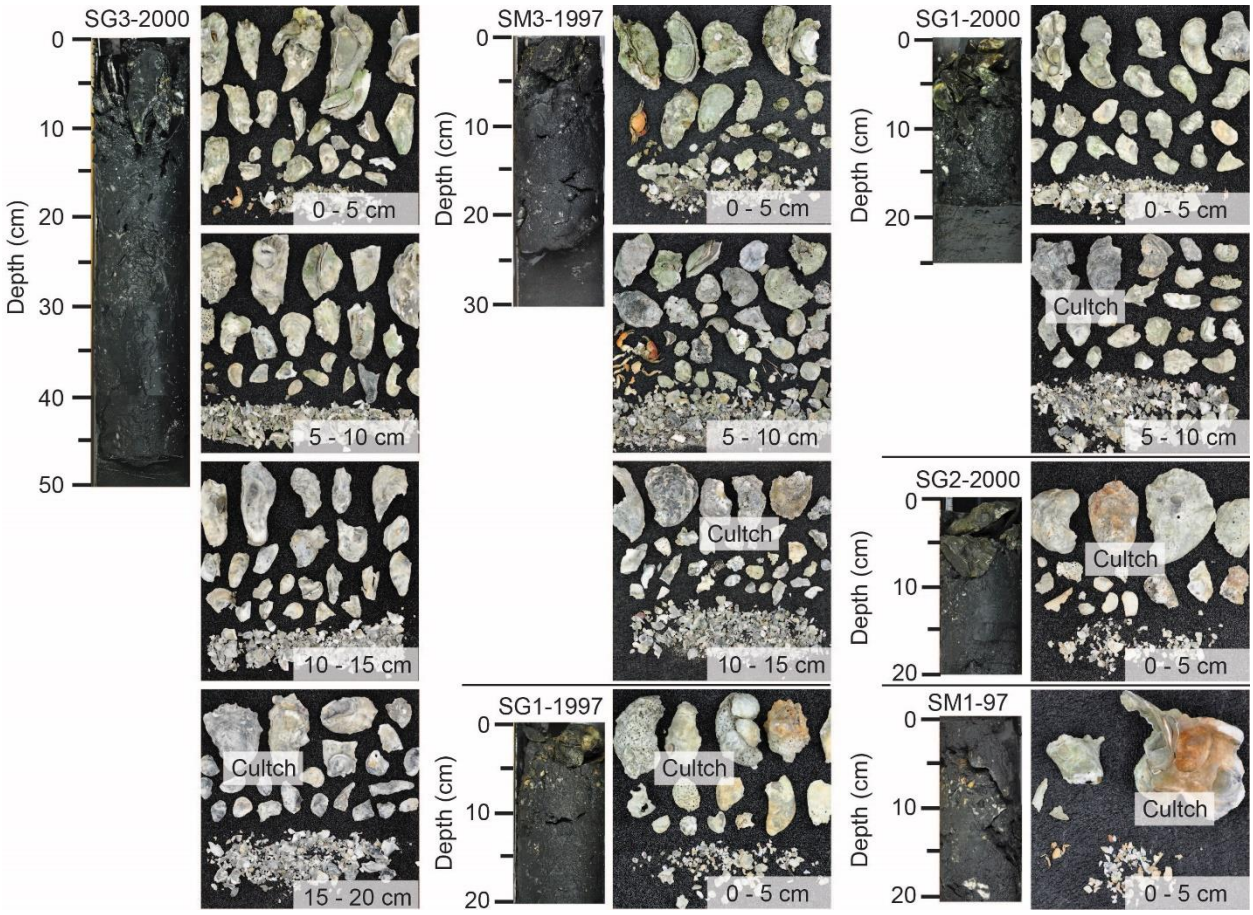

Cultch material placed during initial construction is morphologically distinct from new growth. Cores illustrate the variable depths of the taphonomically active zone (zone of living oyster) among reefs. Shell photos are labeled by depth section in the core, and the presence of cultch material in the "0-5 cm" section indicates no growth on that reef.

APPENDIX 3.1 STATISTICAL COMPARISONS OF WATER QUALITY DATA BETWEEN SCAN TIME STEPS FOR EACH REEF GENERATION

Reef Type	Time Step	Temperature (ºC)‡	Wilcoxon Rank Sums	Salinity (ppt)‡	t-Tests ($_{DF}$)
Decade-old	1	19.7 ± 7.2	$Z = 0.68$	31.8 ± 2.2	$\mathbf{t_{55} = -2.5}$
	2	18.6 ± 7.3	$p = 0.50$	*29.6 ± 4.0	$\mathbf{p = 0.015}$
Young	1	19.7 ± 6.6	$Z = 0.84$	32.4 ± 2.8	$\mathbf{t_{23} = -2.4}$
	2	18.2 ± 7.0	$p = 0.40$	*29.7 ± 3.0	$\mathbf{p = 0.025}$
Centennial	1	18.8 ± 6.9	$Z = -0.02$	30.6 ± 2.9	$t_{32} = -1.7$
	2	18.5 ± 8.5	$p = 0.99$	27.7 ± 5.6	$p = 0.10$

‡ Mean ± Standard Deviation

* Significant difference ($P < 0.05$) from previous timestep.

APPENDIX 4.1 LOI-CHN CALIBRATION CURVE

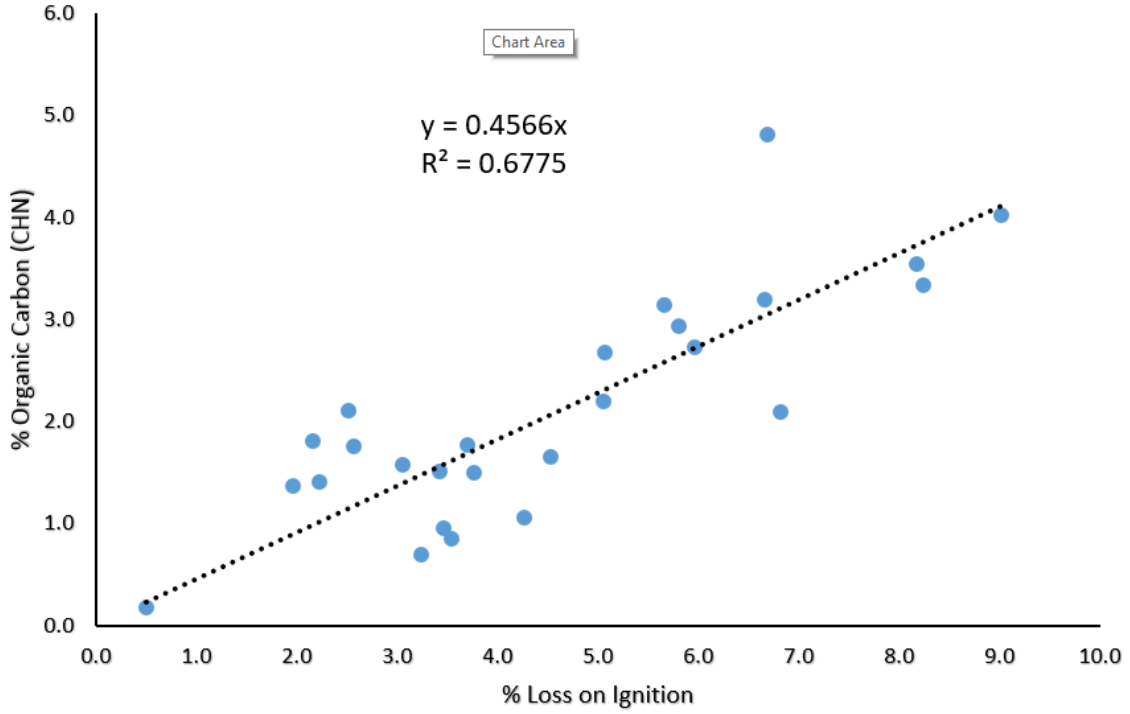

APPENDIX 4.2 ADDITIONAL CORE DATA